| | |
|---|---|
| **Titre:** Title: | Scaling the Production of Solid-Stabilized Emulsions |
| **Auteur:** Author: | Alexandre Al-Haiek |
| **Date:** | 2018 |
| **Type:** | Mémoire ou thèse / Dissertation or Thesis |
| **Référence:** Citation: | Al-Haiek, A. (2018). Scaling the Production of Solid-Stabilized Emulsions [Thèse de doctorat, École Polytechnique de Montréal]. PolyPublie. https://publications.polymtl.ca/3737/ |

UNIVERSITÉ DE MONTRÉAL

# SCALING THE PRODUCTION OF SOLID-STABILIZED EMULSIONS

ALEXANDRE AL-HAIEK

DÉPARTEMENT DE GÉNIE CHIMIQUE

ÉCOLE POLYTECHNIQUE DE MONTRÉAL

THÈSE PRÉSENTÉE EN VUE DE L'OBTENTION

DU DIPLÔME DE PHILOSOPHIAE DOCTOR

(GÉNIE CHIMIQUE)

DÉCEMBRE 2018

UNIVERSITÉ DE MONTRÉAL

ÉCOLE POLYTECHNIQUE DE MONTRÉAL

Cette thèse intitulée :

SCALING THE PRODUCTION OF SOLID-STABILIZED EMULSIONS

présentée par : AL-HAIEK Alexandre

en vue de l'obtention du diplôme de : Philosophiae Doctor

a été dûment acceptée par le jury d'examen constitué de :

Mme HEUZEY Marie-Claude, Ph. D., présidente

M. FRADETTE Louis, Ph. D., membre et directeur de recherche

M. DOUCET Jocelyn, Ph. D., membre

M. LARACHI Faïçal, Ph. D., membre externe

# DEDICATION

*To my family,*

*Nizar, Mona, Noor & Karim.*

*To every child who did not get the same opportunities I got.*

*To Syria.*

# ACKNOWLEDGEMENTS

I would need a whole thesis-long document just for a list of people that positively impacted my life and helped me become a better human, man, citizen, engineer, and researcher.

There are no words that can express my gratitude towards professor Louis Fradette. Being in his team will positively impact the rest of my career and I am grateful for that. It has been a pleasure since day one! He is an example for present and future generations of what an engineer and a researcher should be. The efficiency he is capable of has no limit…and I think he reached 100% (which challenges thermodynamics). Every time we had a meeting, I acted like a sponge: absorbing as much information as I could because I knew I was learning from *la crème de la crème*.

I am also eternally thankful to Dr. Èmir Tsabet. I have always considered him as my unofficial co-supervisor. He has been a source of inspiration regarding what a researcher should be. He has and will always be a mentor. Personally, I was extremely happy to see him come back to the department in 2017. All the discussions we had and his generosity were key in my road to a Ph.D.

My dear colleagues Bing Wan and Rahi Avazpour complete what I call: *the Pickering team*. I enjoyed all the time we spent together: group meetings, conferences…and getting hundreds of liters of deionized water on the J.A. Bombardier building. I learned so much from our discussions and the work in our laboratory. You are excellent engineers and researchers and I wish you great success in your professional and personal careers.

It was also a pleasure and an honor to be part of the URPEI with my dear friends and colleagues: Bouchra Orabi (as a sister), Igor Barnabé Belot (as a brother), David Vidal, Jean-Michel Tucny, Bastien Delacroix, Christine Beaulieu, Bruno Blais, Sebastien Leclaire, Olivier Bertrand, and Rémi Demol.

This project would not have been possible without the help of key personnel from the department of chemical engineering: Martine Lamarche and Gino Robin (known as *the dream team*), Matthieu Gauthier (known as *the master of rheology* and a very nice person to be around), Jean Huard (known as *the artist*), Sylvain Fleury Simard, Hélène Chatillon, Daniel Pilon, Robert Delisle, Kalonji Mbelu, Pr Nick Virgilio, Wendell Raphaël, Richard Silverwood, Carmen Aguilar, Monique Malouin, Yoan Ayassamipoullé, Karine Pilon, Chi Yuan Chang, Valérie Baudart,

Évelyne Rousseau, Mariia Kopach, Josée Rivest, Sylvie Taillon, Yanik Landry-Ducharme, Mehdi Bentounes, and Sébastien Chénard.

I am very grateful to professor Jason R. Tavares. He is a source of inspiration regarding hard and efficient work, dedication and success, both professionally and personally.

I am also very thankful to Dr. Philippe Leclerc. I have the pleasure of working with him and learning a lot on how a great engineer and researcher should be. He has a bright career in front of him and I wish him great success in all his endeavors.

I have recently joined the company Pyrowave. It is such a joy to wake up every day to do what we do. I could not have thought of a better place to challenge myself on a daily basis. The project and the team are awesome: Jocelyn Doucet, Jean-Philippe Laviolette, Philippe Leclerc, and Olivier Leblanc.

I want to conclude this section by dedicating this thesis and sending my most affectionate thoughts to the people I love more than anything: Nizar, Mona, Noor, and Karim. Simply put, I would give my life to you! It is an honor to be with you and I dedicate this thesis to you.

# RÉSUMÉ

Un processus d'émulsification est rencontré chaque jour ! Que ce soit simplement en lavant les mains ou nettoyant les vêtements, en utilisant une vinaigrette ou en buvant du lait, ou avec l'émulsification de l'eau dans l'huile extraite par la suite. Ce peut être un objectif ou un problème. Néanmoins, l'émulsification fait partie d'un plus grand domaine en ingénierie appelé *mélange*... et ce dernier ne manque pas de lacunes. Sur le plan industriel, la résolution des problèmes de mélange repose principalement sur l'expérience de l'ingénieur et sur une méthode basée sur l'essai et l'erreur. Cette façon de faire mène à des produits non conformes aux spécifications et génère des pertes de l'ordre de millions de dollars. Heureusement, ce comportement est en disparition grâce aux méthodes scientifiques qui sont étudiées et publiées chaque année. L'objectif principal ici est de comprendre le procédé et non pas simplement d'atteindre les spécifications requises.

Les émulsions stabilisées par des particules, souvent appelées émulsions de Pickering, ont fait l'objet de nombreuses recherches depuis la fin des années 1900. Avec le développement de la science des matériaux, les chercheurs se sont généralement concentrés sur l'effet de chaque ingrédient sur l'émulsion résultante. Le traitement de ces émulsions a suscité peu d'intérêt, ce qui est surprenant si l'on considère le fait suivant : comment les formulations développées à l'échelle laboratoire peuvent-elles être reproduites à plus grande échelle si le traitement n'est pas encore compris ?

Le manque de documentation sur le traitement a été abordé comme suit. Premièrement, il est apparu évident qu'aucun effort n'a été consacré à la quantification de l'impact de la présence de particules sur la capacité de génération d'interface. C'est une lacune scientifique due au fait que plusieurs études ont démontré que les particules ont bel et bien un impact sur le média dans lequel elles sont suspendues. D'un autre côté, il n'y a pas de consensus sur les conclusions : certains concluent que la présence de particules augmente la turbulence et vice-versa. Par conséquent, afin de bien comprendre le traitement des émulsions stabilisées par des particules, le processus d'émulsification a été divisé en ses composantes principales **:** une suspension solide suivie d'une dispersion liquide. L'impact de chaque composante sur l'émulsion finale a été identifié et quantifié pour une large gamme de conditions d'émulsification. Deux mécanismes principaux ont été étudiés : la suspension de particules et l'émulsification. Bien que la génération et la stabilisation d'interface affectent l'émulsification, la suspension de particules n'a pas été étudiée. La taille des gouttelettes augmente

lorsque la taille des particules ou la viscosité de l'huile augmente et lorsque la concentration des particules diminue. Cependant, des gouttelettes plus larges sont obtenues en augmentant la concentration en particules dans certaines conditions. Ce comportement inattendu a été analysé en examinant l'interaction entre les propriétés des particules solides et l'énergie injectée. Une analyse des échelles de longueur de turbulence a montré que ce comportement se produit lorsque la taille des particules est plus grande que l'échelle de Kolmogorov.

Le deuxième objectif était le suivant : comment peut-on accomplir la mise à l'échelle des émulsions de Pickering à l'aide d'une cuve agitée ? L'objectif principal de cette partie était de déterminer si l'utilisation de particules au lieu de tensioactifs aura un impact sur la procédure de mise à l'échelle tout en gardant à l'esprit que la méthode de stabilisation est complètement différente pour ces deux agents émulsifiants. Les critères de mise à l'échelle classiques utilisés pour les émulsions à base de tensioactifs ont été rassemblés et testés sur des émulsions diluées et concentrées. Les critères standard pour les émulsions stabilisées par les tensioactifs ainsi que pour des suspensions solides ont été appliqués aux émulsions concentrées et diluées. Aucun des paramètres étudiés ne pouvait être utilisé comme critère de mise à l'échelle pour la production d'émulsions de Pickering. L'utilisation du nombre de Weber, du nombre de Reynolds et de la vitesse en pointe comme critères de montée en puissance a entraîné des diamètres plus élevés avec la plus grande échelle, tandis que la tendance inverse a été observée avec le temps de circulation et la dissipation d'énergie. La meilleure mise à l'échelle a été obtenue avec le taux de dissipation d'énergie et la vitesse de pointe, ce qui porte à penser que l'exposant de mise à l'échelle appropriée serait compris entre 2/3 (taux de dissipation d'énergie) et 1 (vitesse de pointe).

Le dernier objectif était, sur la base des conclusions du deuxième article, de trouver un critère d'échelle approprié, de l'expliquer et de trouver ses limites. Bien que la principale différence concernant la procédure de mise à l'échelle fût mise en évidence dans l'objectif précédent, cette dernière section définit une règle de mise à l'échelle pour les émulsions de Pickering. Un exposant de mise à l'échelle de 0.8 est approprié pour la mise à l'échelle des SSE, indiquant qu'une combinaison de critères est plus appropriée qu'un critère unique comme pour une émulsification standard. L'exposant de mise à l'échelle a ensuite été mis au défi à l'aide d'un réservoir pilote de 250 litres et s'est révélé être un critère de mise à l'échelle approprié pour les émulsions de Pickering, car il permet de prédire correctement la vitesse de rotation requise sur un facteur d'échelle de 1000, rarement vu dans la littérature.

# ABSTRACT

An emulsification process is encountered every single day! Whether it is simply when washing hands or clothes, using vinaigrettes or milk, or with water emulsified in oil that is then extracted. It can be either an objective or a problem. Nonetheless, emulsification is part of a larger engineering field called *mixing* which does not lack issues. Industrially, resolving mixing issues have mainly relied on the engineer's experience and on a trial-and-error method. Products that did not match specifications generated millions of dollars in losses. However, this behavior is changing with a large amount of scientifically based methods that are investigated and published every year. The main objective here is to understand the process and not simply achieve the required specifications.

Solid-stabilized emulsions (SSEs) often referred to as Pickering emulsions, have been the focus of a large amount of research since the late 1900s. With the development of material science, investigators generally focused on the effect of each ingredient on the resulting emulsion, i.e. droplet size. There has been little interest in the processing of these emulsions which is surprising regarding this simple fact: how the formulations developed in the laboratory can be scaled if processing is not yet understood?

The lack of literature towards processing was tackled as following. First, it appeared that there has been no effort dedicated to quantifying the impact of the presence of particles on the interface generation capacity. This scientific gap is due to the fact that several studies showed that particles impact a stream, even if there is no consensus: some say that the presence of particles increases the turbulence and vice-versa. Therefore, in order to fully understand the processing of solid-stabilized emulsions, the emulsification process has been divided into its main components: solid suspension and liquid dispersion. Their impact on the resulting emulsion has been identified and quantified for a wide range of emulsification conditions. Two main mechanisms were studied: particle suspension and liquid dispersion. The droplet size increased when the particle size or the oil viscosity was increased and when the particle concentration was decreased. However, larger droplets were obtained by increasing the particle concentration under certain conditions. This unexpected behavior was analyzed by examining the interaction between the properties of the solid particles and turbulent energy. An analysis of turbulence length scales showed that this behavior occurs when the particle size is larger than the Kolmogorov scale.

With the previous conclusions, the next question becomes: how can Pickering emulsions be scaled using impeller agitated tanks? The main goal of this part was to determine whether using particles instead of surfactants would impact the scaling procedure while keeping in mind that the stabilization method is completely different for these two emulsifying agents. Conventional scaling criteria used for surfactant-based emulsions and solid suspensions were gathered and tested on diluted and concentrated particle-stabilized emulsions. Scale-up effects on the production of solid-stabilized emulsions were investigated. Standard criteria for surfactant-stabilized emulsions and solid suspensions (constant energy dissipation rate, Weber number, Reynolds number, impeller tip speed, and circulation time) were applied to concentrated and diluted emulsions. None of the parameters investigated was suitable for use as a scale-up criterion for the production of Pickering emulsions. The use of the Weber number, Reynolds number, and tip speed as scale-up criteria resulted in higher diameters with the largest scale while the opposite tendency was observed with circulation time and energy dissipation. The best scale-up was obtained with the energy dissipation rate and tip speed, suggesting that the suitable scale-up exponent would be between 2/3 (scale-up exponent with the energy dissipation rate) and 1 (scale-up exponent with the tip speed).

The last objective was, based on the conclusions of the second paper, to find a proper scaling criterion, explain it and finds its limitations. While the main difference regarding the scaling procedure was highlighted in the previous objective, this last section defined a scaling rule for Pickering emulsions that could be applied to systems that have been tested. Furthermore, the scaling method was validated on a pilot scale of 250 liters thus reaching a scaling factor of 1000 which is uncommon in the literature. We previously showed that solid-stabilized emulsions cannot be scaled using conventional emulsion scaling rules. A 0.8 scaling exponent was found to be suitable for scaling SSE processes, indicating that a combination of criteria is more appropriate than a single criterion as with a standard emulsification. This finding was validated using diluted and concentrated emulsions and a wide range of oil viscosities (10 to 200 cSt), particle sizes, and coverage potentials. The scaling exponent was then challenged using a 250 L pilot tank and proved to be a suitable scaling criterion for Pickering emulsions in that it can correctly predict the required rotational speed over a scaling factor of 1000. To better understand the significance of this new scaling exponent, free particle systems were also investigated. The presence of particles reduced coalescence efficiency by reducing the collision frequency between droplets.

# TABLE OF CONTENTS

# LIST OF TABLES

# LIST OF FIGURES

# LIST OF APPENDICES

# LIST OF SYMBOLS AND ABBREVIATIONS

## SYMBOLS

| | |
|---|---|
| A | Surface – in $m^2$ |
| $A_H$ | Hamaker constant – in *Joules* |
| $A_{cov}$ | Coverage potential – in $m^2$ |
| $A_{gen}$ | Interface generation potential – in $m^2$ |
| $A_{th}$ | Theoretical coverage potential – in $m^2$ |
| $\theta_{ij}$ | Contact angle at an interface formed with fluid *i* and *j* (wettability) – in ° |
| $\phi_d$ | Dispersed phase volume fraction – in *%* |
| cSt | Centistokes |
| $d_{32}$ | Sauter mean diameter – in $\mu m$ |
| $d_{Vi}$ | *i*% of the droplets (or particles) are of sizes less than that diameter – in $\mu m$ |
| D | Separation distance AND impeller diameter – both in m |
| E | Energy – in *J* |
| $E_{col}$ | Collision efficiency – in % |
| $E_{TPCL}$ | Three-phase contact line efficiency – in % |
| $E_{Att}$ | Attachment efficiency – in % |
| $E_{cov}$ | Coverage efficiency – in % |
| $\varepsilon$ | Energy dissipation rate – in $W/m^3$ |
| $f_n(d_i)$ | Number frequency of droplet (or particle) of diameter $d_i$ |
| $f_v(d_i)$ | Volume frequency of droplet (or particle) of diameter $d_i$ |
| $F_{vdW}$ | van der Waals force – in Newtons |
| $G^0$ | Gibbs standard surface free energy – in J/mole |

| | |
|---|---|
| $k_H$ | Consistency index |
| $k_s$ | Metzner constant |
| L | Liter |
| $\alpha$ | Power-law exponent |
| $\gamma_{ij}$ | Interfacial tension between fluid *i* and *j* – in *N/m* |
| $\gamma_{eff}$ | Effective shear rate – in $s^{-1}$ |
| mL | Mililiters |
| N | Impeller speed – in rpm |
| $N_p$ | Impeller power number |
| $n$ | Number of droplets (or particles) |
| $\rho_i$ | Density of component *i* – in $kg/m^3$ |
| R | Particle radii – in m |
| $S^0$ | Standard entropy – in J/mole/K |
| St | Stokes numbers |
| $\sigma$ | Surface tension – in N/m |
| T | Temperature AND tank diameter – in K and m, respectively |
| $\tau$ | Shear strees – in Pa |
| $\tau_0$ | Yield strees – in Pa |
| $V_D$ | Dispersed phase volume – in $m^3$ |
| $V_C$ | Continuous phase volume – in $m^3$ |
| $\mu_D$ | Dispersed phase viscosity – in Pa.s |
| $\mu_C$ | Continuous phase viscosity – in Pa.s |

# ABBREVIATIONS

| | |
|---|---|
| AFM | Atomic Force Microscopy |
| DHR | Double helical ribbon |
| DLVO | Derjaguin, Landau, Verwey and Overbeek |
| HLB | Hydrophilic-lipophilic balance |
| O/W | Oil-in-water |
| PBT | Pitched-blade turbine |
| PTFE | Polytetrafluoroethylene |
| PVM | Particle vision microscope |
| Re | Reynolds number |
| RT | Rushton turbine |
| SEM | Scanning electron microscope |
| SSE | Solid-stabilized emulsion |
| TPCL | Three-phase contact line |
| We | Weber number |
| W/O | Water-in-oil |

# CHAPTER 1 INTRODUCTION

*The objective of Chapter 1 is the contextualization of this project. Basics, such as emulsion preparation, characterization, and stabilization, are presented as well as the general focus of this thesis.*

## 1.1 What is an emulsion?

The easiest answer would be that an emulsion is a stable dispersion of two (or more) immiscible fluids. The best-known example of a dispersion is the mixing of water and olive oil. Emulsions are found in numerous applications such as food (ex. mayonnaise, vinaigrette, milk), pharmaceutical (ex. drug delivery), cosmetic (ex. skincare, sunscreen) and others (ex. paint, bitumen). Oil-in-water emulsions have the general creamy (ex. cream) consistency while water-in-oil emulsions have a greasy texture (ex. butter). They are not only encountered as end-products but also as a possible problem such as water droplets in crude oil (Fig. 1-4). In that case, for example, the objective would be to destabilize, i.e. separate, the emulsion to avoid further processing problems being corrosion and increased energy consumption due to the presence of water.

During a dispersion process, one fluid will occupy the role of the dispersed phase (as droplets or bubbles) and the second fluid will be surrounding the dispersed phase, i.e. continuous phase. However, maintaining droplet stability against coalescence will require the use of an emulsifying agent or stabilizer resulting in an emulsification process. Without it, the fluid dispersion tends to get to its most thermodynamically stable state, i.e. the smaller contact area between the liquids as soon as the energy input is stopped. It will result in a phase separation (Fig. 1-1).

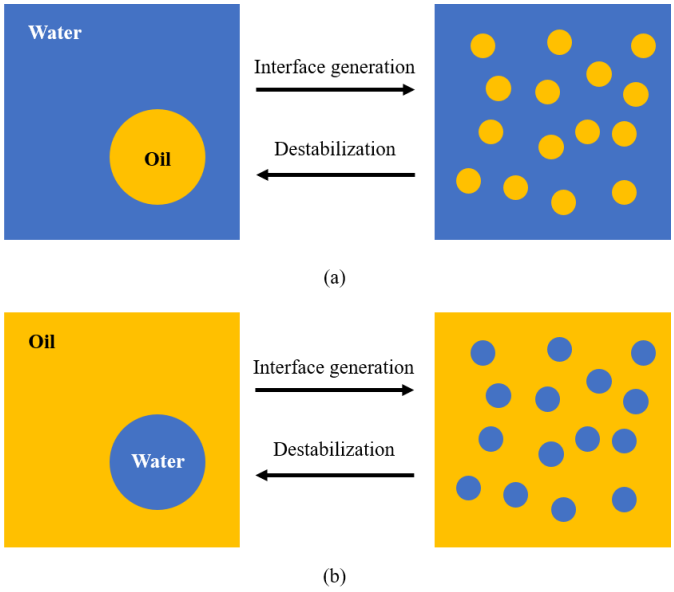


Figure 1-1 – Formation and destabilization of a (a) oil-in-water and (b) water-in-oil dispersion [taken and adapted from Tadros (2013)]

## 1.2 How to characterize an emulsion?

### 1.2.1 Emulsion type

There are two main possible simple-type assuming an immiscible mixture of water and oil: oil-in-water (O/W) or water-in-oil (W/O). Figure 1-1(a) exhibits an O/W dispersion and Figure 1-1(b) shows a W/O dispersion. It is possible, under certain conditions, to obtain a multiple-type emulsion, i.e. oil-in-water-in-oil (O/W/O) or water-in-oil-in-water (O/W/O). As it will be described in section 2.2.2, emulsion type is dictated by parameters such as the particle wettability (contact angle, $\theta$) in case of Pickering emulsions or the hydrophilic-lipophilic balance (HLB) in case of surface-active agents, oil polarity and water pH.

### 1.2.2 Dispersed phase fraction

Emulsions are also classified according to their dispersed phase volume fraction ($\phi_d$ in Equation 1.1).

$$\phi_d = \frac{V_D}{V_D + V_C} \quad (1.1)$$

where $V_D$ is the dispersed phase volume and $V_C$ is the continuous phase volume, both in $m^3$. With this data, it is possible to determine if an emulsion is diluted, concentrated or in-between. This parameter has a major impact on the processing of emulsions (ex. hydrodynamics) and their transport (rheology) which will be detailed later in this thesis. According to Tsabet (2014), an emulsion is said to be diluted when $\phi_d < 0.01$ and concentrated when $\phi_d > 0.2$.

### 1.2.3 Droplet size and size distribution

Emulsions are also characterized by their droplet size. More than often, droplet size is not uniform, i.e. not monodispersed. In that case, a droplet size distribution analysis is performed to obtain polydispersity data such as $d_{10}$, $d_{50}$, $d_{90}$, and the Span.

$$Span = \frac{d_{90} - d_{10}}{d_{50}} \quad (1.2)$$

Another important droplet size parameter is the Sauter mean diameter ($d_{32}$) because it relates the dispersed phase volume fraction to the interface generated ($A_{gen}$) during emulsification.

$$d_{32} = \frac{6\phi_d}{A_{gen}} = \frac{\sum_{i=1}^{i=m} n_i d_i^3}{\sum_{i=1}^{i=m} n_i d_i^2} \quad (1.3)$$

Droplet and/or particle size distributions are generally presented as histograms with the frequency of each size class. This frequency can be expressed either by number (Equation 1.4) or volume (Equation 1.5).

$$f_n(d_i) = \frac{n_i}{\sum_{j=1}^{m} n_j} \quad (1.4)$$

$$f_v(d_i) = \frac{n_i d_i^3}{\sum_{j=1}^{m} n_j d_j^3} \quad (1.5)$$

Number- and volume-based frequencies should be used depending on what the objective is. Imagine a box containing three golf balls and one basketball and the objective is to obtain a size distribution of the whole system (golf balls plus the basketball). Using a number-based frequency, the distribution will be more representative of the golf balls because there are three times more of them than the basketball. However, using a volume-based frequency will result in a distribution more representative of the basketball. How this relates to solid-stabilized emulsions? In this type of emulsions, there are droplets and free particles in suspension in the sample. In order to get a size

distribution which represents the droplets, it is necessary to use a volume frequency. Number-based frequency will exhibit a size distribution according to free particles in the system.

## 1.3 How to achieve stability?

The equilibrium between the fluids is achieved when minimizing Gibbs free energy thus reducing the contact area (Equation 1.7). Equation 1.7 is the simplified form of Equation 1.6 (Gibbs-Deuhem) for a system at constant temperature and composition. Dispersions are not thermodynamically stable systems. Therefore, stopping power input or not using a stabilizer (or emulsifying agent) will end in phase separation, i.e. smallest contact area possible.

$$dG^0 = -S^0 dT + A d\gamma + \sum n_i d\mu_i \quad (1.6)$$

$$\gamma = \left(\frac{\partial G^0}{\partial A}\right)_{T,n_i} \quad (1.7)$$

where $G^0$ is the surface free energy (in $J/mol$), $S^0$ is the entropy (in $J/mol.K$), $A$ is the surface (in $m^2$), $\gamma$ is the interfacial tension (in $N/m$), $n_i$ is the number of moles of the component $i$ and $\mu_i$ is the chemical potential of the component $i$.

Molecules that are in the bulk phase of the fluid are under equal forces from all sides. However, molecules at the interface are under unequal inward attractive forces. This explains the spherical shape of droplets. Table 1-1 presents the surface and interfacial tension of liquids against water.

Table 1-1 – Surface and interfacial tensions for liquids with water [taken from Shaw (1991)]

| *Liquid* | *Surface tension (mN/m)* | *Interfacial tension (mN/m)* |
|---|---|---|
| *Water* | 72.8 | N/A |
| *Benzene* | 28.9 | 35.0 |
| *n-Octanol* | 27.5 | 8.5 |
| *n-Hexane* | 18.4 | 51.1 |

### 1.3.1 Surfactants (surface active agents)

Surfactants are the most commonly used emulsifying agents. They stabilize droplets by reducing the interfacial tension between the fluids. They are molecules composed of a hydrophobic tail having an affinity with the oil (non-polar) phase and a hydrophilic head having an affinity with the aqueous (polar) phase (Fig. 1-2). Also known as amphiphilic molecules, they reduce interfacial tension by gathering at the interface. The hydrophilic-lipophilic balance (HLB), introduced by Griffin (1949), defines the ratio of hydrophilic to lipophilic parts of the molecule.

$$HLB = 20 \cdot \left(\frac{Molar\ weight\ of\ the\ hydrophilic\ part}{Molar\ weight\ of\ the\ molec0ule}\right) \qquad (1.8)$$

It varies from 0 to 20 where 0 is obtained for a completely hydrophobic product and 20 for a fully hydrophilic product. The HLB is calculated using Equation 1.8.

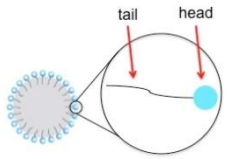


Figure 1-2 – Surfactant configuration: hydrophobic tail and hydrophilic head [taken and adapted from Tsabet (2014)]

Table 1-2 presents the common classification of surfactants along with their advantages and disadvantages and some interesting applications.

Table 1-2 – Classification of surface-active agents [taken and adapted from Shaw (1991)]

| *Class of surface-active agents* | *Examples of molecules* | *Advantages/Disadvantages* | *Applications* |
|---|---|---|---|
| *Anionic* | $CH_3(CH_2)_{16}COO^-Na^+$<br>$CH_3(CH_2)_{11}SO_4^-Na^+$ | Cost and performance effective | Shampoos, laundry detergents |
| *Cationic* | $CH_3(CH_2)_{11}NH_3^+Cl^-$<br>$CH_3(CH_2)_{15}N(CH_3)_3^+Br^-$ | Expensive but great germicidal effect | Anti-microbials, anti-fungals |
| *Non-ionic* | $CH_3(CH_2)_{11}(OCH_2CH_2)_6OH$ | Lengths of hydrophilic and hydrophobic groups can be modified | Wetting agent, clearners, polishes |
| *Ampholytic* | Dodecyl betaine | Low toxicity and irritation | Latex paint |

Nevertheless, their use is generally associated with a higher cost and a negative impact on the environment due to their petrochemical origins. Moreover, in certain industrial applications such as skincare, the use of surfactants is often associated with toxicity and irritation. Therefore, an alternative should be considered: the use of solid particles as stabilizers will be the main focus of this thesis.

### 1.3.2 Polymers

Polymers can adsorb at an interface and stabilize liquid-liquid dispersions from coalescence by forming a physical barrier. It is recommended to choose polymers that have hydrophilic and lipophilic portions and to avoid the use of long chains polymers that could cause droplet

flocculation leading to coalescence. (Tsabet, 2014) This stabilizing agent will not be discussed in this document.

### 1.3.3 Solid particles

Without reducing the interfacial tension, solid particles stabilize a droplet by creating a physical barrier around it, which prevents coalescence (destabilization of the emulsion). Solid-stabilized emulsions (SSEs) are also known as *Pickering emulsions* thanks to S.U. Pickering who observed this phenomenon in 1907. (Pickering, 1907) The reader should be aware that despite being called *Pickering emulsions*, it was W. Ramsden who first observed it in 1903. (Ramsden, 1903) Even though the capacity of stabilizing droplets using solid particles was discovered in the early 1900, the interest by the scientific community did not come until the late 20$^{th}$ and the beginning of the 21$^{st}$ century. This interest is due to the development of material science, which led to the production of a wide range of particles. Moreover, the lower cost and the environmentally friendly behavior of this emulsification method have also their share of interest, economically and socially. (Yan et al., 2001) (Aveyard et al., 2002)

Solid particles can contribute to the production of emulsions that are more stable than the surfactant-based ones. They can be recovered after the emulsion destabilization, which is an advantage regarding the particle life cycle. These particles can be obtained from a variety of organic and mineral powders. However, there is a fundamental difference between surfactants and solid particles: the first stabilize emulsions by reducing the interfacial tension between the fluids while the second creates a physical barrier between the phases (Fig. 1-3). This difference suggests that scaling parameters for conventional emulsions cannot suitable for solid-stabilized emulsions.

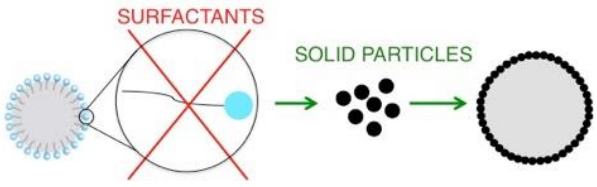


Figure 1-3 – Surfactants replacement with solid particles [taken and adapted from Tsabet (2014)]

## 1.4 Why is there an interest in the use of solid particles?

### 1.4.1 Comparison between surfactants and solid particles

Solid-stabilized emulsions have the advantage of higher resistance against droplet coalescence because the particles irreversibly adsorb at the interface, which renders the emulsion its stability. The strong anchoring of solid particles is due to their affinity to both water and oil, while surfactants need to be amphiphilic. Pickering emulsions are also famous for their "surfactant-free" character enabling them to be attractive to the pharmaceutical and cosmetic industries where surfactants show negative effect due to their toxicity. Another difference resides in the solubilization phenomenon that is absent from SSEs. Indeed, surfactants can aggregate to form micelles, which are soluble. It is not the case when particles aggregate.

Pickering emulsions have also been studied at a laboratory scale for other applications. Research groups have prepared microcapsules, which are interesting for the pharmaceutical industry regarding drug delivery. The biomedical field has also its own interest in SSEs because of their higher stability at freezing temperatures. Surfactant-based emulsions tend to destabilize at freezing temperature while SSEs show stability at low temperatures. Others have prepared porous and composite materials using different methods such as polymerization. Moreover, nowadays, the industries and the society are looking for *greener* alternatives to reach a sustainable development. In this axis, SSEs can be considered *greener* than their surfactant counterpart because of their ability to be recycled. Indeed, using a centrifuge, applying a magnetic or electrical field or changing the particle wettability can break SSEs. This could lead to the recuperation of the particles and their reuse. (Tsabet, 2014)

Furthermore, the reader should be aware that solid- (or particle-) stabilized emulsions can also be an undesirable state such as water droplets in oil (petroleum industry). These water drops have to be removed to reach refining specifications (less than 1% of water) to avoid risks of corrosion (due to soluble salt in the water) and premature catalyst activation. It also prevents the accumulation of water throughout the process. In that case, the main objective will rely on the destruction of the emulsion, i.e. phase separation by particle desorption from the interface.

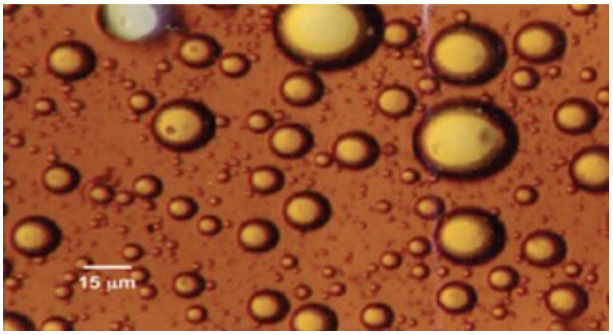


Figure 1-4 – Water emulsified in oil [taken from Amani et al. (2017)]

### 1.4.2 What am I interested at in this project?

Since they have been characterized at the laboratory scale only, solid-stabilized emulsions cannot be produced on an industrial scale following a proper methodology. From an engineering standpoint, this research project will aim to answer the following question: *How solid-stabilized emulsions can be scaled for process design following a methodology soundly based on the physical sciences?* This experimental project will cover oil-in-water emulsions stabilized by solid particles in an intermittent (batch) mode of production using scales ranging from 0.25 liter to a pilot scale of 250 liters. Diluted and concentrated emulsions with oil viscosities ranging from 10 to 5000 cSt will be studied. The effect of particle characteristics (wettability and size), dispersed phase properties (viscosity and concentration) and mixing configuration will also be studied. This project will also include the design of impellers as well as mixing tanks. Finally, this study will explain why, if it is the case, scaling SSEs varies from conventional emulsions. It should be noted that, throughout this document, surfactant-stabilized emulsions are also referred to as conventional emulsions. In the case of liquid-liquid dispersions, no emulsifying agent or stabilizer has been used.

### 1.4.3 Key originality of this thesis

This thesis was completed by doing things differently than what is commonly found in the literature. First and foremost, solid-stabilized emulsions have been so far interesting to researchers regarding their potential end-uses, i.e. applications. However, no interest has been given to the following question: how do we get there, i.e. the processing? In other words, the processing of Pickering emulsions is still lacking. SSEs were assessed from an engineering standpoint. A scaling factor of 1000 has been achieved using two dispersion methods (radial and axial turbines). If the

reader takes a look at the literature under our hand, it will be noticed that this is an element rarely seen in this area of interest.

Another interesting key originality is how problems have been addressed. Throughout this thesis, problems have been solved by decomposing them to their main constituents. Understanding each component of a process is the main key that leads to success solving. In the case of solid-stabilized emulsions, the literature presents these emulsions as a whole rather than a combination of well-known processes: solid suspension followed by a liquid dispersion! This key approach was the main reason for the completion of this thesis and the contribution resulting from it. It was also validated using experimental work.

# CHAPTER 2 LITERATURE REVIEW

*The objective of Chapter 2 is to "set the table" on what has already been subject for investigation and what has not in order to identify remaining scientific gaps from a process engineering point of view.*

## 2.1 A bit of history

Ramsden (1903) and Pickering (1907) introduced particle stabilization at an interface more than a century ago. Solid-stabilized emulsions (SSEs) were named after S.U. Pickering, who published a report on particle stabilized oil-in-water (O/W) emulsions in 1907. Pickering noticed that finely divided solid particles can act as stabilizers. He reported a stable oil-in-water emulsion stabilized by solid particles adsorbed at the surface of paraffin oil droplets. Improved stability is shown in comparison with surfactant-stabilized emulsions. Although the advantages of SSEs are explained quite clearly by Pickering, surfactant-based emulsions were still preferred by the industry. It was not until a few decades ago that SSEs attracted the attention of the scientific field with the development of material science, which brought a wide range of particles.

## 2.2 What has been studied?

### 2.2.1 Pickering emulsions generation process

Since the late 20$^{th}$ and the early 21$^{st}$ century, numerous studies using different types of particles have been dedicated to SSEs at a laboratory scale. The main conclusion was that the emulsion stability results from the formation of a steric barrier around the droplets. (Binks, 2002) In other words, the stabilization process is linked to the formation of a particle network around generated droplets. This stabilization mechanism can be described in three steps (Tsabet, 2014):

(1) Particle approaches and reaches the fluid/fluid interface (film drainage and contact time between particle and droplet)
(2) Particle adsorbs at the interface (through capillary rise)
(3) Formation of a particle network to stabilize droplets

These steps were highlighted through atomic force microscopy (AFM) experiments. Tsabet et al. (2016) investigated the ingredient properties (oil, particles, and water) on particle adsorption

dynamics at fluid/fluid interfaces using steps presented by Figure 2-1. The main conclusion was that a repulsive force is involved during approach and contact steps and an attractive force during adsorption. The ingredients effect on different steps is summarized in Table 2-1.

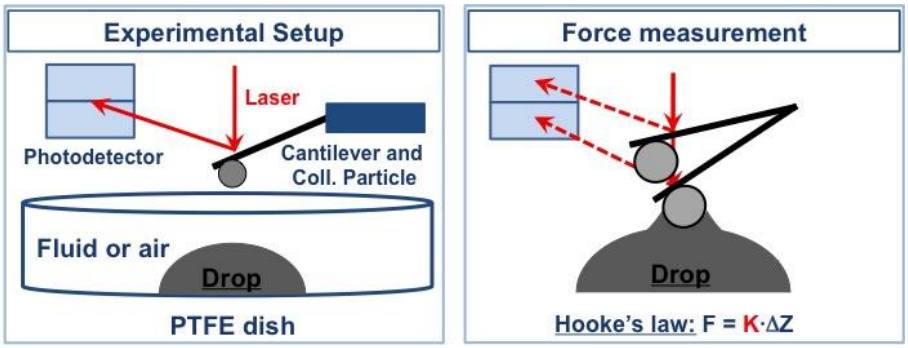


Figure 2-1 – Schematic representation of the AFM setup [taken from Tsabet et al. (2016)]

Table 2-1 – Effect of emulsion properties on the particle adsorption [taken and adapted from Tsabet et al. (2016)]

| *Parameters* | *Particles properties* | *Oil viscosity* | *Water pH & salinity* |
|---|---|---|---|
| *Approach* | Significant impact on these steps | | Significant (Effect on electrostatic double layer force) |
| *Contact* | | Significant | |
| *Adsorption* | | | |
| *Detachment* | | | |
| *Adsorption time* | | Significant | |

#### 2.2.1.1 Particle approaching the fluid-fluid interface

The approach step is when a particle first approaches and reaches the fluid/fluid interface. Many studied the particle/fluid approach and collision. To do so, most of them used a method based on the flow analysis of film drainage between the particle and the interface. (Jones & Wilson, 1978) (Davis et al., 1989) (Chesters, 1991) (Abid & Chesters, 1994) (Saboni et al., 1995) (Jeelani & Hartland, 1994) However, some interactions were not considered at the scale of the particle in this method. These interactions are the following: van der Waals and electrical double layer forces (defined by the DVLO theory which explains the stability of colloidal suspensions) and non-DVLO forces such as hydration, hydrodynamic, hydrophobic and steric forces. Van der Wall forces operate at an atomic and molecular level. Nevertheless, it can be defined at a macroscopic level using the Hamaker constant ($A_H$), which can be obtained using AFM measurements. Table 2-2 presents typical values of this constant. The van der Waals force ($F_{vdW}$) expression between two spheres is determined using equation 2.1. (Butt et al., 2005)

$$F_{vdW} = -\frac{A_H}{6D^2} \cdot \frac{R_1 R_2}{R_1 + R_2} \qquad (2.1)$$

where $R_1$ and $R_2$ are the radii of both interacting bodies (spheres in this case) and $D$ is their separation distance. $R_i$ and $D$ are expressed in meters and the Hamaker constant in Joules.

Table 2-2 – Hamaker constant ($A_H$) for different materials [taken and adapted from Butt et al. (2005) and Tsabet (2014)]

| *Material 1* | *Material 2* | *Medium* | *$A_H$ (x $10^{-20}$ J)* | *Reference* |
|---|---|---|---|---|
| *Teflon* | Teflon | Air | 3.9 | Drummond et al. (1996) |
| *$SiO_2$* | $SiO_2$ | Water | 1 | Biggs et al. (1997) |
| *$SiO_2$* | Au | Water | 12-15 | Hillier et al. (1996) |
| *$SiO_2$* | Mica | Water | 1.2 | Vakarelski et al. (2000) |

As for the electrostatic double layer force, it was shown taking place between bodies in liquid media with a high dielectric constant. It is present due to surface dissociation or from the adsorption of free charges in the aqueous medium. (Liang et al., 2007) These forces can be observed in colloidal dispersions. At low salt concentrations, there is a formation of a double layer charge resulting in a repulsive interaction. When increasing the salt concentration, an attractive interaction appears resulting in particle coagulation.

Non-DLVO forces appear at short ranges (1-3 nm) and can be much larger than DLVO forces. Appendix A presents these forces.

#### 2.2.1.2 Particle adsorption at the fluid-fluid interface

It starts when the liquid film between the particles and the droplet is completely drained and the particle collides the interface, and it finishes when the particle reaches its equilibrium position at the interface. The final position of a particle can be deduced from its contact angle, i.e. wettability ($\theta$ in °). This step can be assessed using two approaches: (A1) the free energy or (A2) the force balance approach. (Binks and Horozov, 2006) The free energy approach (A1) consider particle adsorption only if there is a reduction in the interfacial energies of particles (Equation 2.2) and droplets (Equation 2.3) after adsorption. (Tsabet, 2014)

$$E_{p/interf} < E_{p/disp} \quad (2.2)$$

$$E_{d/with\ p} < E_{d/without\ p} \quad (2.3)$$

It also assumes that the equilibrium position at the interface is reached when,

$$\frac{dE_{p/interf}}{d\theta} = 0 \quad (2.4)$$

$$\frac{dE_{d/with\ p}}{d\theta} = 0 \quad (2.5)$$

where $E_{p/interf}$ is the interfacial energy of the particle at the interface, $E_{p/disp}$ is the interfacial energy of the particle in the bulk phase (when dispersed), $E_{d/with\ p}$ is the interfacial energy of the droplet with adsorbed particles and $E_{d/without\ p}$ is the interfacial energy of the droplet without particles. Interfacial energies are expressed in Joules/$m^2$.

The force balance approach (A2) assumes that equilibrium is reached when the sum of all the external forces is equal to zero. These forces are the capillary (Equation 2.6 from Princen (1969) and Rapacchietta et al., (1977)), the buoyancy (Equations 2.7 and 2.8), the hydrostatic (Equation 2.9), and the gravity (Equation 2.10). Joseph et al. (2003) and Singh et al. (2005) did the force balance using the following equations:

$$F_{\gamma/z} = \gamma_{OW_z}(2\pi r_c) = 2\pi r\, \gamma_{OW}\, sin\, \phi_c\ \sin\ (\theta + \phi_c) \quad (2.6)$$

$$F_{B/w} = \rho_w V_{pw} g = \frac{\rho_w g \pi r^3\ (2 - 3\ cos\phi_c + cos^2\phi_c)}{3} \quad (2.7)$$

$$F_{B/o} = \rho_o g\ \left(V_p - V_{pw}\right) = \frac{\rho_o g \pi r^3\ (2 + 3cos\phi_c - cos^2\phi_c)}{3} \quad (2.8)$$

$$F_p = -(\rho_o - \rho_w)\ g\ z_c\ (r\ sin\phi_c)^2 \quad (2.9)$$

$$F_g = \frac{\rho_p g 4\pi r^3}{3} \quad (2.10)$$

Thus, the particle equilibrium position (Equation 2.11) can be deduced using the force balance approach.

$$\sin\phi_c\ \sin(\theta + \phi_c) = \frac{g r^2(\rho_o - \rho_w)}{6\gamma_{OW}} \cdot \left(4 \cdot \frac{\rho_p - \rho_o}{\rho_w - \rho_o} - (1 - \cos\phi_c)^2 \cdot (2 - \cos\phi_c) + \frac{z_c}{r} sin^2\phi_c\right) \quad (2.11)$$

#### 2.2.1.3 Particles form a network at the fluid-fluid interface

The third and final step is the formation of a particle network. Emulsion stability depends on the network compactness and number of layers at the interface. Some studies showed that particles must form at least one layer to prevent destabilization. (Yan et al., (1994, 1995)) Others showed that stable solid-stabilized emulsions could be generated without covering the entire interface. (Midmore, 1998) (Vignati et al., 2003) Therefore, there are many possible network configurations that can stabilize emulsions. They can be divided into five categories (Lopetinsky et al., 2006) (Binks and Horozov, 2006) (Tsabet, 2014):

1. Droplets are entirely covered (close-packed hexagonal particles) (Figure 2-2a)
2. Droplets are entirely covered (with a common layer between two droplets) (Figure 2-2b)
3. Partial particle flocculation (Figure 2-2c)

4. Particle aggregation at the interface (Figure 2-2d)
5. Particles form a 3D network (Figure 2-2e)

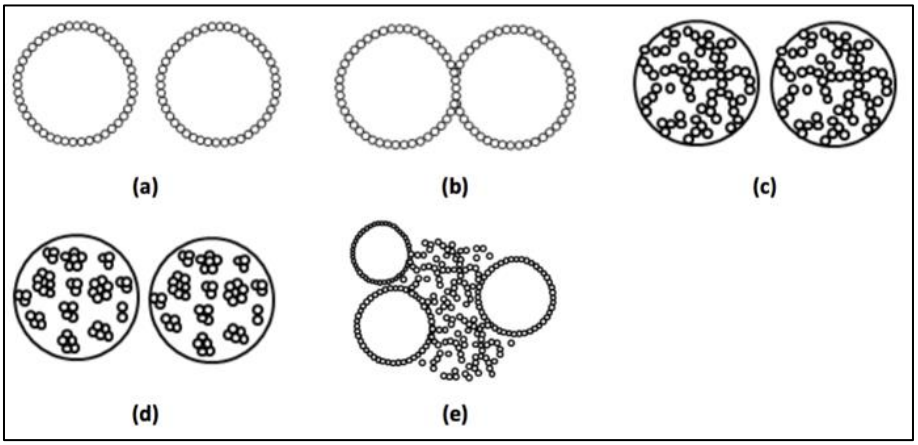


Figure 2-2 – Particle network configurations [taken from Tsabet (2014)]

### 2.2.2 Properties of Pickering emulsions

One important research angle was the investigation of Pickering emulsion properties. Similarly, to surfactant emulsions, Pickering emulsion type, size distribution, stability, and rheology were widely considered. Table 2-3 presents a summary of studies related to the impact of the properties of involved parameters on solid-stabilized emulsions.

Results are showing that particle wettability defining the particle affinity for both fluids (i.e. water and oil) is a central parameter that is affecting both emulsion type and stability through the control of particle position at the interface (Fig. 2-3). The contact angle giving this position can be determined using equation 2.12 from Hey and Kingston (2006),

$$\cos\theta_{ow} = \frac{\gamma_{so} - \gamma_{sw}}{\gamma_{ow}} \quad (2.12)$$

where $\gamma_{so}$ is the interfacial tension between the solid particle and the oil phase, $\gamma_{sw}$ is the interfacial tension between the solid particle and the water phase and $\gamma_{ow}$ is the interfacial tension between the oil and water phases. Interfacial tension is expressed using Newton per meter (N/m), which is equivalent to $J/m^2$.

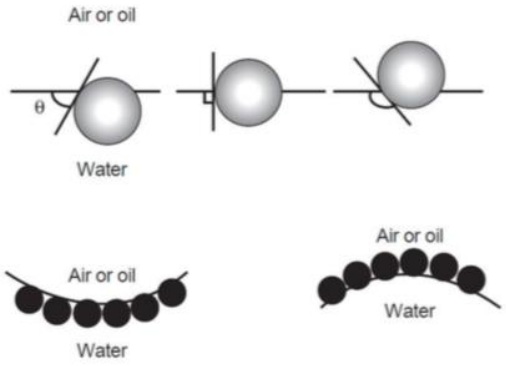


Figure 2-3 – Contact angle for particles adsorbed at an interface [taken from Langevin et al. (2004)]

Zhou et al. (2011) proposed the following equation 2.13 in order to determine the oil-water contact angle ($\theta_{ow}$) knowing the air-oil and air-water contact angles, respectively $\theta_{ao}$ and $\theta_{aw}$.

$$\cos\theta_{ow} = \frac{\gamma_{aw}}{\gamma_{ow}}\cos\theta_{aw} - \frac{\gamma_{ao}}{\gamma_{ow}}\cos\theta_{ao} \quad (2.13)$$

Contact angles smaller than 90° will tend to form o/w emulsions because of their hydrophilic affinity (ex. metal oxides) and vice-versa for contact angles bigger than 90° (ex. silica). (Binks, 2002) Kruglyakov et al. (2004) proposed a relationship between the particle contact angle and the surfactant HLB (Equation 2.14) which makes it easier to compare these two stabilizers.

$$HLB_{particle} = \left(\frac{1 + cos\,\theta_{ow}}{1 - \cos\theta_{ow}}\right)^2 \quad (2.14)$$

When a particle sits at an oil droplet interface, for example, it forms a steric barrier and is locked in place. Levine et al. (1989) presented an expression to quantify the required energy (*E*) to desorb, i.e. extract a particle from a given interface (Equation 2.15).

$$E = \pi r^2 \gamma_{OW} \cdot (1 \pm \cos\theta_{ow})^2 \quad (2.15)$$

where $r$ is the particle radius (in m). The "+" sign is used when particles are desorbed into the oil phase and vice-versa with the "-" sign. The higher desorption energy needed to destabilize Pickering emulsions is in contrast with surfactant-based emulsions where surfactants adsorb and desorb at a faster scale. (Binks, 2002)

Table 2-3 – Pickering emulsion properties: type, size, and stability [taken from Tsabet (2014)]

| *Emulsion property* | *Parameter* | *Reference* |
|---|---|---|
| *Emulsion type*<br>*Controlled by particle affinity to oil and water* | Particle wettability<br>Hydrophilic: O/W, Hydrophobic: W/O<br>Hydrophilic + hydrophobic: O/W/O or W/O/W | N. Yan et al. (2001)<br>B.P. Binks et al. (2000, 2005)<br>R. Aveyard et al. (2003) |
| | Oil polarity<br>Oil/particle affinity | B.P. Binks et al. (2002, 2005)<br>K. Golemanov et al. (2006)<br>J. Frelichowska et al. (2009) |
| | Aqueous phase pH<br>Particle wettability is affected by the mean surface charges and/or surfactants | N. Yan et al. (1996, 1997)<br>B.P. Binks et al. (2006) |
| *Emulsion size*<br>*Droplet size is reduced by* | Particle size<br>Decreasing particle size | B.P. Binks et al. (2001)<br>S. Tarimala et al. (2004) |
| | Particle concentration<br>Increasing particle concentration | S. Arditty et al. (2003) |

Table 2-3 – Pickering emulsion properties: type, size, and stability [taken from Tsabet (2014)] (continued)

| *Emulsion property* | *Parameter* | *Reference* |
|---|---|---|
| *Emulsion stability*<br>*Emulsion stability is improved by* | Particle wettability<br>Contact angle ~90° | B.P. Binks et al. (2000, 2005)<br>R. Aveyard et al. (2003) |
| | Particle size distribution<br>Using small monodisperse particles | S. Tarimala et al. (2004) |
| | Particle concentration<br>Increasing particle concentration | S. Arditty et al. (2003)<br>B.P. Binks et al. (2003, 2004, 2005) |
| | Salt concentration<br>Increasing the salt concentration to promote partial particle flocculation | B.P. Binks et al. (2005, 2006)<br>T.S. Horozov et al. (2007) |
| | Oil viscosity<br>Decreasing oil viscosity | K. Golemanov et al. (2006)<br>C.-O. Fournier al. (2009) |
| | Particle shape<br>Increasing the particle aspect ratio | B. Madivala et al. (2009) |

While the effect of the formulation on emulsion properties has been widely investigated, the processing was much less considered. This aspect was investigated by some members of the URPEI at Polytechnique Montreal and interesting findings have been reported in the literature. (Fournier et al., 2009) (Reyjal et al., 2013) (Tsabet and Fradette, 2015a, 2015b, 2016) (Wan and Fradette, 2017) Tsabet et al. (2015) studied the combined effect of the impeller speed and oil viscosity, as well as the effect of the impeller speed and particle concentration on emulsion size and stability. They proposed a correlation to predict the droplet Sauter mean diameter from operating conditions. Starting by comparing the interface generation potential ($A_{gen}$) to the particle coverage potential ($A_{cov}$), the proposed model associated efficiency to each stabilization step to determine the effectively covered interface:

$$A_{th} = Min\left(A_{gen}, A_{cov}\right) \quad (2.16)$$

$$A_{Eff} = A_{Th} \cdot (E_{col} \cdot E_{TPCL} \cdot E_{Att} \cdot E_{cov}) \quad (2.17)$$

The first efficiency is the particle/droplet collision efficiency ($E_{col}$). It is related to the film drainage process between a particle and a droplet during approach. The second efficiency is the three-phase contact line (TPCL) efficiency ($E_{TPCL}$) related to the probability of formation of a stable meniscus around the adsorbed particle. The particle attachment efficiency ($E_{Att}$) is the third efficiency. It is a function of attachment and detachment forces exerted on the particle. It defines the particle stability at the interface. The last efficiency is the droplet coverage efficiency ($E_{cov}$). It defines the system capacity to prevent coalescence through the formation of a particle network around the droplets. Details on the calculation of these efficiencies are presented in Appendix B. The model was validated in a 1 L vessel for a wide range of oil viscosities (20 – 5000 cSt), Weber numbers (100 – 600) and coverage potentials (5 – 20 $m^2$). Figure 2-4(a) presents a comparison between the model prediction and the effectively covered interface obtained experimentally for different oil viscosities. Figure 2-4(b) presents the same comparison, but for different interface coverage potentials, also known as the theoretically covered interface.

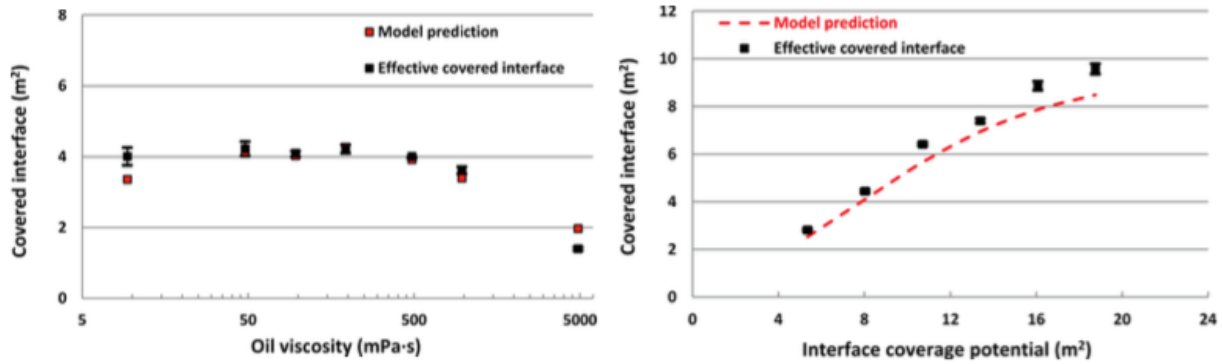


(a) (b)

Figure 2-4 – Comparison between the correlation and experimental results for different (a) oil viscosities and (b) interface coverage potentials [taken from Tsabet et al. (2015)]

Tsabet et al., (2015) determined optimal conditions to obtain the smallest and narrowest droplet size distribution. Impeller speed and emulsification time results showed that the shear level at the impeller zone, the energy dissipation rate and the circulation time are the important parameters regarding stabilization.

Rheological behavior of SSEs was also considered by several studies. Results showed a shear-thinning behavior with a yield stress following the Herschel-Bulkley model (Herschel and Bulkley, 1926):

$$\tau = \tau_0 + k_{HB}\,\dot{\gamma}^{\alpha} \quad (2.18)$$

where $\tau$ is the shear stress (in Pa), $\tau_0$ is the apparent yield stress (in Pa), $k_{HB}$ is the consistency index, $\alpha$ is the power law index and $\dot{\gamma}$ is the shear rate (in $s^{-1}$).

Torres et al. (2007) showed that the yield stress, the consistency, and the power law index are sensitive to particles concentration. Thixotropy and viscoelasticity were also reported. (Torres et al. 2007) (Braisch et al., 2009) (Simon et al., 2010) It was also highlighted that the rheological behavior is closely linked to the particle concentration and aggregation and to the phase's rheology. Table 2-4 summarizes relevant works and their results. The emulsion viscosity increases when the dispersed phase fraction is increased due to the increase in the number of droplet and aggregate formation. The increase of the dispersed phase fraction induces a transition towards a rheofluidifier behavior with thixotropic or viscoelastic effects.

Table 2-4 – Studies on Pickering emulsions rheology [adapted from Tsabet (2014)]

| *Reference* | *System* | *Particle* |
|---|---|---|
| *Midmore (1998)* | Concentrated (75%) carnation oil in water | Partially flocculated silica particles |
| *Torres et al. (2007)* | Hexane in water | Silica, bentonite or kaolin |
| *Braisch et al. (2009)* | Concentrated corn oil in water | Silica nanoparticles |
| *Simon et al. (2010)* | Water in decane or decane in water | Hydrophobic or hydrophilic silica particles |

### 2.2.3 Applications of Pickering emulsions

Solid-stabilized emulsions can be used to generate new materials either as a final or intermediate product. A literature review by Leal-Calderon et al. (2008) presented the potential of SSEs towards new materials. Table 2-5 presents a summary of this review.

Table 2-5 – Potential applications of SSEs [adapted from Leal-Calderon et al. (2008)]

| *Application* | *How?* | *Advantage/Application* | *Reference* |
|---|---|---|---|
| *Monodisperse emulsions*<br>*(Fig. 2-5)* | Limited coalescence method: producing excess of interface compared to the amount of available solid particles | (1) Surfactant-free monodisperse emulsions<br>(2) Tuneable mean size (μm to cm)<br>(3) Simple and multiple emulsions<br>(4) Long stability (over months) | Arditty et al. (2003, 2004) |
| *Stimulus-responsive materials* | Use of stimulus-responsive particle which acts when modifying a parameter such the pH, temperature, ionic strength, magnetic field, etc. | (1) Destabilizing an emulsion "on-demand"<br>(2) Drug delivery opportunities | Fujii et al. (2004, 2005a, 2005b, 2006)<br>Binks et al. (2006)<br>Ngai et al. (2005, 2006)<br>Melle et al. (2005) |
| *Naturally occurring particles used for SSEs* | Use of bacteria and virus particles (also known as bio-nanoparticles) | (1) Biocompatibility<br>(2) Monodisperse particles<br>(3) High stability | Dorobantu et al. (2004)<br>Russell et al. (2005)<br>Binks et al. (2005) |
| *Permeable capsules*<br>*(Fig. 2-6)* | Completely cover droplet with particles. Then, locking the particles together by either aggregation, polymer adsorption or particle fusion (sintering). Use centrifugation with a solvent comparable to what is inside droplets | (1) Functional foods<br>(2) Drug delivery for biomedical applications<br>(3) Controllable permeability | Dinsmore et al. (2002)<br>Hsu et al. (2005)<br>Simonic et al. (2004)<br>Prestidge et al. (2006) |

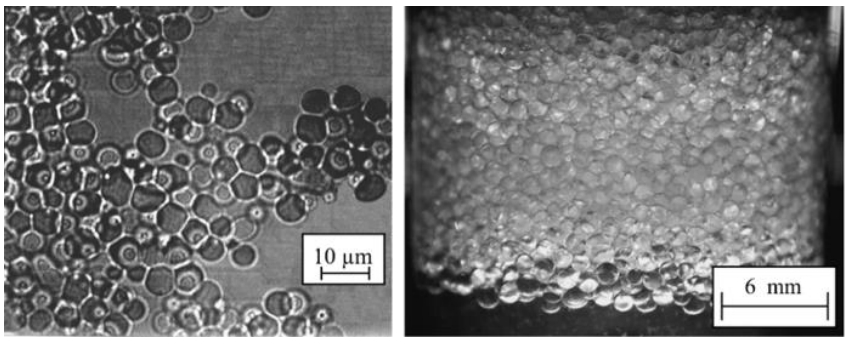


Figure 2-5 – Monodisperse O/W emulsions using limited coalescence [taken from Arditty et al. (2003 and 2004)]

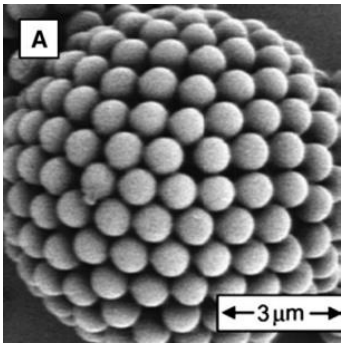


Figure 2-6 – SEM image of a capsule [taken from Hsu et al. (2005)]

### 2.2.4 Scaling Solid-Stabilized Emulsions

Similar to most mixing processes involving several mechanisms, the definition of a scaling rule for solid-stabilized emulsions is not a straightforward operation and no work was dedicated to this aspect. For conventional emulsions, criteria were defined depending on the system (Table 2-6).

The studies on scaling conventional dispersions and emulsions are useful in the sense that they will be considered as a starting point for this project. Indeed, as it will be presented later, conclusions drawn from these studies will be tested on Pickering emulsions. The results generated from this starting point will be helpful in the orientation that this project took.

Table 2-6 – Studies on the scaling of conventional emulsions

| *Reference* | *Emulsification system* | *Geometrical parameters* | *Formulation & Physical properties* | *Characterization method* | *Scale-up factor* | *Recommended rule* |
|---|---|---|---|---|---|---|
| *Podgórska et al., 2001* | Stirred tanks with 6-blades Rushton turbine | $T_1$ = 0.15 m<br>T/D = 1.49//2.11//3 | $\phi_d = 0.05$<br>$\mu_D/\mu_C = 1.3$ &<br>$\rho_D/\rho_C = 1.03$<br>$\sigma = 0.034$ N/m | Numerical analysis based on solving the population balance equation to obtain droplet size distribution | $T_i/T_1$ = 3.33//6.66//16.66 | Constant P/V and average circulation time without geometrical similarity |
| *Podgórska, 2005* | Baffled stirred tanks with a 6-blades Rushton turbine | $T_1$ = 0.15 m<br>T/D = 3 | $\phi_d = 0.15$<br>$\mu_D/\mu_C = 1$ &<br>$\mu_D/\mu_C = 500$<br>$\rho_D/\rho_C = 1$<br>$\sigma = 0.04$ N/m | Numerical analysis based on solving the population balance equation to obtain droplet size distribution | $T_2/T_1$ = 6.66 | Constant P/V and average circulation time without geometrical similarity |

Table 2-6 – Studies on the scaling of conventional emulsions (continued)

| *Reference* | *Emulsification system* | *Geometrical parameters* | *Formulation & Physical properties* | *Characterization method* | *Scale-up factor* | *Recommended rule* |
|---|---|---|---|---|---|---|
| *Capdevila et al., 2010* | Stirred tanks with a helix mixer | $V_{tank1}$ = 100 mL<br>$D_1$ = 11 mm | Highly concentrated W/O emulsions<br>Oil: decane, dodecane, hexadecane<br>% Water = 91 - 95 wt%<br>Stabilizer: Span 80<br>S:O (wt./wt.) = 15:85 - 29:71 | Emulsion stability: Back scattering light analysis (Turbisoft MA2000)<br>Droplet size distribution: Optical microscopy (Zeiss Axiovert 100 A)<br>Emulsion rheology: HAAKE RS150 rheometer | $V_{tank1}$ = 100 mL<br>$V_{tank2}/V_{tank1}$ = 6.85 | No dimensionless variables commonly used in scale-up studies, such as the Reynolds number, was suitable for this system |

Table 2-6 – Studies on the scaling of conventional emulsions (continued)

| *Reference* | *Emulsification system* | *Geometrical parameters* | *Formulation & Physical properties* | *Characterization method* | *Scale-up factor* | *Recommended rule* |
|---|---|---|---|---|---|---|
| *(Suárez et al., 2013)* | Flat metallic membranes in baffled & unbaffled tanks with different impellers (2 Paddle impellers & 1 marine propeller) | Paddle impellers: $D_1$ = 60//90 mm<br>Marine propeller: $D_1$ = 60 mm<br>D/T = 0.33 & D/T = 0.5<br>H/T = 1<br>$D_{impeller-membrane}$ = 5 mm | O/W emulsions (1.5 wt%)<br>Continuous phase: Water with viscosity modifier (CMCNa)<br>Dispersed phase: Food-grade extra virgin olive oil ($\mu_D$ = 51 mPa·s, $\rho_D$ = 886 kg/m$^3$)<br>Stabilizer: Tween 20® (2 wt%) | Droplet size distribution: Laser diffraction technique (Malvern Mastersizer S) | $T_i/T_1$ = 1.5//2.25 | Constant impeller tip speed with geometrical similarity |

Table 2-6 – Studies on the scaling of conventional emulsions (continued)

| *Reference* | *Emulsification system* | *Geometrical parameters* | *Formulation & Physical properties* | *Characterization method* | *Scale-up factor* | *Recommended rule* |
|---|---|---|---|---|---|---|
| *(May-Masnou et al., 2013)* | Glass jacketed vessels Agitated with a three-level P-4 pitched blade impeller | $T_1$ = 50 mm<br>D/T = 0.9 & H/T = 0.8 | Highly concentrated W/O emulsions<br>Continuous phase: Dodecane<br>Dispersed phase: Milli-Q water ($\phi_d = 0.9$)<br>Stabilizer: Span 80® (HLB = 4.3) | Droplet size distribution: Optical microscopy (Optika) | $T_i/T_1 = 2$ | Low surfactant concentration: $N_2 = N_1 (D_1/D_2)^{0.5}$<br>High surfactant concentration: $N_2 = N_1 (D_1/D_2)^{0}$ |

Table 2-6 – Studies on the scaling of conventional emulsions (continued)

| *Reference* | *Emulsification system* | *Geometrical parameters* | *Formulation & Physical properties* | *Characterization method* | *Scale-up factor* | *Recommended rule* |
|---|---|---|---|---|---|---|
| *(May-Masnou et al., 2014)* | Glass jacketed vessels Agitated with a three-level P-4 pitched blade impeller | $T_1$ = 50 mm<br>D/T = 0.9 & H/T = 0.8 | Highly concentrated W/O emulsions<br>Continuous phase: Dodecane<br>Dispersed phase: Milli-Q water ($\phi_d$ = 0.9)<br>Stabilizer: Span 80® (HLB = 4.3) | Emulsion stability: Back scattering light analysis (Turbisoft MA2000)<br>Droplet size distribution: Optical microscopy (Optika)<br>Emulsion rheology: HAAKE Mars III rheometer | $T_i/T_1$ = 2//4 | Constant P/V with geometrical similarity |

## 2.3 What has not been studied?

Since the interest in the use of solid particles for liquid-liquid stabilization is still recent, studies were mainly focused on the production and study of these emulsions at a laboratory scale. So far, research aimed at evaluating emulsion stability, according to different parameters: particles, water and oil characteristics. However, from an engineering point of view, the processing and scaling have not yet been covered. Indeed, a literature review reveals that no methodology for scaling SSEs has been established. The concept of scaling is important in engineering since it allows the large-scale production of formulations developed in the laboratory. It was covered by the literature regarding conventional liquid-liquid mixtures (with and without surfactant) as presented in Table 2-6. Paul et al. (2004), a reference book in the field of mixing presented different scaling criteria for conventional blends (Table 2-7).

Table 2-7 – Scaling criteria for conventional liquid-liquid dispersions [taken and adapted from Paul et al. (2004)]

| *Parameter* | *Non/slowly coalescing system* | *Rapidly coalescing system* |
|---|---|---|
| *Scaling criterion* | P/V = constant | Circulation time = constant |
| *Limitation ($V_L/V_S$)* | 100:1 | 10:1 to 20:1 |
| *D/T* | 0.3-0.5 | $\geq$ 0.5 |

# CHAPTER 3 THESIS ORGANIZATION

*The objective of Chapter 3 is to present the research problem that this thesis will answer. Furthermore, the general and specific objectives will be detailed in order to "map out a route".*

## 3.1 Research problematic and scientific gap

Literature review highlighted the high potential of solid-stabilized emulsions in different industrial fields. Nonetheless, the lack of information on processing and does not allow a proper and intelligent design of a large-scale production facility. Moreover, differences between surfactants and solid particles suggest that scaling parameters for surfactant-based emulsions could be not applicable to SSEs.

Indeed, due to the complexity of involved mechanisms, most of mixing operations at the industrial scale are governed as "trial-and-error" experiments. Decisions are taken based on experience rather than a fundamental understanding of involved phenomena because several gaps remain in the literature. Thus, engineers will have to rely on previous tests to achieve the desired properties. However, for (often!) economical and obvious reasons, this practice should be changed. Poor mixing can be responsible for almost $100M in losses every year for a large company. (Paul et al., 2004) From a scientific point of view, this practice demonstrates the lack of knowledge of phenomena taking place in a mixing system. The deficiency raised by the literature review, which will be the subject of this project, *is the lack of information on the scaling and processing of Pickering emulsions*.

Since interest in Pickering emulsions is recent, it is quite normal that this void exists. Several research groups are interested in SSEs due to the significant potential they provide. Studies by these groups contributed to the scientific progress. From an industrial perspective, establishing scaling methods and a good knowledge of phenomena involved in the production of these emulsions can reduce costs regarding process development as well as losses in terms of material and human resources. This project is also in a continuity of projects done by Polytechnique Montreal on Pickering emulsions. Indeed, several students contributed to the knowledge expansion on these emulsions: Tsabet and Fradette (2015 and 2016), Wan and Fradette (2017), Reyjal et al. (2013), Fournier et al. (2009).

## 3.2 General objective

The literature review showed that an increased interest in Pickering emulsions has emerged in recent years. This subject has been extensively researched. However, as shown, scientific gaps remain, especially regarding the processing and scaling of these emulsions. Therefore, this thesis has the general objective of *developing a methodology for scaling solid-stabilized emulsions*. In order to achieve this main objective, three specific objectives will be detailed in the next section.

This thesis will mainly focus on the generation of Pickering emulsions. Why? The author of this thesis relies on the principle that in order to efficiently decompose an emulsion to its main constituents it is important to understand its formation. However, work done by Bing and Fradette (2017 and 2018) is kindly recommended for readers seeking information about SSEs destabilization.

## 3.3 Specific objectives

### 3.3.1 Determine the impact of the presence of particles on the processing of solid-stabilized emulsions.

This is the topic of the first paper. In order to fully understand the processing of solid-stabilized emulsions, the emulsification process has been divided into its main components: solid suspension and liquid dispersion. Their impact on resulting emulsion has been identified and quantified for a wide range of emulsification conditions using several characterization techniques (ex. particle vision microscope, laser diffraction method).

### 3.3.2 Verify the applicability of conventional emulsions scaling criteria on solid-stabilized emulsions.

This is the topic of the second paper. The main goal of this part is to determine whether using particles instead of surfactants will impact the scaling procedure while keeping in mind that the stabilization method is completely different for these two emulsifying agents. Conventional scaling criteria used for surfactant-based emulsions were gathered and tested on diluted and concentrated particle-stabilized emulsions in three geometrically similar scales with two impeller flows (radial and axial).

### 3.3.3 Identify parameters regulating solid-stabilized emulsions scaling.

This is the topic of the third and last paper. While the main difference regarding the scaling procedure was highlighted in the previous objective, this last section will define a scaling rule for Pickering emulsions that could be applied to the systems that have been tested in this project. Furthermore, the scaling method will be validated on a pilot scale of 250 liters thus reaching a scaling factor of 1000 which is uncommon in the literature.

# CHAPTER 4 ARTICLE 1: DETERMINATION OF SCALING RULES FOR SOLID-STABILIZED EMULSIONS: THE COUNTERINTUITIVE EFFECT OF PARTICLES ON DROPLET SIZE

**Alexandre Al-Haiek, Èmir Tsabet, and Louis Fradette**

**URPEI, Chemical Engineering Department**

**Polytechnique Montréal, 2900 Édouard-Montpetit, Montréal, Canada, H3C 3A7**

**Submitted in *AIChE Journal***

## Abstract

The processing of solid-stabilized emulsion (SSEs) was analyzed to identify mechanisms that are relevant for suitable scaling. Two main mechanisms were studied: particle suspension and emulsification. While interface generation and interface stabilization affect the emulsification process (Tsabet and Fradette, 2015), particle suspension has not been studied. We experimentally investigated the effect of particle suspension on SSEs. Oil-in-water emulsions were produced using off-centered pitched blade and Rushton turbines in unbaffled 5-L tanks. Silicone oils were used as the dispersed phase, glass beads ($d_{32} \approx 3$, 35, and 65 µm) were used as stabilizers, and deionized water was used as the continuous phase. Emulsions were characterized by droplet size distribution measurements using a Malvern Mastersizer 3000. Liquid dispersions were characterized by analyzing images obtained using a particle vision microscope (PVM). The droplet size increased when the particle size or oil viscosity was increased and when the particle concentration was decreased. However, larger droplets could be obtained by increasing the particle concentration under certain conditions. This unexpected behavior was analyzed by examining the interaction between the properties of the solid particles and turbulent energy. An analysis of turbulence length scales showed that this behavior occurs when the particle size is larger than the Kolmogorov scale. We tested different Stokes regimes and showed that a viscous flow regime (larger fluid response time) exhibits the same behavior as that reported in the literature. On the other hand, high particle concentrations in the inertia flow regime (larger solid response time) stabilized larger droplets.

**Keywords:** Pickering emulsions, scaling, power-law, suspension, emulsification, and stirred tanks.

## 4.1 Introduction

Although W. Ramsden and S.U. Pickering were the first to describe solid-stabilized (Pickering) emulsions in 1903 and 1907, respectively, these emulsions only began to attract serious attention in the late 1990s. William Haynes (1860) and the Bessel brothers (1877) reported that particles adsorb to interfaces. The Bessel brothers, for example, who were trying to concentrate ore minerals, used a graphite flotation process to adsorb graphite flakes to air bubbles (Chelgani et al., 2015). Solid-stabilized emulsions have recently received increasing attention from the scientific community due to the huge potential of their structures and properties. Figure 4-1 presents the number of papers published on Pickering emulsions over the past 100 years, with an emphasis on the past 25 years.

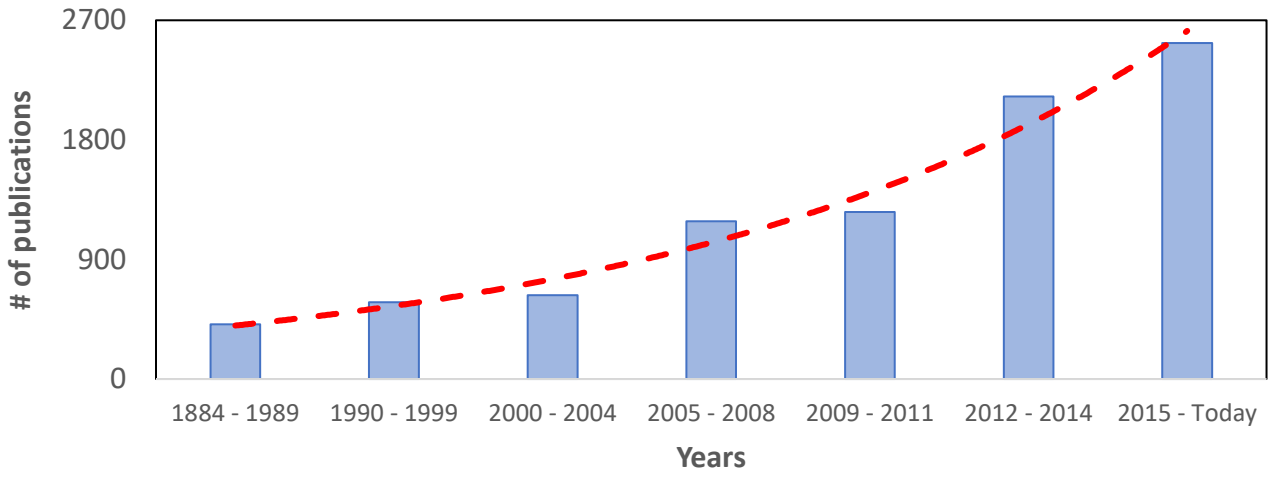


Figure 4-1 – Data obtained from EngineeringVillage.com using a *Pickering AND emulsion** within Subject/Title/Abstract search criterion

Because so many articles have been published on Pickering emulsions, the following literature review has been divided into the six main research groups that have worked on solid-stabilized emulsions, with a focus on the particle types they used and their main conclusions. The first group, which is headed by Bernard P. Binks, has published over 200 articles on the subject. Over the years they have used a large variety of particles ranging from bentonite, silica, latex, and a composite microgel to wax and $Fe_3O_4$. They have worked with modified and unmodified particles (by changing their wettability) and with different liquid mixtures. They reported that particles of

intermediate hydrophobicity ($\theta_{ow} \sim 90°$) produce highly stable emulsions and that highly hydrophobic ($\theta_{ow} > 90°$) and hydrophilic ($\theta_{ow} < 90°$) particles produce less stable emulsions. They used mixtures of hydrophilic and hydrophobic particles to produce emulsions at the phase inversion point. They also investigated the use of amphiphilic or Janus particles to produce emulsions and found that these emulsions are more stable than conventional solid-stabilized emulsions. They also reported that increasing the particle concentration leads to smaller stable droplets due the higher coverage potential. Binks et al. (2001) also showed that it is possible to produce stable emulsions without covering the entire droplet surface and that the stability of emulsions can be enhanced by reducing the particle size. Pickering emulsions can be stabilized by using particle/surfactant mixtures or particles alone and by adjusting the pH if pH-sensitive surfactants and/or particles are used. The pH of the aqueous phase has an impact on particle adsorption at the interface through particle flocculation. Binks et al. (1999) showed that a medium degree of particle flocculation resulting from the addition of electrolytes and their impact on the repulsive electrical double layer force enhances the stability of emulsions. Higher particle flocculation, however, decreases the stability of emulsions. They also showed that oil polarity has an impact on oil/particle affinity and interfacial tension, which also control emulsion stability. A higher oil polarity reduces interfacial tension and increases wettability. Polar oils tend to form water-in-oil emulsions and non-polar oils tend to form oil-in-water emulsions (Binks and Clint, 2002). Modifying the emulsion temperature using thermo-sensitive particles has been shown to be a main parameter for controlling phase inversion. One recurring key point is that the studies by this group have only been carried out with nanoparticles. However, it should be noted that interparticle forces lead to the formation of clusters that do not exceed a few microns in diameter (single digit numbers).

Chevalier et al. (1991) worked with bare silica and recently published a review on Pickering emulsions. They reported that suspensions of polar oils and hydrophilic particles tend to give more stable oil-in-water emulsions. Oil polarity has an impact on interfacial tension and particle wettability and thus on droplet size and emulsion type. Once again, these studies were conducted exclusively with nanoparticles. They also stated in their review that most of the studies on SSEs were conducted using nanoparticles < 100 nm in size or ranging from 0.1 μm to 1 μm in size.

Jacob Masliyah and Bruce Bowen have together published more than 400 articles on oil sands and emulsification. They worked with fine kaolinite clay, fumed silica nanospheres, and polystyrene

particles (references). Levine et al. showed that particle stability depends on energy wells at the interface in which particles get trapped (reference). They proposed equation 4.1 to deduce the energy ($E$ in Joules) needed to remove a particle from an interface,

$$E = \pi R^2 \gamma_{OW}(1 \pm \cos\theta_{ow})^2 \quad (4.1),$$

where R is the particle radius (in m), $\gamma_{OW}$ (in N/m) is the interfacial tension, and $\theta_{ow}$ is the particle wettability (in °). They showed that particle wettability has an impact on emulsion type. Oil-in-water emulsions are more likely to form with hydrophilic particles and water-in-oil emulsions are more likely to form with hydrophobic particles, while mixtures of hydrophobic and hydrophilic particles tend to produce multiple emulsions. They reported that one layer of particles must form at the droplet interface to prevent destabilization, that numerous particle layers and increasing particle compactness reduce the demulsification rate, and that a high contact angle results in a compact particle layer at the interface. On the other hand, hydrophilic particles tend to flocculate and form a less compact layer. In addition, high particle concentrations tend to reduce the demulsification rate. They controlled emulsion stability using particle/surfactant mixtures. They also showed that decreasing the pH reduces the adsorption rate of a particle at the interface. Furthermore, an increase in pH will lead to an increase in the demulsification rate. They mainly worked on the impact of the pH of the aqueous phase on particle wettability and on emulsion type and stability. Liu et al. (2006) showed that adding an electrolyte to the aqueous phase reduces repulsive double layer forces due to the presence of free ions, which screen surface charges. Like others, Masliyah and Bowen worked with particles under 1 µm in size.

Dai et al. (2008) worked with particles (polystyrene beads, for example) up to a few microns (4 µm) in size. They reported that particle motion at the interface is dependent on particle size and wettability, oil viscosity, and interface curvature, that it is not necessary to cover the entire interface to get stable dispersions, and that small monodispersed particles increase the stability of emulsions. Tarimala et al. (2004) also showed that reducing particle size reduces droplet size.

Di Sun et al. worked with layered double hydroxide particles no more than 300 nm in size. They showed that emulsion stability can be improved by adding electrolytes, which results in partial particle flocculation, and that emulsion stability decreases if the particles are highly flocculated.

The studies mentioned above used different particle types with specific properties, including nanoparticles. In some cases, clusters formed but never exceeded a few microns in size. This is

important to keep in mind. These studies never investigated the processing or generation of solid-stabilized emulsions. Much research has been devoted to investigating the impact of particle and aqueous and oil phase properties on the stability of the final emulsion. However, to our knowledge, no articles on the processes and the characteristics of the processes used to produce emulsions have been published. Although the stabilization of droplets by particles has been extensively documented, little information is available on how to make particles accessible to the oil-water interface by solid suspension. The aim of the present study was to determine the impact of the solid suspension step on the processing of solid-stabilized emulsions and to quantitatively assess the characterization techniques commonly used for solid suspensions and liquid dispersions.

In addition to stabilization, one of the main and first steps involved in the production of solid-stabilized emulsions is the suspension of particles (stabilizers) in the continuous phase. Solid suspension is essentially determined by the minimum impeller speed required to suspend all the particles in the continuous phase. A useful criterion for characterizing solids suspension is the just-suspended speed ($N_{js}$) (Zwietering, 1958). Although numerous studies have used Zwietering's correlation to study various conditions (impeller type, geometrical ratio of the tank, particle size, mixing regime), the correlation has many limitations and lacks accuracy. Ayranci and Kresta (2013) proposed the following correlation, which is based on Zwietering's correlation under a fully turbulent regime ($Re > 10^4$), to better deduce the just-suspended speed:

$$N_{js} = A\left(\frac{g(\rho_s - \rho_l)}{\rho_l}\right)^{0.5} \frac{d_p^{1/6} X^n}{N_p^{1/3} D^{2/3}} \frac{T}{D} \quad (4.2)$$

where,

$$A = S\left(\frac{d_p^{\frac{1}{30}} N_p^{\frac{1}{3}} v^{0.1}}{D^{\frac{11}{60}}}\right) \frac{D}{T} \left(\frac{g\Delta\rho}{\rho_l}\right)^{-0.05} \quad (4.3),$$

where $g$ is the acceleration due to gravity ($m/s^2$), $\rho_s$ is the solid density ($kg/m^3$), $\rho_l$ is the liquid density ($kg/m^3$), $d_p$ is the particle diameter (m), $N_p$ is the impeller power number, $D$ is the impeller diameter (m), $T$ is the tank diameter (m), and $X$ is particle loading (%). Increasing the particle size ($d_p$) and/or particle concentration ($X$ in Equation 4.2) increases $N_{js}$. We used Equation 4.2 to calculate $N_{js}$.

Although numerous studies have been devoted to investigating the effect of particle properties on the stabilization of Pickering emulsions and the effect of these properties on pure solid suspensions, to the best of our knowledge, no studies have looked at the interaction between these two effects in the emulsification process.

The effect of particles on turbulence has been extensively studied. There is, however, no consensus on the way it effects the entire system. Ebert (1992) and Yang and Shy (2005) found that increasing the particle concentration reduces turbulent kinetic energy levels in turbulent flows in horizontally positioned cylindrical vessels. Elghobashi and Truesdell (1993) remarked that the experimental data available to them at the time showed that the presence of particles in a system can increase or decrease the kinetic energy of the main carrier fluid. Jianren et al. (1997) showed that increasing the particle size results in greater fluid turbulence dampening in a gas crossflow over a cylinder. Druzhinin and Elghobashi (1999), Druzhinin (2001), and Ferrante and Elghobashi (2003) studied the particle size to Kolmogorov length scale ratio and showed that the dissipation rate of turbulent kinetic energy decays at a higher rate in a particle-free system, and that smaller particles cause a reduction in the turbulent energy decay rate. Ferrante and Elghobashi (2003) used a direct numerical stimulation to show that particles with a Stokes number lower than 1 increase the turbulent kinetic energy rate and the energy dissipation rate ($\varepsilon_{av}$). They attributed this to an increase in inertia as the solid particles follow the streamline. On the other hand, they showed that particles with a Stokes number greater than 1 reduce both $\varepsilon_{av}$ and turbulent kinetic energy due to particles moving across the streamline and counteracting the energy in the flow. Unadkat et al. (2009) and Micheletti and Tianneskis (2004) also reported that particles with a Stokes number greater than 1 cause a decay in the turbulent kinetic energy rate.

Gabriele et al. (2011) used particle image velocimetry (PIV) to study the effect of large particles on the liquid mean velocity, turbulent kinetic energy, and energy dissipation rates. They used a PBT-agitated cylindrical vessel with an up-and-down pumping configuration and observed small variations in liquid velocities when particle concentrations were increased. However, the turbulent kinetic energy rate near the impeller dropped significantly (30-40%) while the solid hold-up increased.

Li et al. (2017) recently used the PIV technique to study the impact of particles on the turbulence rate in a PBT-agitated tank in a turbulent regime, i.e., a Reynolds numbers > $10^4$. They observed a

strong turbulence dampening effect in the presence of the particles and very strong phase coupling with particles in the fluid velocity fields. When the solid volume fraction was increased, this dampened the overall circulation pattern as well as the fluid velocity fluctuation levels. They attributed this to the obstruction of the flow by the particles near the bottom of the tank, which disturbed the main recirculation pattern, i.e., the flow pattern, and shifted it upward. The effect of the particles weakened in the volume above the impeller, slowing the recirculation pattern and resulting in reduced turbulence. More recently, Li et al. (2018) used the PIV technique to show that particles dampen the average velocity fields in the tank as well as the turbulence rate (Reynolds number) in the fluid both experimentally and using a direct numerical simulation in a stirred tank operated in the transitional regime (Reynolds number between 1000 and 10,000).

Based on results showing that the fluid turbulence rate controls the production of the interface during emulsification (references) as well as particle attachment when solid-stabilized emulsions are generated (reference), we investigated the impact of solid suspension during emulsification on the resulting solid-stabilized emulsion. More generally, we clarified the impact of the presence of particles on the resulting emulsion.

Most studies to date have focused on emulsion stability. However, the few that have focused on processing considered an average power dissipation rate ($\varepsilon_{av}$, Equation 4.4) in a stirred tank.

$$\varepsilon_{av} = \frac{P}{V_{liq}} = \frac{N_p\, \rho\, N^3 D^5}{V_{liq}} \quad (4.4),$$

where $P$ is the power (in J/s), $V_{liq}$ is the liquid volume in the tank (in $m^3$), $N_p$ is the dimensionless power number, $\rho$ is the fluid density (in $kg/m^3$), $N$ is the impeller speed (in $s^{-1}$), and $D$ is the impeller diameter (in m).

While experimental results indicate that particles have an impact (no consensus on the type of impact) on the flow, the role of particles in energy splitting between the production of an interface and the suspension of particles in a stirred tank is poorly understood. There are thus many unanswered questions concerning how energy is distributed in a stirred tank during particle-stabilized emulsification processes.

## 4.2 Materials and methods

The general experimental methodology we used can be divided into three main steps. The first step was to prepare the emulsification setup (5-L scale) using a pitched-blade turbine (PBT) or a Rushton turbine (RT). The second step was to prepare the emulsion. The particles (3, 35, or 65 µm) were first suspended in the continuous phase (deionized water), and the dispersed phase (silicone oil of the desired viscosity) was then added to the suspension. In the third step, the droplet size and distribution of the emulsions were characterized using a laser diffraction method. The parameters considered were diameters ($d_i$ where $i$ is 10, 50, 90, or 32) and polydispersity (span).

### 4.2.1 Materials

Pure silicone oils (Clearco Inc., USA) of different viscosities (Table 4-1) were used as the dispersed phase, deionized water was used as the continuous phase, and glass beads were used as stabilizers. Particle sizes and contact angles were measured using a laser diffraction technique (section 4.2.2.4.4) and a capillary rise method (section 4.2.2.4.1), respectively (Table 4-2).

Table 4-1 – Properties of the silicone oils

| *Viscosity (cSt)* | *Density (kg/m$^3$)* | *Dynamic viscosity (mPa.s)* | *Surface tension (mN/m)* |
|---|---|---|---|
| 10 | 935 | 9.35 | 20.1 |
| 50 | 960 | 48.00 | 20.8 |
| 100 | 966 | 96.60 | 20.9 |
| 200 | 968 | 193.60 | 21.0 |

Table 4-2 – Properties of the glass beads

| *Particle size (µm)* | *Density (kg/m$^3$)* | $\theta_{aw}(°)$ | $\theta_{ao}(°)$ | $\theta_{ow}(°)$ | *Type* | *Supplier* |
|---|---|---|---|---|---|---|
| 3 | 2520 | $90 \pm 4$ | $81 \pm 1$ | $94 \pm 4$ | Hydrophilic | Cospheric LLC |
| 35 | 2520 | $74 \pm 2$ | $55 \pm 4$ | $78 \pm 6$ | Hydrophilic | Potters Inc. |
| 65 | 2520 | $72 \pm 2$ | $26 \pm 3$ | $84 \pm 3$ | Hydrophilic | Potters Inc. |

## 4.2.2 Experimental methods

### 4.2.2.1 Emulsification setup

Emulsions were produced in an unbaffled 5-L tank using a 4-blade PBT or a 6-blade RT (USI-MAX, Canada). The impellers were off-centered to prevent the formation of a vortex (Fig. 4-2). This configuration has the same mixing performance as a baffled tank with a centered impeller (Nishikawa et al., 1979) (Novak et al., 1982) (King et al., 1985) (Karez et al., 2004) (Karez et al., 2005) (Montante et al., 2006). Table 4-3 gives the dimensions of the emulsification setup.

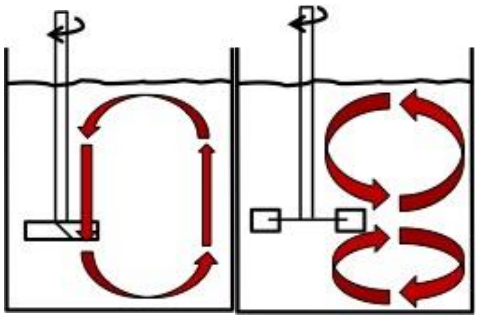

(a) (b)

Figure 4-2 – Emulsification systems with (a) a PBT or (b) an RT [taken from Tsabet and Fradette (2015)]

Table 4-3 – Geometrical parameters of the components for each scale

| *Geometrical parameters* | *Dimension (cm)* |
|---|---|
| Tank diameter (T) | 16.30 |
| Impeller diameter (D) | 5.43 |
| Length of one blade (L) | 1.36 |
| Height of one blade (W) | 1.09 |
| Baffle thickness (J) | 1.63 |

### 4.2.2.2 Formulation

Diluted and concentrated oil-in-water (O/W) emulsions were prepared using 5% and 30% dispersed phase fractions ($\phi_d$).

$$\phi_d = \frac{V_D}{V_D + V_C} \quad (4.5),$$

where $V_D$ is the volume of the dispersed phase (in $m^3$) and $V_C$ is the volume of the continuous phase (in $m^3$).

#### 4.2.2.3 Emulsification preparation

The solid particles were dispersed in the desired amount of deionized water for 10 min at 480 rpm. The oil was then gently added, and the mixing was continued for a further 24 h. Samples were collected under agitation using a large-tip opening pipette to prevent droplet breakage. The emulsification steps are illustrated in Figure 4-3.

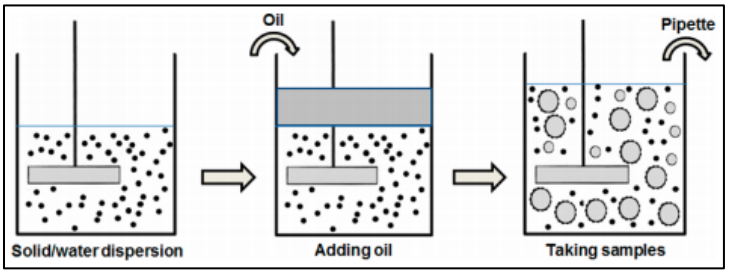


Figure 4-3 – Steps used to prepare a solid-stabilized emulsion [taken from Tsabet et al. (2015)]

#### 4.2.2.4 Emulsion characterization

##### *4.2.2.4.1 Particle wettability*

Particle wettability was evaluated by taking contact angle measurements using the capillary rise method developed by Fournier et al. (2009). This method is also detailed in Al-haiek et al. (*submitted, see article 2 of this thesis*).

##### *4.2.2.4.2 Viscosity and rheological behavior*

The viscosities of the solid suspensions were measured using a Malvern Bohlin Gemini rheometer. A double helical ribbon (DHR) geometry was used to determine the rheological behavior of the solid suspensions. The geometric parameters of the DHR are given in Figure 4-4 and Table 4-4. A DHR is recommended for solid suspensions because of its pumping capacity (Bertrand et al., 2018), which prevents particle sedimentation even at low shear rates (Patterson et al., 1979) (Ait-Kadi et al., 1997) (Brito-De et al., 1997) (Brito-De et al., 1998).

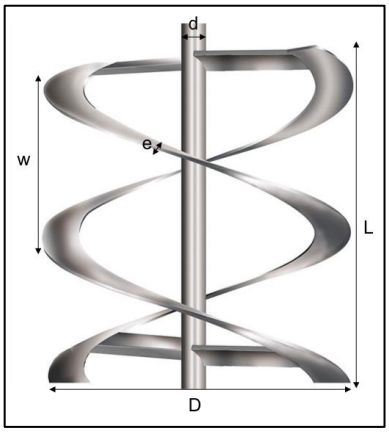


Figure 4-4– Double helical ribbon

Table 4-4 – Geometrical parameters of the double helical ribbon

| *Geometrical parameters* | *DHR (in mm)* |
|---|---|
| Shaft diameter (d) | 5.87 |
| Impeller diameter (D) | 39.56 |
| Height of the impeller (L) | 55.38 |
| Distance between ribbons (w) | 18.78 |
| Impeller thickness (e) | 1.63 |

The effective shear rate generated by the DHR was determined using the Metzner constant $(k_s)$ given by:

$$\dot{\gamma}_{eff} = k_s N \text{ (4.6)},$$

where $\dot{\gamma}_{eff}$ is the effective shear rate $(s^{-1})$ and N is the rotational speed (in rpm). The Metzner constant was deduced using the experimental methodology of presented in Fradette (1999). This method requires to first determine the power number for the impeller ($N_p$) as a function of the Reynolds number for a Newtonian fluid. Second, the torque is measured for different speeds for the non-Newtonian fluid and therefore $N_p$ can be calculated. The effective Reynolds number can also be calculated and used to obtain the effective, i.e. process viscosity. This effective viscosity is then used to determine the effective shear rate. Last step is to calculate $k_s$ using equation 4.6. Experimental measurements showed that the Metzner constant was approximately 20 ± 2, which

is close to the values reported in the literature (Brito-de la Fuente et al., 1997) (Coulson and Richardson, 1993).

#### *4.2.2.4.3 Emulsion type*

Emulsion type was determined by measuring conductivity using an Okton conductivity meter (CON 110 series).

#### *4.2.2.4.4 Droplet size distributions*

The droplet size distributions in the emulsions were determined using a Malvern Mastersizer 3000 combined with a laser diffraction technique. Plastic pipettes were used for sampling. The narrow tip was cut off to provide a large opening and prevent shear that could break larger droplets and result in unrepresentative samples of the emulsion. The pipette was inserted halfway in the tank, and three samples were taken at 10-s intervals. The sampling interval was higher than the circulation time to ensure that the samples were representative of the whole tank. Low-density plastic pipettes were used rather than glass pipettes because of their inherently hydrophobic nature, which prevents droplets from sticking to the wall of the pipette.

The droplet size distribution in the liquid dispersions was determined by analyzing images acquired using a particle vision microscope (PVM). Bing and Fradette (2017) have reviewed and compared these methods.

Emulsions were characterized using the Sauter mean diameter ($d_{32}$), which is the relationship between the dispersed phase volume fraction ($\phi_d$) and the generated interface ($A_{gen}$).

$$d_{32} = \frac{6\phi_d}{A_{gen}} \quad (4.7)$$

#### *4.2.2.4.5 Theoretical coverage potential*

The capacity of the system to cover the generated droplets ($A_{cov}$) was determined from the particle properties using equations 4.8 to 4.11 (Tsabet and Fradette, 2015 and 2016):

$$V_{1/particle} = \frac{4\,\pi R_p^3}{3} \quad (4.8)$$

$$N_{particles} = \frac{m_p}{\rho * V_{1/particle}} \quad (4.9)$$

$$A_{cov/1p} = \pi\left(R_p \sin\theta_{ow}\right)^2 \quad (4.10)$$

$$A_{cov} = A_{cov/1p} * N_{particles} \quad (4.11),$$

where $R_P$ is the radius of the particles (in m), $V_{1/particle}$ is the volume of the particles (in $m^3$), $m_p$ is the mass of the particles in the system (in kg), $\rho$ is the density of the particles (in $kg/m^3$), $N_{particles}$ is the number of particles in the system, and $\theta_{ow}$ is the contact angle (in °).

## 4.3 Results and discussion

### 4.3.1 Effect of particle loading and oil viscosity on the droplet size of diluted emulsions

Figure 4-5 shows the evolution of the Sauter mean diameter with respect to different particle concentrations and oil viscosities. In the case of 10 cSt silicone oil, the droplet size increased when the coverage potential was reduced or the particle size was increased. Higher particle concentrations stabilized more interface while larger particle sizes reduced particle attachment efficiency (Fig. 4-5). The RT, as expected, generated smaller droplets than the PBT because it produces higher shear levels and shorter circulation times. A more viscous silicone oil (200 cSt) exhibited different behavior. The increase in droplet size when the coverage potential was reduced was only observed with the smallest particles (3 µm), while a surprising decrease in droplet size was observed when larger particles with lower coverage potentials were used. This counterintuitive behavior was observed with both impellers, indicating that the shear level has no impact on the results. The particle size effect was seen with both impellers, with the droplet size decreasing at the lowest coverage potential when the particle size was switched from 3 µm to 35 µm. The surprising decrease in droplet size was also observed at the highest coverage potential when the particle size was switched from 35 µm to 65 µm. This inversion in droplet size versus particle size and coverage potential suggests that two competitive mechanisms affect interface generation and emulsion stabilization.

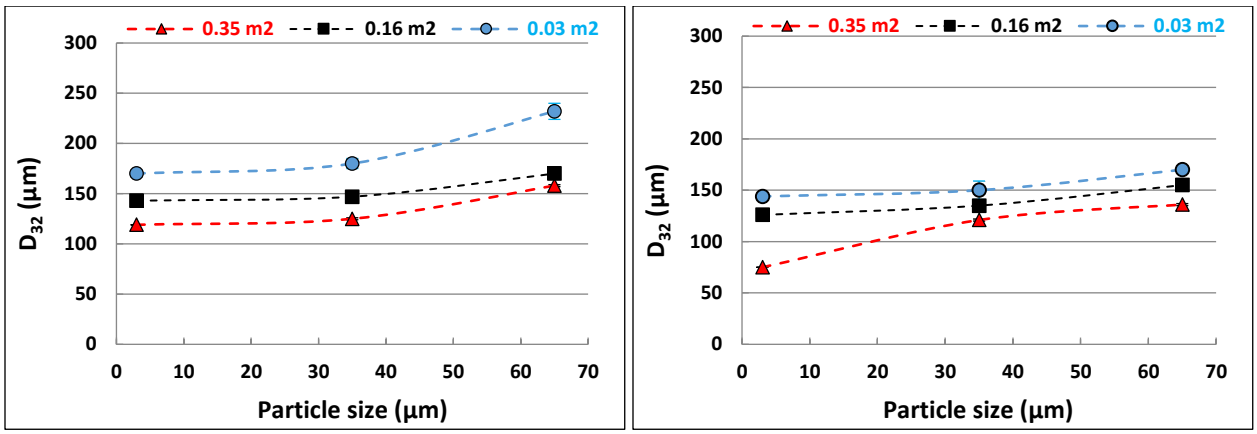


**(1-a) 10 cSt oil - PBT** **(1-b) 10 cSt oil - RT**

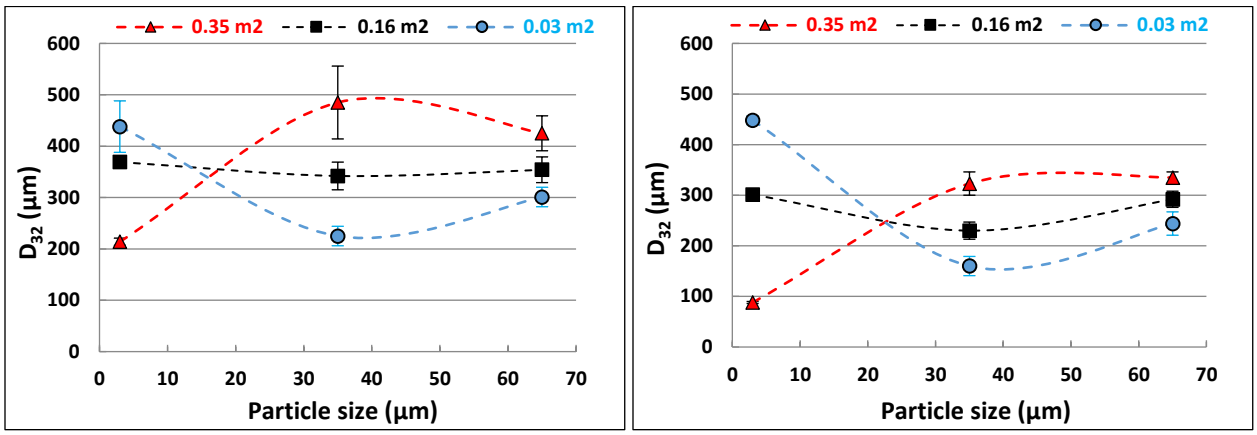


**(2-a) 200 cSt oil - PBT** **(2-b) 200 cSt oil - RT**

Figure 4-5 – Effect of particle size on emulsion size using different impellers, with $\phi_d = 5\%$ v/v and (1) 10 cSt oil or (2) 200 cSt oil

The effect of oil viscosity was investigated further in order to pinpoint the reasons for this unexpected behavior (Fig. 4-6). Larger droplet sizes were produced with higher particle concentrations when 50 cSt oil and 35 µm particles were used (Fig. 4-6(a)) and when 10 cSt oil and 65 µm particles were used (Fig. 4-6(b)). These results confirmed that competitive processes related to particle size and oil viscosity affect interface generation and emulsion stabilization.

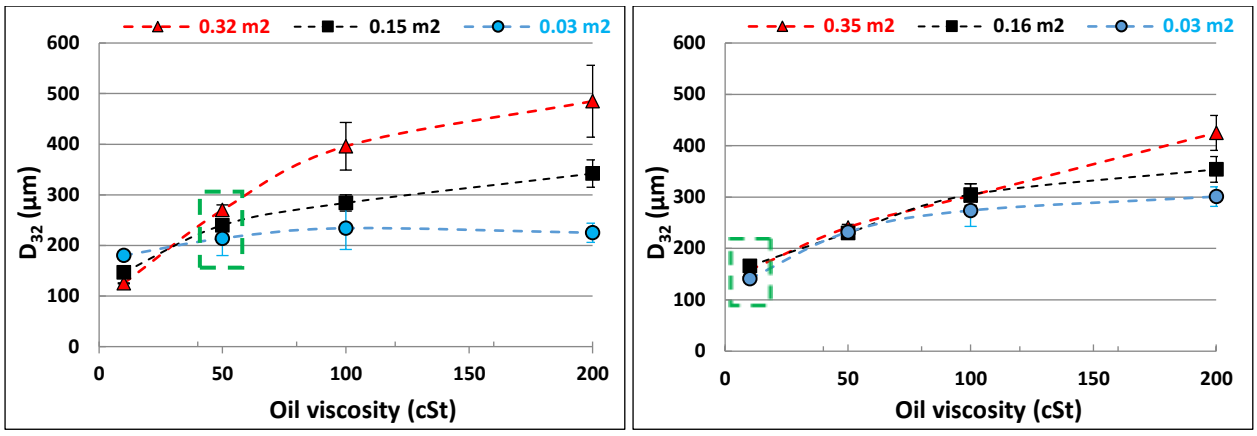


**(a) 35 µm particles** **(b) 65 µm particles**

Figure 4-6 – Effect of oil viscosity on emulsion size using a PBT, with $\phi_d = 5\%$ (v/v) and (a) 35 µm or (b) 65 µm particles

### 4.3.2 Effect of particle loading and oil viscosity on the droplet size of concentrated emulsions

We also investigated the behavior of concentrated emulsions. Figure 4-7 shows the Sauter mean diameters of concentrated emulsions with different particle concentrations and oil viscosities. Both impellers produced the same size of droplets and exhibited the same variation in particle size with both viscosities, confirming that these phenomena are independent of the flow pattern.

An increase in droplet size was observed once again when higher concentrations of larger particles (35 and 65 µm) were used than when higher concentrations of smaller particles (3 µm) were used. These results showed that the unexpected effect of particle concentration on droplet size is more pronounced with concentrated emulsions.

Based on a thorough analysis of the emulsification procedure, three main conditions must be met to produce stable Pickering emulsions. The first condition is that the system must be able to suspend and disperse the particles because they cannot attach to an interface and droplets cannot be stabilized if they are not suspended. The second condition is that the emulsification system must be able to generate an interface for droplets to be produced. The third condition is that the properties of individual particles must control particle attachment to the interface. Since the coverage potential acts on a global scale, the observed phenomena must be related to the complex and combined influence of the particles on their own suspension and on interface generation.

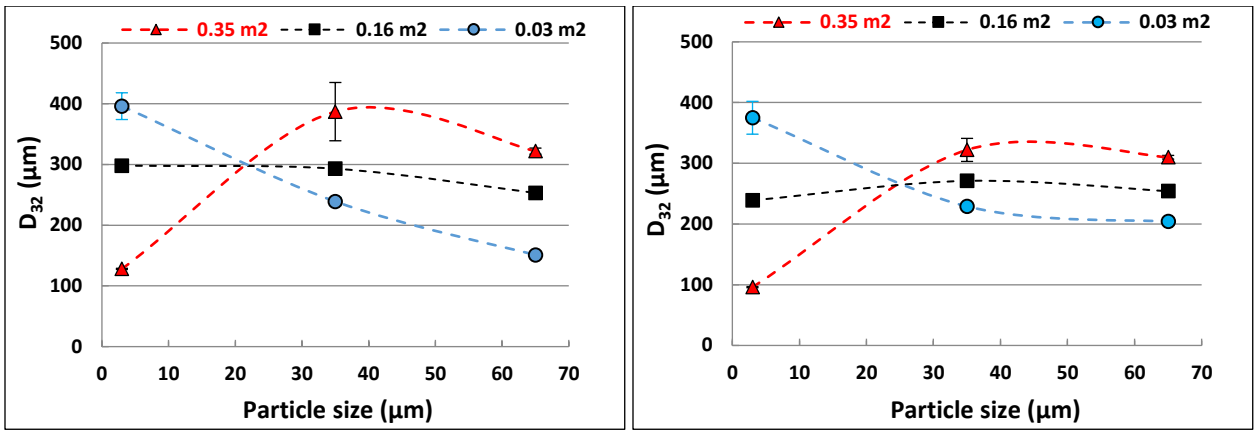


**(1-a) 10 cSt oil – PBT** **(1-b) 10 cSt oil - RT**

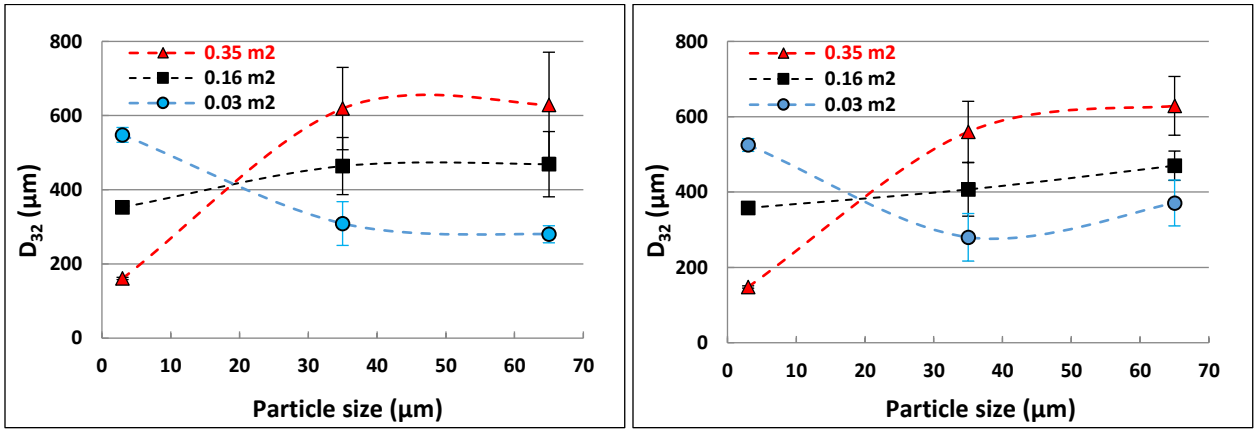


**(2-a) 200 cSt oil – PBT** **(2-b) 200 cSt oil - RT**

Figure 4-7 – Effect of particle size on emulsion size using different impellers, with $\phi_d =$ 30% (v/v) and (1) 10 cSt oil or (2) 200 cSt oil

### 4.3.3 Effect of particle loading on interface generation

To assess the effect of particle loading on the ability of the system to generate an interface, the surfaces of the particles were modified to make them highly hydrophilic ($\theta_{ow} \rightarrow 0°$) and to make their attachment at the interface impossible. Droplet size was measured by image analysis (PVM) during mixing after reaching the equilibrium state.

Figure 4-8 presents the effect of the coverage potential on the droplet size of the dispersions produced with 30% (v/v) 200 cSt silicone oil and 3 µm and 65 µm glass beads using the PBT at 480 rpm. Typical PVM images are presented near their corresponding droplet size.

As with Figure 4-7, the black curve in Figure 4-8 shows that there was an increase in droplet size when more 65 µm glass beads were added to the system. The increase in size was caused by a less effective interface generation mechanism due to the presence of more particles and was not related to the stabilization process. There was also an increase in droplet size when more 3 µm glass beads were added, especially with respect to the case without particles with the lowest coverage potential when the addition of more particles had almost no effect on droplet size. However, Figure 4-8 also shows that the 3 µm particles produced larger droplets at the lowest coverage potential, suggesting that the capacity of the system to generate an interface is reduced in the presence of 3 µm particles compared to the system without particles. These findings show that particle size has an impact on the process leading to an increase in droplet size when the particle concentration is increased.

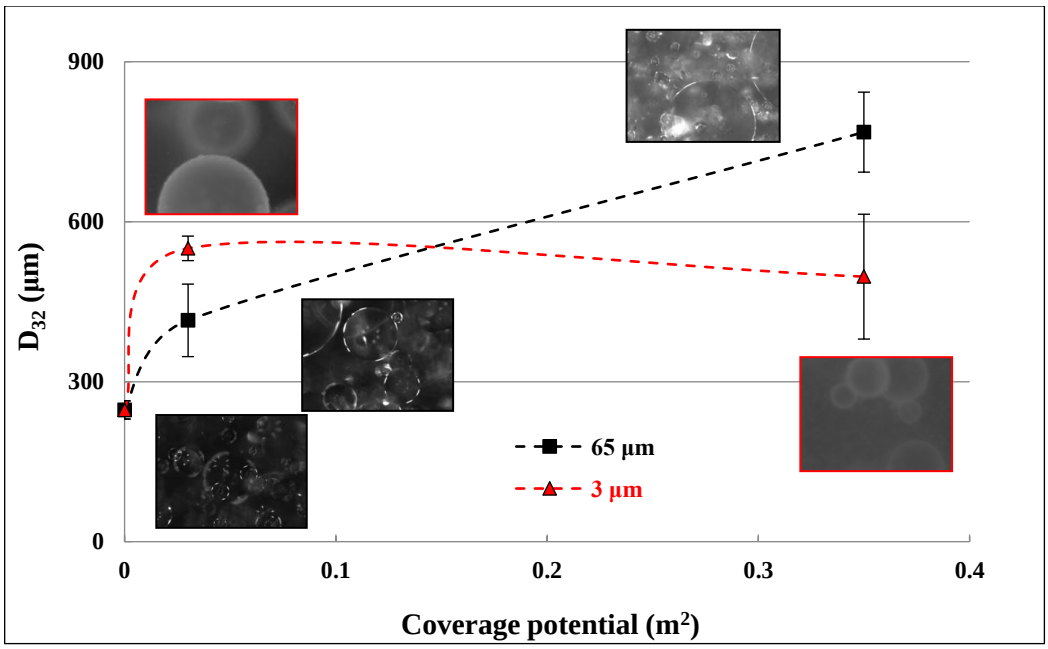


Figure 4-8 – Effect of coverage potential on dispersion size using a PBT, with 3 µm and 65 µm glass beads ($\phi_d = 30\%$ (v/v) and 200 cSt oil)

### 4.3.4 The influence of solid particles on suspension viscosity

The rheological behavior of solid suspensions was analyzed and was compared to the properties of the continuous phase to determine the effect of the presence of solids using the method described in section 4.2.2.4.2. The results are shown in Figure 4-9.

The experiments yielded some interesting findings, some reported in the literature, others not. The 3 µm glass bead suspensions exhibited Newtonian behavior, with a viscosity similar to that of deionized water (~1 mPa.s), regardless of the level of particle loading. However, the 65 µm glass bead suspensions behaved in a shear-thinning mode, with viscosities 10 to 100 times higher than the 3 µm particle suspensions. An increase in viscosity with an increase in particle concentration has been reported in the literature (Ovarlez et al., 2006) (Stickel and Powell, 2005) (Buscall, 1991) (Zhu et al., 2017). On the other hand, an increase in viscosity with an increase particle size is the opposite of what has been reported in the literature (Mewis and Wagner, 2012) (Konijn et al., 2014) (Chen, 2006) (Del Gaudio et al., 2013). For the same solids loading, for example 0.65 $m^2$, the viscosity of the 65 µm glass bead suspension was 100 times higher than that of the 3 µm glass bead suspension.

The lowest solids loading with 65 µm glass beads resulted in a viscosity that was 10 times higher than water at the same shear rate in the mixing tank, while the highest solids loading resulted in a viscosity that was 100 times higher.

Various models have been developed to describe the impact of dispersed solids on the viscosity of suspensions. Although most of the models state that viscosity is mainly affected by the solids volume content, as shown in Table 4-5, they do not take particle size into account.

Table 4-5 – Models showing the impact of dispersed solids on the viscosity of the suspension

| *Authors* | *Equation* | *Conditions* |
|---|---|---|
| *Einstein (1906)* | $\eta = \eta_{medium}(1 + [\eta]\phi)$ (4.12) | - $\phi < 0.05$<br>- Flow field around a single sphere<br>- Independent of particle size |
| *Batchelor (1977)* | $\eta = \eta_{medium}(1 + [\eta]\phi + \chi\phi^2)$ (4.13) | - Adapted Eq. 4.12 for many monodispersed spheres<br>- $0.15 < \phi < 0.2$ |
| *Roscoe (1952)* | $\frac{\eta}{\eta_{medium}} = \left(1 - \frac{\phi}{\phi_m}\right)^{-[\eta]}$ (4.14) | - First attempt to express $\eta$ as a function of $\phi_m$<br>- $\phi > 0.05$ |

| | | |
|---|---|---|
| *Krieger-Dougherty (1959)* | $\frac{\eta}{\eta_{medium}} = \left(1 - \frac{\phi}{\phi_m}\right)^{-[\eta]\phi_m}$ (4.15) | - Valid for low and high $\dot{\gamma}$<br>- $\phi > 0.2$ |

where $\eta$ is the viscosity of the suspension, $\eta_{medium}$ is the viscosity of the suspending medium, $\phi$ is the particle volume fraction, $\phi_m$ is the maximum particle packing volume fraction, $[\eta]$ is the intrinsic viscosity of the suspension, and $\eta/\eta_{medium}$ is the relative viscosity of the suspension. It should be remembered that Einstein's equation is considered as a starting point in suspension rheology (Pabst, 2003).

Particle aggregation may occur in a high solids content suspension, which has an impact on the rheology of the suspension. Particle aggregates encompass part of the suspending medium, which in return increases the apparent particle content thus increasing its apparent viscosity (Graham et al., 1984) (Tsutsumi et al., 1994). While the viscosity of the suspension increases even with low particle fractions, particle interactions are assumed to be negligible, meaning that the viscosity of the suspension is controlled by the flow medium (Newtonian because of water in this case). Particles in dilute suspensions move randomly, and their behavior does not change when the shear rate increases. At higher particle concentrations, this random movement will cease due to the closeness of the particles, which start to pack, aggregate, and form networks. This results in a higher viscosity and a higher particle content. (Zaman et al., 1996)

A higher solids content increases particle collision, which in turn increase the friction and the resulting shear force required to maintain the flow (higher suspension viscosity). Particle interactions result in a higher viscosity at a lower shear rate. On the other hand, increasing the shear rate breaks up aggregates, reducing the apparent particle content and thus lowering the viscosity, i.e., shear-thinning behavior. Shamlou (1993) stated that $\phi_m$ is a function of the shear rate. At a lower $\dot{\gamma}$ there is a random three-dimensional particle distribution, where $\phi_m = 0.632$ for monodispersed spherical particles. Increasing $\dot{\gamma}$ increases $\phi_m$ to 0.708, resulting in shear-thinning behavior (see Equation 4.15). This can be explained by a change in the flow around particles from random to ordered. This has been validated by simulations and scattering experiments, with layers of particles forming as the shear rate increases (Krieger and Dougherty, 1959).

As mentioned in Chen (2006), particle size and distribution have their share of impact on suspension viscosity due to their influence on collisions and packing. At any given solids volume content, the presence of smaller particles results in a higher suspension viscosity because of the shorter distance between the particles, which increases the strength of the interactions compared with larger particles. It has also been reported that the shear-thinning phenomenon is more present with smaller particles (Van der Werff and De Kruif, 1989) (Zaman et al., 1996) (Zaman and Moudgil, 1998) (Lee et al., 1999) (Olhero and Ferreira, 2004). Indeed, finer particle suspensions are more viscous at lower shear rates due to higher interparticle attraction, which increases the resistance to flow. This is in contradiction with our results, which show that larger particles lead to higher viscosities (Fig. 4-9). (Mewis and Wagner, 2012). This is where the notion of particle size distribution becomes important. Indeed, it has been observed that suspensions of polydispersed particles are less viscous than suspensions of monodispersed particles due to the higher packing rate ($\phi_m$) of polydispersed suspensions, which results in a higher flow capacity of particles with identical volume loading. Smaller particles can fill the interstices between larger particles (Chong et al., 1968) (Chong et al., 1971) (Olhero and Ferreira, 2004) (Mewis, 1996) (Zaman and Moudgil, 1998).

The particle sizes (based on the Sauter mean diameter) used in the present study are presented in Table 4-2. The polydispersity of the 3 µm particles was higher than that of the 65 µm particles (Table 4-6). As mentioned previously, increasing polydispersity increases $\phi_m$ due to the finer particles moving between the larger particles. This increase in maximum packing reduces the relative viscosity of the suspension.

Table 4-6 – Polydispersity of the solids used in this study and for Figure 4-9

| | $D_{32}$ | $D_{10}$ | $D_{50}$ | $D_{90}$ | Span |
|---|---|---|---|---|---|
| | $\mu m$ | | | | $\frac{d_{90}-d_{10}}{d_{50}}$ |
| *3* | 1 | 3 | 9 | | 2.72 |
| *65* | 35 | 65 | 95 | | 0.92 |

This result (Fig. 4-9) can explain the larger droplets observed when the coverage potential increases with 65 µm glass beads. Indeed, a higher suspension viscosity results in a decrease in the effect of turbulent energy on the interface generation process, leading to an increase in droplet size. Some studies, including the one by Stamatoudis and Tavlarides (1985), showed that smaller droplets can be produced by increasing the viscosity of the continuous phase. However, this does not explain the results of the present study. In fact, Figure 4-10(b) shows that there was a decrease in droplet size when the viscosity of the continuous phase was increased. There is, however, one key point, i.e., the studies mentioned above used a Newtonian continuous phase. The viscosity of a Newtonian fluid remains constant regardless of the shear rate whereas the viscosity of a non-Newtonian fluid, such as the suspensions investigated in the present study, changes throughout the agitated vessel. Indeed, as the results in Figure 4-9 show, once the solid-liquid mixture (for a large particle load) is in the high shear zone near the impeller, its effective viscosity will decrease until it reaches a medium viscosity. Based on the literature, large droplets are generated in the impeller zone because of the low viscosity in this zone. The droplets then follow the streamline to a zone far from the impeller where the viscosity is higher due to the lower shear rate. According to Tsabet and Fradette (2015), the higher viscosity of the continuous phase reduces stabilization efficiency by increasing the drainage time during the particle-to-droplet approach.

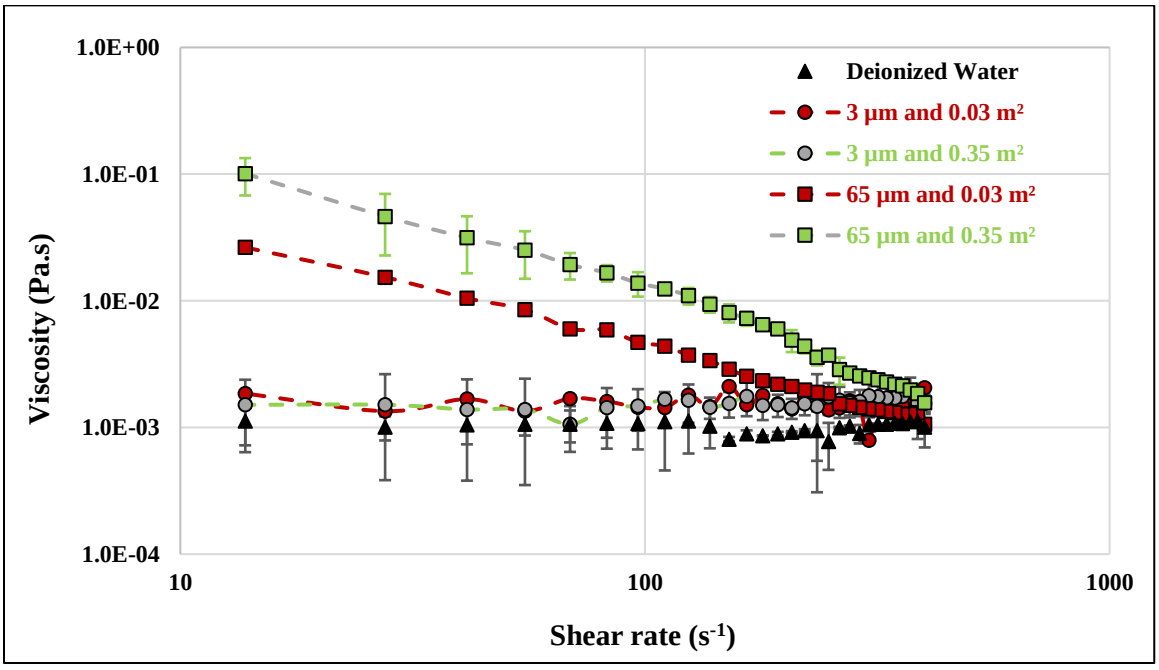


Figure 4-9 – Viscosity of solid suspensions using deionized water as the dispersing medium

Nonetheless, the increase in droplet size was observed with the largest particle size, indicating that the decrease in the capacity of the system to generate an interface is not just associated with friction between suspended particles that results in an increase in the viscosity of the continuous phase. Indeed, much work has been devoted to studying the impact of suspended particles on turbulence, as discussed above.

### 4.3.5 The impact of the presence of particles on turbulence

The interaction between particles and turbulence is usually characterized by the Stokes number (St), which is the particle to fluid response time ratio (Equation 4.16).

$$St = \frac{\pi \rho_p d_p N D}{9 \mu_l} \quad (4.16),$$

where $\mu_l$ is the viscosity of the continuous liquid phase (in Pa.s), $\rho_p$ is the particle density (in kg/m$^3$), $d_p$ is the particle diameter (in m), N is the impeller rotational speed (in s$^{-1}$), and D is the impeller diameter (in m). Table 4-7 gives the calculated Stokes numbers under the conditions considered.

Table 4-7 – Calculated Stokes numbers under the conditions considered

| *Particle $D_{32}$(μm)* | *3* | *35* | *65* |
|---|---|---|---|
| *Stokes number* | 1 | 13 | 25 |

Depending on the value of the Stokes number, two regimes can be defined. The first regime occurs when the particle response time is larger than the fluid response time. In this case, the particle no longer follows the streamlines. On the other hand, a particle with a smaller response time will adhere tightly to the fluid streamlines. Whether or not a particle follows the streamlines can be related to the Kolmogorov scale (η), which represents the smallest eddies generated in the agitated vessel (Equation 4.17). Shaw (1991) proposed that when $\eta > d_p$, the particle will tend to follow the flow of the medium, which is related to Stokes' second regime.

$$\eta = \left(\frac{v^3}{\varepsilon}\right)^{1/4} \quad (4.17)$$

According to the Stokes numbers calculated above, the 3 µm glass bead suspension behaved as a viscous flow, i.e., the 3 µm particles tended to follow the fluid streamline. The particle response time was shorter than that of the fluid response time. On the other hand, the 35 µm and 65 µm glass bead suspensions were either in the transitional or the inertial regime, suggesting that these particles tended to move across the streamlines and not along the fluid streamlines. Furthermore, the smallest eddy size calculated based on the system conditions we used was 50 µm in size, which clearly demarcated the 3 µm particles from the 35 µm and 65 µm particles. It should be noted that even if the $d_{32}$ of the 35 µm particles was lower than the Kolmogorov scale, we used polydispersed particles, which included particles above 50 µm. Moreover, the size is considered more relevant than the absolute value itself. The calculations given in Table 4-7 show that there is a demarcation, with the 3 µm particles on one side of the Stokes regime values and the 35 µm and 65 µm particles on the other.

The positive and negative impacts of particles on turbulence have been investigated in depth by others. However, there is no consensus as to whether particles impact turbulence positively or negatively based on flow regimes and eddy size. In the present study, an increase in the particle concentration of either the 35 µm or the 65 µm particles generated larger droplets, which could be interpreted as a decrease in the overall emulsification efficiency of turbulence. Indeed, an efficient emulsification process will tend to generate the smallest and most uniform (monodispersed) droplet size possible.

When the 3 µm glass beads were suspended in the aqueous phase, and based on the analysis of the Stokes regime given above, the particles followed the streamline, minimizing energy loss from the system. These conditions did not increase the energy dissipation rate or decrease the turbulent kinetic energy of the system, but they did free up energy for surface generation during the addition of the oil phase. The opposite was true for the 35 µm and 65 µm glass beads, which behaved "negatively," that is, they crossed over the streamlines, which reduced the turbulent kinetic energy available for droplet generation and resulted in a larger droplet size.

The impact of the Stokes regime on the various emulsification systems can be validated by varying the solid and/or fluid response time by modifying the particle density and/or fluid viscosity. For the 35 µm particles, the fluid viscosity had to be increased to 9 mPa.s to reach a Stokes number equal to 1. For the 65 µm particles, the fluid viscosity had to be increased to 17 mPa.s to reach a

Stokes number equal to 1. The fluid viscosity was increased using a range of diluted glucose solutions.

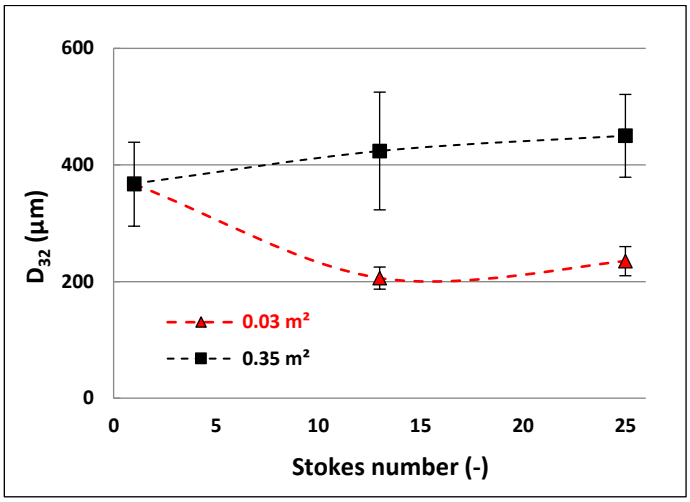


(a)

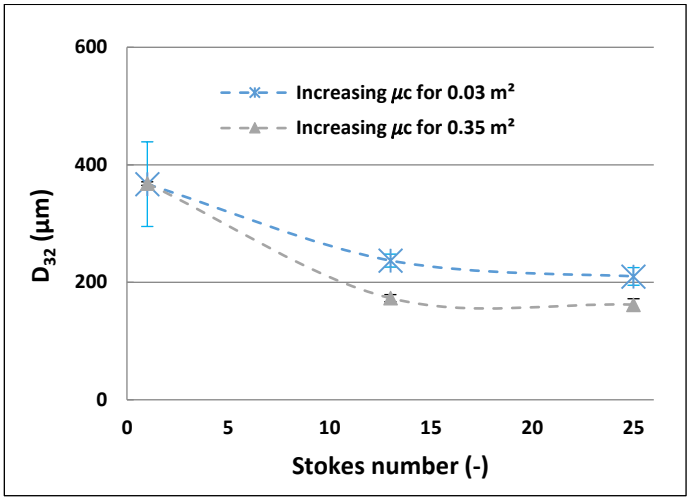


(b)

Figure 4-10 – Effect of adjusting the Stokes regime by controlling the viscosity of the continuous phase using (a) deionized water (1 mPa.s) and (b) two glucose solutions (9 and 17 mPa.s to give Stokes values of 13 and 25, respectively) as the continuous phase

The response time of particles can also be adjusted by modifying particle density. The 35 µm glass beads used so far had a density of 2520 kg/m$^3$, which resulted in a Stokes number that was related to the inertial flow regime. To decrease the particle response time until the viscous flow regime is

reached (the same regime as for the 3 µm particles), 35 µm hollow glass beads with a density of 220 kg/m$^3$ were used. The emulsification results using these low-density particles are shown in Figure 4-11. Decreasing the Stokes number to the viscous flow regime while keeping the particle size constant resulted in a droplet size similar to that reported in the literature. Consequently, if more particles are used, the droplets generated by the emulsification conditions are smaller, which is in line with the expected behavior. Once again, this indicates that the Stokes number is the most important parameter for monitoring particle behavior in emulsions. A lower particle density decreases the amount of energy required by the solid suspension process and, consequently, increases the fraction of available energy required to generate a liquid-liquid interface. This increase in available energy was also seen with smaller droplets. It is important to remember that the inertia of a moving particle is a function of its weight, i.e., its density. If this is expressed in terms of just-suspended speed (Equation 4.1), lower density particles will suspend more easily than higher density particles.

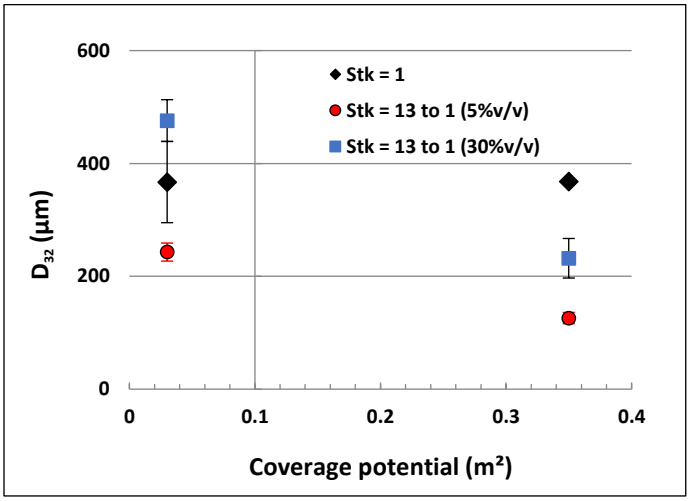


Figure 4-11 – Effect of adjusting the Stokes regime by varying the particle density using 35 µm hollow glass beads with diluted (5% v/v) and concentrated (35% v/v) emulsions using a PBT and 200 cSt oil as the dispersed phase

As mentioned above, the 3 µm glass bead suspensions exhibited Newtonian behavior, with a viscosity of the same order of magnitude as water at both high and low particle concentrations. However, the 65 µm glass bead suspensions exhibited non-Newtonian shear-thinning behavior and, as such, higher particle concentrations produced smore viscous suspensions. In terms of energy, a

higher viscosity decreases the Reynolds number, i.e., the turbulence in the mixing tank. A higher viscosity also consumes a larger amount of the power input from the motor, leaving less energy to generate an interface. During stabilization, a more viscous continuous phase will reduce coalescence and smaller droplets will be stabilized. In the present case, energy is consumed by the system to suspend the particles, leaving less energy to generate an interface. This only occurs when the particles in the system are in the inertial regime, i.e., when the particle response time is larger than that of the fluid response time.

The increase in the viscosity of the continuous phase also has an impact on the stabilization process. For instance, the drainage time between a particle and a droplet increases with viscosity, resulting in lower collision efficiency, as reported by Tsabet and Fradette (2015). The reduction in collision efficiency reduces the stabilized interface, resulting in the production of larger droplets. In addition, the lower energy dissipation rate following solid suspension results in a lower collision frequency between particles and droplets, which reduces the stabilized interface.

## 4.4 Conclusions

Our objective was to investigate the counterintuitive relationship between droplet size and coverage potential. Emulsions were produced in 5-L agitated vessels with either a PBT or an RT. We show for the first time that droplet size increases in tandem with an increase in the coverage potential (or particle fraction). This counterintuitive behavior only occurred when 35 µm and 65 µm glass beads were used. The 3 µm glass beads gave the same results as those reported in the literature. The smallest particles moved in viscous flows at lower orders of magnitude than the Kolmogorov scale according to their calculated Stokes number. The Stokes number calculated for the 35 µm and 65 µm particles placed these particles in a transitional/inertial regime. They thus moved in flows of the same order of magnitude as the Kolmogorov scale. Our results and analyses indicated that larger particles interact negatively with the main flow, i.e., they decrease the amount of energy available for droplet generation and, as a result, they reduce emulsification efficiency. Our analyses also provide a partial explanation for the inconsistencies reported in the literature on the impact of particles on turbulence. The Stokes number can be used to predict the behavior of a given system.

## 4.5 Acknowledgments

The authors gratefully acknowledge the financial support from the Natural Sciences and Engineering Research Council of Canada and from TOTAL.

# CHAPTER 5 ARTICLE 2: SCALING UP THE PRODUCTION OF SOLID-STABILIZED EMULSIONS. PART I – ARE CONVENTIONAL EMULSION AND DISPERSION SCALE-UP RULES APPLICABLE?

**Alexandre Al-Haiek, Èmir Tsabet and Louis Fradette**

**Chemical Engineering Department**

**Polytechnique Montréal, 2900 Édouard-Montpetit, Montréal, Canada, H3C 3A7**

**Submitted in *Chemical Engineering Research and Design***

## Abstract

Scale-up effects on the production of solid-stabilized emulsions were investigated. Given the geometrical similarities of the three scales used (0.25, 5, and 35 L), emulsions were prepared using off-centered pitched blade and Rushton turbines in unbaffled tanks. Standard criteria for surfactant-stabilized emulsions (constant energy dissipation rate, Weber number, Reynolds number, impeller tip speed, and circulation time) were applied to concentrated and diluted emulsions. Silicone oil (50 cSt) was used as the dispersed phase in water, and glass microspheres ($d_{32} \approx 3$ µm) were used as a stabilizer. Emulsions were characterized by droplet size measurements using a Malvern Mastersizer 3000. The Sauter mean diameter ($d_{32}$) as well as $dv_{10}$ and $dv_{90}$ were used to compare emulsions. A decolorization technique was used to evaluate mixing times. None of the parameters investigated was suitable for use as a scale-up criterion for the production of Pickering emulsions. The use of the Weber number, Reynolds number, and tip speed as scale-up criteria resulted in higher diameters with the largest scale while the opposite tendency was observed with circulation time and energy dissipation. The best scale-up was obtained with the energy dissipation rate and tip speed, suggesting that the suitable scale-up exponent would be between 2/3 (scale-up exponent with the energy dissipation rate) and 1 (scale-up exponent with the tip speed).

**Key words:** Pickering emulsions, scale-up, suspension, emulsification process, and stirred tanks.

## 5.1 Introduction and theoretical basis

Emulsification processes are used in a wide range of applications, including the production of foods, cosmetics, pharmaceutics, and chemicals (Chappat, 1994). In general, emulsions are stabilized by decreasing the interfacial tension using amphiphilic molecules called surfactants. However, solid particles have attracted growing interest as stabilizing agents in recent years. They have proved to be quite useful in generating emulsions that are more stable and have a longer shelf-life than their surfactant-stabilized counterparts. The stabilization of emulsions using particles is becoming increasingly popular, especially for cosmetics and pharmaceutics, in which surfactants are a major cause of skin irritation and can be toxic. (Chevalier et al., 2013) (Wu et al., 2016) The biomedical industry is also interested in these emulsions because of their higher stability at freezing temperatures. They have also been used to prepare porous and composite materials. In addition, various industries, as well as consumers, are increasingly looking for "greener" alternatives with a view to sustainable development. Pickering emulsions can be considered "greener" than their surfactant counterparts because the solid particles can be recycled. Centrifugation and magnetic fields can be used to break up properly designed Pickering emulsions. This powerful and unique feature makes it possible to recover and reuse the particles.

The ability of solid particles to act as stabilizers in emulsions was first reported by W. Ramsden and S.U. Pickering (Ramsden, 1903) (Pickering, 1907). These two pioneers showed that it is possible to produce emulsions that are more stable than surfactant-stabilized emulsions for longer periods and in harsher conditions. However, these types of emulsions attracted no significant interest until the 1980s when studies on solid-stabilized emulsions (SSEs) explored the effects of different components on emulsion stability, type, size, and rheology. Several studies have shown that the high stability of SSEs is mainly due to the formation of steric particle networks around the droplets (Yan et al., 1994) (Binks B. , 2007) (Horozov et al., 2005) (Arditty et al., 2003), which is facilitated by the elevated energy of attachment of the particles to the interface. Studies on emulsion stability have also shown that particles of intermediate hydrophobicity (with a contact angle of ≈90° between the particle and the liquid phases) generate the most stable emulsions (Binks et al., 2000) (Aveyard et al., 2003) (Binks et al., 2005). Research on particle size (Tarimala et al., 2004) and concentration (Arditty et al., 2003) has revealed that droplet size decreases when particle size is decreased or when particle concentration is increased. Studies on oil viscosity have shown that

emulsion stability is enhanced with higher viscosity oils (Golemanov et al., 2006) (Fournier et al., 2009). Emulsion type has also been studied by investigating the effect of particle wettability (Yan et al., 2001) (Binks et al., 2000) (Binks et al., 2005) (Aveyard et al., 2003), oil polarity (Golemanov et al., 2006) (Frelichowska et al., 2009), and the pH of the aqueous phase (Yan et al., 1996) (Binks et al., 2006). Emulsion type is controlled by particle affinity with oil and water, such that hydrophilic particles stabilize oil-in-water droplets and hydrophobic particle stabilize water-in-oil droplets. Particle wettability is also affected by the pH of the aqueous phase, which in return dictates emulsion type. The effects of particle size (Binks et al., 2001) (Tarimala et al., 2004) and particle concentration (Arditty et al., 2003) on the size distribution of emulsions have also been studied. Rheology studies have shown that SSEs follow the Herschel-Bulkley model (Midmore, 1998) (Torres et al., 2007) (Braisch et al., 2009).

While the effect of the formulation on SSE properties has been investigated in depth, emulsion processing has received much less attention. Tsabet et al. (2015a) did, however investigate the effect of oil viscosity, impeller speed, and particle coverage potential on emulsion properties. They proposed a modelling procedure to predict droplet size from process conditions (Tsabet et al., 2015b). They first determined and compared the interface generation potential and the particle coverage potential to deduce a theoretical covered interface, and then determined the stabilization efficiencies in order to deduce the effectively covered interface and mean droplet size. This semi-empirical approach was validated experimentally in a mixing tank using a wide range of oil viscosities (20 – 5000 cSt). The capacity of the system to generate an interface was quantified using Weber numbers (100-600) and coverage potentials (5-20 $m^2$). However, one question remains. Given our current state of knowledge of solid-stabilized emulsions and process design, is this enough to start the mass production of emulsions using solid particles?

Like most mixing processes involving several mechanisms, defining a scale-up rule for solid-stabilized emulsions is not a straightforward task and, to date, not much work has been devoted to this aspect. Different criteria have been defined for conventional emulsions, depending on the system properties. Table 5-1 presents a review of studies on conventional emulsion scale-ups and their conclusions.

Table 5-1 – Review of scale-up rules for conventional emulsions

| *Reference* | *Emulsification system* | *Geometrical parameters* | *Formulation & Physical properties* | *Characterization method* | *Scale-up factor* | *Recommended rule* |
|---|---|---|---|---|---|---|
| *Podgórska et al., 2001* | Stirred tanks with 6-blades Rushton turbine | $T_1$ = 0.15 m<br>T/D = 1.49//2.11//3 | $\phi_d = 0.05$<br>$\mu_D/\mu_C = 1.3$ &<br>$\rho_D/\rho_C = 1.03$<br>$\sigma = 0.034$ N/m | Numerical analysis based on solving the population balance equation to obtain droplet size distribution | $T_i/T_1$ = 3.33//6.66//16.66 | Constant P/V and average circulation time without geometrical similarity |
| *Podgórska, 2005* | Baffled stirred tanks with a 6-blades Rushton turbine | $T_1$ = 0.15 m<br>T/D = 3 | $\phi_d = 0.15$<br>$\mu_D/\mu_C = 1$ &<br>$\mu_D/\mu_C = 500$<br>$\rho_D/\rho_C = 1$<br>$\sigma = 0.04$ N/m | Numerical analysis based on solving the population balance equation to obtain droplet size distribution | $T_2/T_1$ = 6.66 | Constant P/V and average circulation time without geometrical similarity |

Table 5-1 – Studies on the scaling of conventional emulsions (continued)

| *Reference* | *Emulsification system* | *Geometrical parameters* | *Formulation & Physical properties* | *Characterization method* | *Scale-up factor* | *Recommended rule* |
|---|---|---|---|---|---|---|
| *Capdevila et al., 2010* | Stirred tanks with a helix mixer | $V_{tank1}$ = 100 mL<br>$D_1$ = 11 mm | Highly concentrated W/O emulsions<br>Oil: decane, dodecane, hexadecane<br>% Water = 91 - 95 wt%<br>Stabilizer: Span 80<br>S:O (wt./wt.) = 15:85 - 29:71 | Emulsion stability: Back scattering light analysis (Turbisoft MA2000)<br>Droplet size distribution: Optical microscopy (Zeiss Axiovert 100 A)<br>Emulsion rheology: HAAKE RS150 rheometer | $V_{tank1}$ = 100 mL<br>$V_{tank2}/V_{tank1}$ = 6.85 | No dimensionless variables commonly used in scale-up studies, such as the Reynolds number, was suitable for this system |

Table 5-1 – Studies on the scaling of conventional emulsions (continued)

| *Reference* | *Emulsification system* | *Geometrical parameters* | *Formulation & Physical properties* | *Characterization method* | *Scale-up factor* | *Recommended rule* |
|---|---|---|---|---|---|---|
| *(Suárez et al., 2013)* | Flat metallic membranes in baffled & unbaffled tanks with different impellers (2 Paddle impellers & 1 marine propeller) | Paddle impellers: $D_1$ = 60//90 mm<br>Marine propeller: $D_1$ = 60 mm<br>D/T = 0.33 & D/T = 0.5<br>H/T = 1<br>$D_{impeller-membrane}$ = 5 mm | O/W emulsions (1.5 wt%)<br>Continuous phase: Water with viscosity modifier (CMCNa)<br>Dispersed phase: Food-grade extra virgin olive oil ($\mu_D$ = 51 mPa·s, $\rho_D$ = 886 kg/m$^3$)<br>Stabilizer: Tween 20® (2 wt%) | Droplet size distribution: Laser diffraction technique (Malvern Mastersizer S) | $T_i/T_1$ = 1.5//2.25 | Constant impeller tip speed with geometrical similarity |

Table 5-1 – Studies on the scaling of conventional emulsions (continued)

| *Reference* | *Emulsification system* | *Geometrical parameters* | *Formulation & Physical properties* | *Characterization method* | *Scale-up factor* | *Recommended rule* |
|---|---|---|---|---|---|---|
| *(May-Masnou et al., 2013)* | Glass jacketed vessels Agitated with a three-level P-4 pitched blade impeller | $T_1$ = 50 mm<br>D/T = 0.9 &<br>H/T = 0.8 | Highly concentrated W/O emulsions<br>Continuous phase: Dodecane<br>Dispersed phase: Milli-Q water ($\phi_d = 0.9$)<br>Stabilizer: Span 80® (HLB = 4.3) | Droplet size distribution: Optical microscopy (Optika) | $T_i/T_1 = 2$ | Low surfactant concentration:<br>$N_2 = N_1 (D_1/D_2)^{0.5}$<br>High surfactant concentration:<br>$N_2 = N_1 (D_1/D_2)^{0}$ |

Table 5-1 – Studies on the scaling of conventional emulsions (continued)

| *Reference* | *Emulsification system* | *Geometrical parameters* | *Formulation & Physical properties* | *Characterization method* | *Scale-up factor* | *Recommended rule* |
|---|---|---|---|---|---|---|
| *(May-Masnou et al., 2014)* | Glass jacketed vessels Agitated with a three-level P-4 pitched blade impeller | $T_1$ = 50 mm<br>D/T = 0.9 & H/T = 0.8 | Highly concentrated W/O emulsions<br>Continuous phase: Dodecane<br>Dispersed phase: Milli-Q water ($\phi_d = 0.9$)<br>Stabilizer: Span 80® (HLB = 4.3) | Emulsion stability: Back scattering light analysis (Turbisoft MA2000)<br>Droplet size distribution: Optical microscopy (Optika)<br>Emulsion rheology: HAAKE Mars III rheometer | $T_i/T_1$ = 2//4 | Constant P/V with geometrical similarity |

The six studies presented in Table 5-1 are useful because they propose potential scale-up criteria that can be tested on solid-stabilized emulsions. Over the years, an enormous amount of research has been done in an attempt to establish a scaling method for surfactant-stabilized emulsions and dispersions. However, there is no unique method, and scaling methods are more or less system dependent (Table 5-1) and depend on parameters such as the dispersed-to-continuous phase viscosity ratio, the surfactant concentration, and the mixing configuration. Moreover, a methodology for scaling Pickering emulsions is lacking, especially a proper methodology for generating solid-stabilized emulsions. Nonetheless, we collected the scaling methods (Table 5-1) used for conventional surfactant-based emulsions and dispersions in order to investigate their potential applicability to Pickering emulsions. These methods were used as a starting point for understanding SSE scaling. The purpose of the present work was to answer the following questions:

(i) Is it possible to use one of the conventional dispersion and surfactant-based emulsion scale-up criteria on SSEs?

(ii) If not, is it possible to find a clue or gather insights from these criteria for future investigation on SSE scaling?

## 5.2 Materials and methods

The general experimental methodology can be divided into three main steps. The first step was to prepare the emulsification setups (scales from 0.25 to 35 L) using an off-centered pitched-blade or a Rushton turbine. Impeller rotation speeds were set to match the required scaling criteria. The impeller speeds chosen as a function of scale for each criterion are presented in section 5.2.1. The second step was to prepare the emulsion itself. The particles were first suspended in the continuous phase, and the dispersed phase was then added to the suspension. In the third step, the droplet size and distribution of the emulsions were characterized using a laser diffraction method. The relevant parameter for successful scaling was the variation in the diameters ($d_i$, where $i$ is 10, 50, 90, or 32) between two scales. If using one criterion led to $\Delta d_i = 0$ (for all $i$), then scaling was considered successful. The same procedure was repeated for all the criteria (Table 5-2). The steps are detailed in the following sections.

### 5.2.1 Equation development

Based on a literature review, five criteria were selected, and their usefulness as a scale-up rule for Pickering emulsions was investigated. The first parameter investigated was the Reynolds number (equation 5.1), which is the ratio of inertial forces to viscous forces:

$$Re = \frac{\rho_c N D^2}{\mu_e} \quad (5.1)$$

$$\rho_c = \frac{m_w + m_p}{\frac{m_w}{\rho_w} + \frac{m_p}{\rho_p}} \quad (5.2)$$

$$\mu_e = \mu_w \left[1 + 2.5\phi_d \left(\frac{0.4\mu_o + \mu_w}{\mu_o + \mu_w}\right)\right] \quad (5.3),$$

where $\rho_c$ is the apparent density (in kg/m$^3$) of the continuous phase (equation 5.2), $\rho_w$ is the density (in kg/m$^3$) of water, $\rho_o$ is the density (in kg/m$^3$) of the oil, N is the rotational speed of the impeller (in s$^{-1}$), D is the diameter of the impeller (in m), $\mu_e$ is the viscosity (in Pa.s) of the emulsion calculated using Taylor's equation (equation 5.3) (Taylor, 1932), $\mu_w$ is the viscosity (in Pa.s) of water, $\mu_o$ is the viscosity (in Pa.s) of the oil, and $m_w$ and $m_o$ are the weights (in kg) of the water and the particles, respectively, in the system. Assuming a constant formulation of the emulsion, keeping the Reynolds number constant between two geometrically similar scales resulted in equation 5.4, from which the impeller speed at the larger scale (2) can be obtained from a similar system at the smaller scale (1):

$$N_2 = N_1 * \left(\frac{D_1}{D_2}\right)^2 \quad (5.4)$$

Due to the presence of highly concentrated emulsions in the present work (up to 30% v/v), it may have seemed appropriate to use the equation proposed by Phan-Thien et al. (1997) to determine the viscosity of the emulsion. However, this equation does not provide satisfying results with dispersed phase volume fractions below 40%, which is why we used Taylor's equation.

The second parameter investigated was the Weber number (equation 5.5), which is the ratio of inertia forces to surface tension, expressed as

$$We = \frac{\rho_c N^2 D^3}{\sigma} = \frac{\rho_c (ND)^2}{(\sigma/D)} \quad (5.5),$$

where $\sigma$ is the surface tension (in N/m). The Weber number plays an important role in emulsification because it scales the ability of a given system to create droplets by inertia ($(ND)^2$) versus the capacity of the droplets to resist deformation by Laplace pressure ($\sigma/D$). Considering constant physical properties (density and interfacial tension), keeping the Weber number constant between two geometrically similar scales resulted in the following equation for impeller speed at each scale:

$$N_2 = N_1 * \left(\frac{D_1}{D_2}\right)^{\frac{3}{2}} \quad (5.6)$$

The third parameter investigated was the speed of the impeller tip. Keeping this parameter constant resulted in the following equation:

$$N_2 = N_1 * \left(\frac{D_1}{D_2}\right) \quad (5.7)$$

The fourth parameter investigated was the power per unit of volume $\varepsilon$ ($W/m^3$) obtained from equation 5.8. The effect of keeping the specific power constant with respect to the rotational speed is given by equation 5.9.

$$\varepsilon = \frac{P}{V} = \frac{N_p \rho N^3 D^5}{V} \quad (5.8)$$

$$N_2 = N_1 * \left(\frac{D_1}{D_2}\right)^{\frac{2}{3}} \quad (5.9),$$

where V is the volume of the emulsion (in $m^3$) and $N_p$ is the Power number.

The fifth parameter investigated was circulation time, which has been used to scale up rapidly coalescing systems in stirred vessels. It can be calculated using equation 5.10 (Paul et al., 2003):

$$t_c = \frac{V_{tank}}{N_q \cdot D^3 \cdot N} \quad (5.10),$$

where $t_{circ}$ is the mean circulation time, $N_q$ is the flow number (0.79 for a pitched blade turbine and 0.72 for a Rushton turbine under turbulent conditions) (Paul et al., 2003), N is the impeller speed, D is the impeller diameter, and $V_{tank}$ is the tank volume. Considering geometrical similarity, an equal circulation time results in an equal impeller rotational speed.

Table 5-2 summarizes the parameters investigated and their effects on the rotational speed for geometrically similar scales. For each parameter, the relation for calculating the impeller speed at the second scale is presented. Table 3 presents the impact of a constant criterion on the evolution of the other parameters when transitioning from scale 1 to scale 2. In other words, when keeping one parameter constant through all scales, it will force the other parameters to increase or decrease when scaling. Maintaining a constant circulation time ($t_c$) between the 0.25 and 5-L scales, for example, will result in a higher power per unit of volume at the 5-L scale. This is due to the larger power input needed to maintain the same 0.25-L circulation time at a larger scale. Indeed, equation 10 states that when the tank volume is increased ($V_{tank}$), $N_q \cdot D^3 \cdot N$ should be increased to keep $t_c$ constant between the 0.25 and 5-L scales. Table 5-3 is insightful when it comes to explaining the behavior of the resulting droplet size (see section 5.3) while scaling with different criteria. If the correlations for predicting droplet size in a liquid dispersion or a solid-stabilized emulsion process are examined as described in Tsabet and Fradette (2015), the parameters presented in Table 5-3 would be of utmost importance when it comes to understanding the phenomena taking place in an agitated vessel.

These criteria were all tested using conventional emulsions. Some, such as the P/V criterion, allowed for the scale-up of these emulsions. However, Pickering emulsions differ from conventional emulsions by the presence of solid particles in the formulation. Indeed, complete or at least satisfying particle suspensions are required to maximize particle-droplet contact and stabilize Pickering emulsions. Some of these criteria are thus also used to scale up solid-liquid systems. Jafari et al. (2012) published a review of scale-up rules used for solid-liquid dispersions in agitated vessels. A large number of the articles they cite propose the use of power-law exponents ranging from 0.8 to 1. A reasonable scale-up rule for Pickering emulsions would be an amalgam of the procedures used for solid-liquid and conventional liquid-liquid dispersions.

Table 5-2 – Scale-up criteria investigated

| *Criteria* | *Constant* | *$N_2$ = fct ($N_1$)* |
|---|---|---|
| *Reynolds number* | $ND^2$ | $N_2 = N_1 * \left(\frac{D_1}{D_2}\right)^2$ |
| *Weber number* | $N^2D^3$ | $N_2 = N_1 * \left(\frac{D_1}{D_2}\right)^{\frac{3}{2}}$ |
| *Mixing time* | $N\theta_m$ | $N_2 = N_1$ |
| *Impeller tip speed* | $ND$ | $N_2 = N_1 * \left(\frac{D_1}{D_2}\right)$ |
| *Specific power* | $N^3D^2$ | $N_2 = N_1 * \left(\frac{D_1}{D_2}\right)^{\frac{2}{3}}$ |

Table 5-3 – Effect of a constant criterion on parameter evolution

| *Criterion* | *$T_{c2}/T_{c1}$* | *$\varepsilon_2/\varepsilon_1$* | *$v_2/v_1$* | *$We_2/We_1$* | *$Re_2/Re_1$* |
|---|---|---|---|---|---|
| *$T_c$ = constant* | 1 | > 1 | > 1 | > 1 | > 1 |
| *ε = constant* | > 1 | 1 | > 1 | > 1 | > 1 |
| *v = constant* | > 1 | < 1 | 1 | > 1 | > 1 |
| *We = constant* | > 1 | < 1 | < 1 | 1 | > 1 |
| *Re = constant* | > 1 | < 1 | < 1 | < 1 | 1 |

## 5.2.2 Materials

Soda lime glass microspheres (Cospheric LLC, USA) with a density = 2500 kg/m$^3$, a $d_{32}$ = 3.23 μm, a $d_{10}$ = 1.36 μm, a $d_{50}$ = 6.19 μm, a $d_{90}$ = 14.12 μm, and a contact angle ($\theta_{ow}$) = 94° ± 4° were used as stabilizers. The contact angle was determined using the method developed by Fournier et al. (2009), which is described in section 5.2.3.4.4 (Tsabet et al., 2016). Fifty centistoke (cSt) pure silicone oil (Clearco Inc., USA) with a density of 960 kg/m$^3$ was used as the dispersed phase, and deionized water was used as the continuous phase.

## 5.2.3 Experimental methods

### 5.2.3.1 Emulsification setup

Emulsions were produced using unbaffled tanks and off-centered impellers (Fig. 5-1). This configuration prevents the formation of a vortex and has the same mixing performance as a baffled tank with a centered impeller (Nishikawa et al., 1979) (Novak et al., 1982) (King et al., 1985) (Karez et al., 2004) (Karez et al., 2005) (Montante et al., 2006).

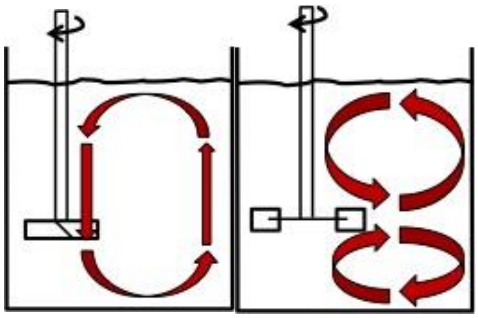

(a) (b)

Figure 5-1 – Emulsification system with (a) a PBT and (b) an RT [taken from Tsabet (2014)]

Three sizes of tanks (0.25, 5, and 35 L) were used to perform the scale-up experiments with a 4-blade pitched-blade turbine (PBT) and a 6-blade Rushton turbine (RT) (USI-MAX, Canada). The characteristic dimensions of each scale are given in Table 5-4 while the geometrical similarities that were kept constant for each scale are given in Table 5-5.

Table 5-4 – Geometrical parameters of the components for each scale

| *Geometrical parameters* | *Scale 1: 0.25 L (in cm)* | *Scale 2: 5 L (in cm)* | *Scale 3: 35 L (in cm)* |
|---|---|---|---|
| Tank diameter (T) | 6.50 | 16.30 | 35.50 |
| Impeller diameter (D) | 2.17 | 5.43 | 11.83 |
| Length of one blade (L) | 0.54 | 1.36 | 2.96 |
| Height of one blade (W) | 0.43 | 1.09 | 2.37 |

Table 5-5 – Geometrical similarities between each scale

| *Geometrical similarities* | *T/D* | *$H_{liq}$/T* | *D/L* | *D/W* | *T/R* | *T/C* |
|---|---|---|---|---|---|---|
| | 3 | 1 | 4 | 5 | 6 | 3 |

where D is the diameter of the impeller, T is the diameter of the tank, $H_{liq}$ is the height of the liquid in the tank, L is the length of the impeller blade, W is the width of the impeller blade, R is the off-centering distance, and C is the clearance of the impeller.

#### 5.2.3.2 Formulation

Oil-in-water emulsions (o/w) were prepared for each experiment. Two dispersed phase fractions were considered (diluted at $\phi_d$ = 5% v/v and concentrated at $\phi_d$ = 30% v/v). The quantities of each phase used at each scale for the two concentrations ($\phi_d$) are given in Table 5-6.

$$\phi_d = \frac{V_D}{V_D + V_C} \quad (5.11),$$

where $V_D$ is the volume of the dispersed phase and $V_C$ is the volume of the continuous phase, both in $m^3$.

Table 5-6 – Composition of each formulation used for each scale

| *Phase* | *Scale 1: 0.25 L (in g)* | | *Scale 2: 5 L (in g)* | | *Scale 3: 35 L (in g)* | |
|---|---|---|---|---|---|---|
| | 30% | 5% | 30% | 5% | 30% | 5% |
| *Continuous phase* | 151.2 | 205.2 | 2380.7 | 3231 | 24596.6 | 33381 |
| *Dispersed phase* | 62.2 | 10.4 | 979.5 | 163.2 | 10119.7 | 1686.6 |
| *Stabilizer* | 5.3 | 0.9 | 83.3 | 13.9 | 860.8 | 143.5 |

### 5.2.3.3 Emulsion preparation

The preparation of an o/w emulsion began by pouring deionized water into the tank. The impeller was turned on and was set at the selected rotational speed. The solid particles were then added and were mixed for 10 min to disperse the particles in the water and break up aggregates, if any. The oil was then gently added to the water/particle mixture, and mixing was continued for a further 24 h. Figure 5-2 illustrates the basic steps for preparing a solid-stabilized emulsion and for sampling the emulsion at the end of the process.

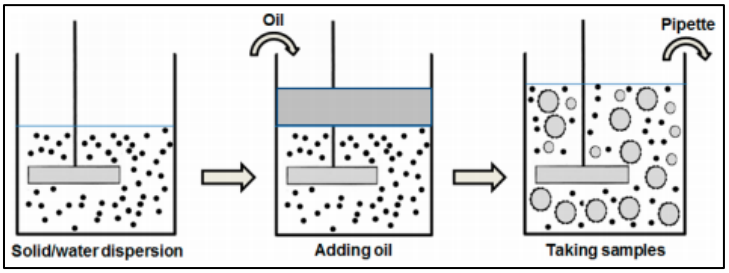


Figure 5-2 – Steps to prepare a solid-stabilized emulsion [taken from Tsabet and Fradette (2015)]

### 5.2.3.4 Emulsion characterization

#### *5.2.3.4.1 Emulsion type*

The emulsion type was determined by conductivity measurements using an OAKTON conductivity meter (CON 110 Series).

*5.2.3.4.2 Emulsion size distribution*

The droplet size distribution was obtained using a Malvern Mastersizer 3000. Emulsions were characterized using the Sauter mean diameter ($d_{32}$), $d_{10}$, and $d_{90}$. Plastic pipettes were used for sampling. The narrow tip was cut off to prevent high shear at the tip that could break larger droplets and result in an unrepresentative sample of the emulsion. The pipette was dipped halfway into the tank, and three samples were taken, with a 10-s delay between samples, which was higher than the circulation time (see section 5.3.1) and which ensured a representative sampling of the whole tank. Low-density polyethylene plastic pipettes were used rather than glass pipettes because of their inherently hydrophobic nature, which prevents droplets from sticking to the wall of the pipette.

*5.2.3.4.3 Mixing and circulation time measurements*

The decolorization technique of Cabaret et al. was used to measure mixing and circulation times (Cabaret et al., 2007). The pH indicator, an aqueous solution of 0.08% (w/w) of bromocresol purple, was poured into the tank and was mixed into the previously prepared emulsion. The pH was controlled using a predetermined quantity of acid (1 M HCl) or base (1 M NaOH). Mixing times were obtained by recording the change in color from purple to yellow, i.e., when the pH changed from 6.8 to 5.2 (Fig. 5-3). The change in color was recorded using a Sony Digital Handycam (DCR-PC101). The video was analyzed using customized software to obtain the decolorization curve and determine the mixing time. The circulation time is 20% of the mixing time (Paul et al., 2003).

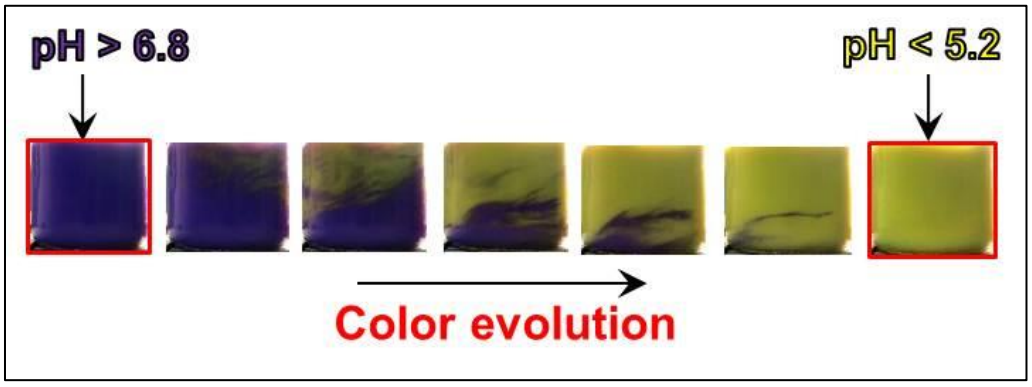


Figure 5-3 – Change in color using the decolorization method [taken from Tsabet and Fradette (2015)]

*5.2.3.4.4 Contact angle measurement*

As mentioned previously, the properties of solid-stabilized emulsions are very sensitive to particle wettability, which affects both emulsion type and stability by modulating the particle attachment process and interactions at the interface. Because they are based on contact angle measurements on flat surfaces, most of the experimental techniques used to quantify this key parameter are unsuitable for solid particles because of the effect of porosity on reproducibility. Capillary rise methods have been proposed as an alternative, but they also have limitations due to particle packing inside the capillary tube. In order to include the effect of particle structure on the capillary rise process, Fournier et al. (2009) proposed that the Blake-Kozeny equation (Equation 5.12), which describes the flow through packed spheres in a cylindrical tube, be used:

$$\frac{h}{t} = \rho g \frac{D_{50}^2}{150\eta} \frac{\varepsilon_{eff}^3}{\left(1-\varepsilon_{eff}\right)^2} \quad (5.12),$$

where $h$ is the height of the liquid front (in m) at time $t$ (in s), ρ is the density of the particles (kg/m$^3$), $D_{50}$ is the mean diameter of the particles (in m), $g$ is equal to 9.81 m/s$^2$, $\eta$ is the viscosity of the liquid (in Pa.s), and $\varepsilon_{eff}$ is the effective porosity of the bed. By measuring $h$ at a given number of times $t$, it is possible to deduce the effective porosity of the bed.

The effective radius given by

$$r = \frac{\sqrt{\varepsilon_{eff}}\, R_C}{K^4} \quad (5.13),$$

where $R_C$ is the radius of the capillary tube (in m) and $K = 25/6$ is the tortuosity factor as determined by Bird et al. (1960). Knowing the immersion depth of the capillary tube in the liquid L (in m) and the liquid surface tension $\gamma_L$ (in N/m), the contact angle θ (in rad) is obtained from the Washburn equation (Equation 5.14) describing the capillary rise kinetics (Siebold et al., 1997):

$$h^2 + 2hL = \frac{r\gamma_L \cos\theta}{2\eta} t \quad (5.14)$$

Once the particle contact angle has been obtained for both phases, the particle contact angle at the water-oil interface can be deduced using the equation of Zhou et al. (2011):

$$\cos\theta_{ow} = \frac{\gamma_{aw}}{\gamma_{ow}} \cos\theta_{aw} - \frac{\gamma_{ao}}{\gamma_{ow}} \cos\theta_{ao} \quad (5.15),$$

where $\theta_{ow}$ is the contact angle at an oil-water interface (in °), $\theta_{aw}$ is the contact angle at an air-water interface (in °), $\theta_{ao}$ is the contact angle at an air-oil interface (in °), $\gamma_{aw}$ is the surface tension of water (in N/m), $\gamma_{ao}$ is the surface tension of the oil (in N/m), and $\gamma_{ow}$ is the interfacial tension between the oil and water (in N/m).

In the present work, the experimental setup was first validated by reproducing the conditions of Fournier et al. (2009). Pyrex capillaries ($d_{Cap}$ = 0.8-1.1 mm) (Corning Inc., NY, USA) were filled with Atomet 95 iron powder ($d_{50}$ = 34 µm and ρ = 2.25 g/cm$^3$) (QMP, Montreal, Canada). To prevent the bed of particles falling from the capillaries, a 4-mm-long column of glass wool was inserted into the capillaries before the iron powder was added. After dipping the capillaries in the liquid, capillary rise was filmed using a Sony Digital Handycam (DCR-PC101). The video was analyzed using customized software to obtain the height of the liquid front "h" using a ruler and the rising time "t" (Fig. 5-4).

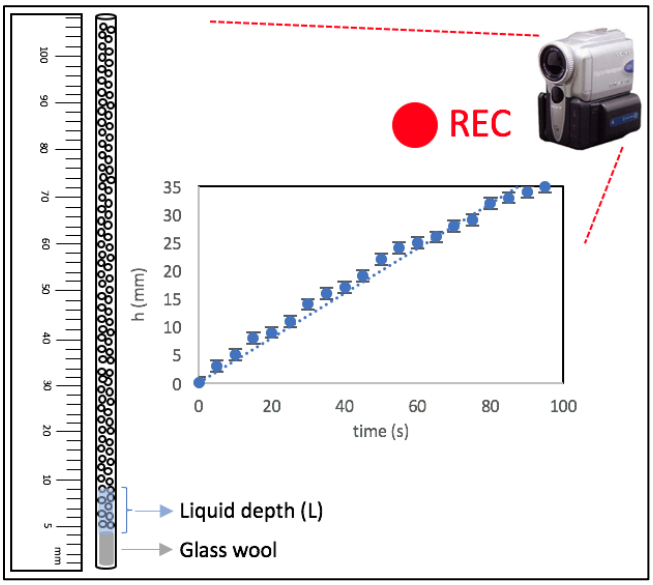


Figure 5-4 – Capillary rise set-up

Very good agreement was observed with the results of Fournier et al. (2009), who reported a contact angle of 67° ± 5° with iron particles while we observed a contact angle of 71° ± 5° with similar particles. The measurements were recorded using iron particles and 3 µm glass beads, for which we obtained a contact angle of 94° ± 5°, and were reproducible (Fig. 5-5).

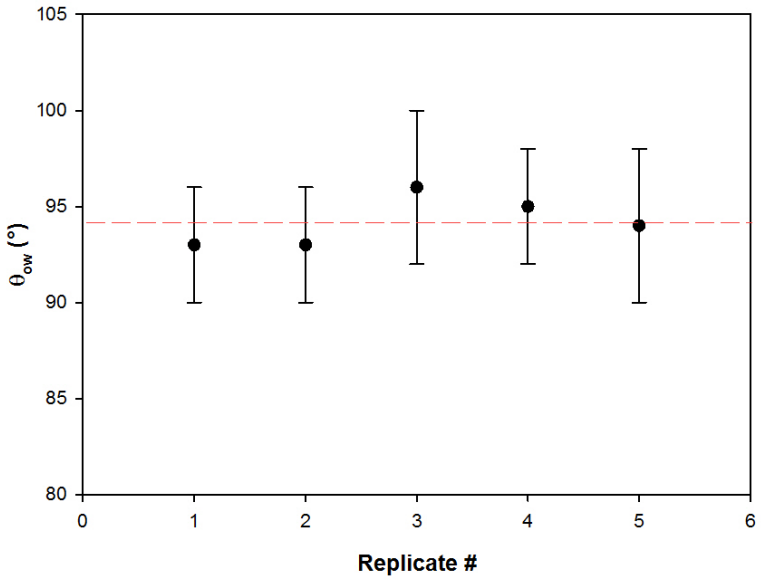


Figure 5-5 – Contact angle with glass beads

## 5.3 Results and discussion

### 5.3.1 Circulation time

The first step was to confirm that the impeller rotational speed corresponded to the same circulation time for a given geometry. Decolorization experiments were performed at different impeller rotational speeds for two scales. Table 5-7 presents an example of when the same rotational speed (900 rpm) resulted in the same mixing time and the same circulation time.

Table 5-7 – Mixing and circulation times using the pitched blade turbine

| *Parameter* | *0.25 L* | *5 L* |
|---|---|---|
| | 900 rpm | |
| *Experimental mixing time (s)* | 5.88 | 5.64 |
| *Experimental circulation time (s)* | 1.18 | 1.13 |
| *Theoretical circulation time (Equation 10) (s)* | 1.78 | 1.79 |

Figure 5-6 presents a comparison of droplet size distributions between two scales when circulation time was used as a scale-up criterion with the PBT for diluted and concentrated systems.

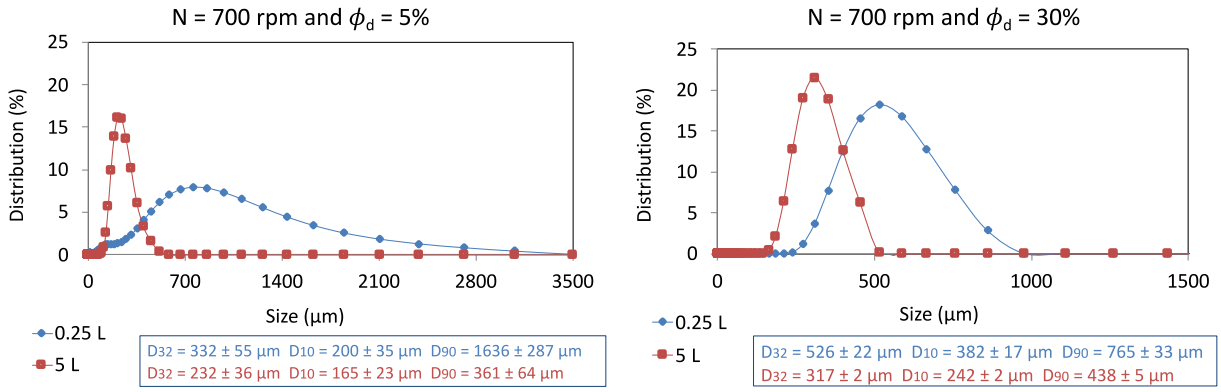


(a) (b)

Figure 5-6 – Droplet size distribution when the same circulation times were used for (a) a diluted and (b) a concentrated system with the PBT

Figure 5-7 presents a comparison of droplet size distributions between scales when circulation time was used as a scale-up criterion with the RT for diluted and concentrated systems.

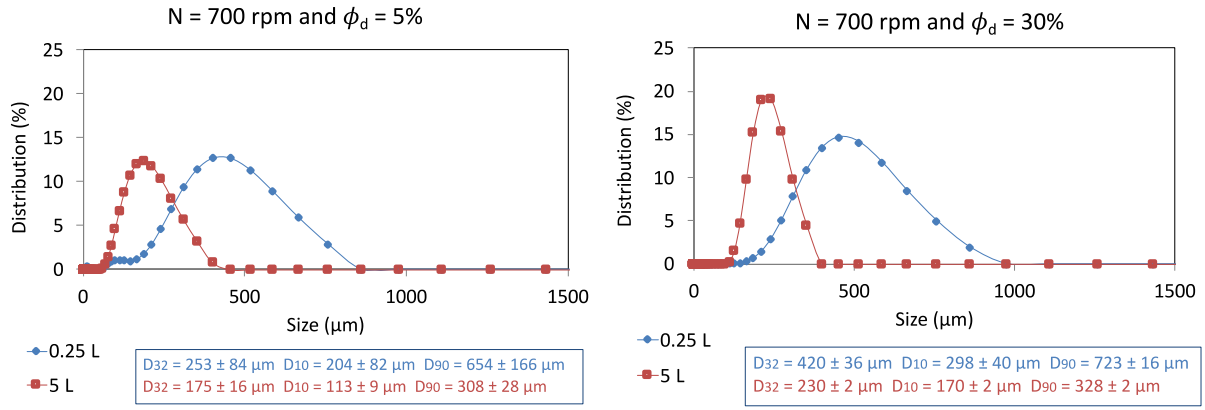


(a) (b)

Figure 5-7 – Droplet size distribution when the same circulation times were used for (a) a diluted and (b) a concentrated system with an RT

Keeping the circulation time constant between two scales did not generate emulsions with the same droplet characteristics for the PBT and RT. Increasing the scale resulted in smaller droplet sizes, indicating that breakage and stabilization were more efficient and/or coalescence was less effective. With the same impeller rotational speed, increasing the scale resulted in a higher Reynolds number, Weber number, ε, and tip speed (Table 5-3), indicating that the ability of the system to generate an interface also increased. It can be assumed that the coalescence frequency also increased as the droplet/droplet collision frequency increased with the energy dissipation rate. However, the particle/droplet collision rate also increased with the energy dissipation rate, promoting droplet stabilization and counterbalancing the increase in droplet/droplet collision frequency. A comparison of the PBT and the RT results showed that smaller sizes were obtained with the RT, indicating that the RT had a higher breakage capacity. This was mainly due to the number of blades (6 blades for the RT vs. 4 blades for the PBT) and the nature of the flow patterns generated. The RT generates two circulation loops while the PBT generates one longer loop with fewer passages of droplets in the high shear impeller zone where breakage occurs. The scale-up operation with the PBT also gave slightly better results than those obtained with the RT for concentrated emulsions while the opposite occurred with diluted systems. This effect is related to the breakage and coalescence mechanisms. For concentrated emulsions, droplet size is controlled by the coalescence mechanism while breakage is the dominant phenomenon associated with diluted systems. Breakage was less efficient with the PBT while coalescence was more efficient because of the larger circulation loop. It should be noted that these experiments were only carried out at the 0.25 and 5 L scales due to safety considerations with respect to the operation of the 35 L impeller shaft at such a high speed (700 rpm).

### 5.3.2 Reynolds number

Figures 5-8 and 5-9 present a comparison of droplet size distributions between two scales when using the Reynolds number as a scale-up criterion with the PBT and the RT for diluted and concentrated systems. The impellers produced completely different emulsion characteristics between the two scales. Smaller droplets were obtained with the smaller scale for the same Reynolds number with the PBT and the RT. This was due to the fact that the speed of the impeller tip, the Weber number, and the power input were greater in the smaller system at a constant Reynolds number, which generates more interface (Table 5-2). In addition, for the same Reynolds

number, the circulation time decreased at the smaller scale, resulting in a decrease in droplet/droplet collision efficiency and thus in coalescence efficiency. The RT produced smaller droplets than the PBT for both scales and for both emulsion concentrations. In these cases, the experiments were only conducted at the 5 and 35 L scales. Achieving such a highly turbulent Reynolds condition at the 0.25 L scale would have required a very high speed due to the small impeller diameter, which could not be achieved with our setup. In addition, it would not be safe to use such a high speed.

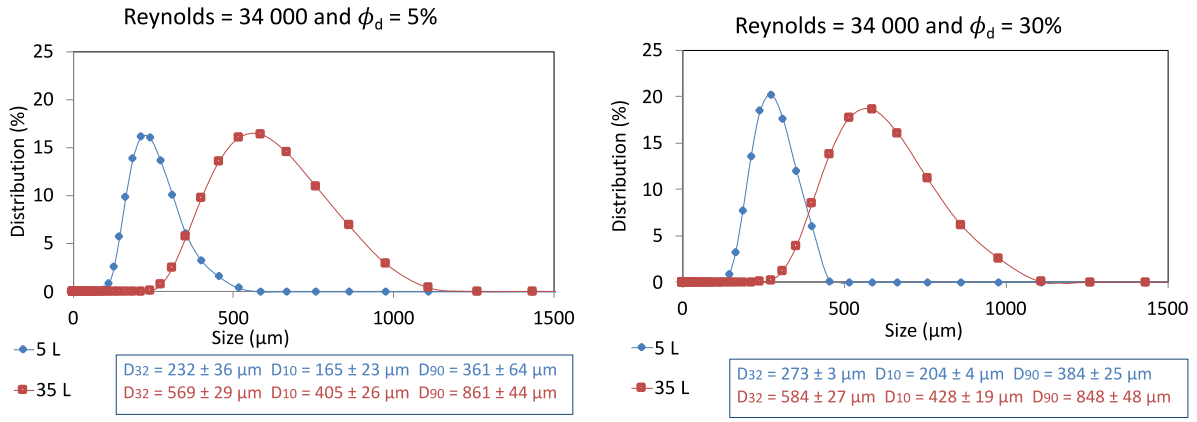


(a) (b)

Figure 5-8 – Droplet size distribution using the same Reynolds number for (a) a diluted and (b) a concentrated system with the PBT

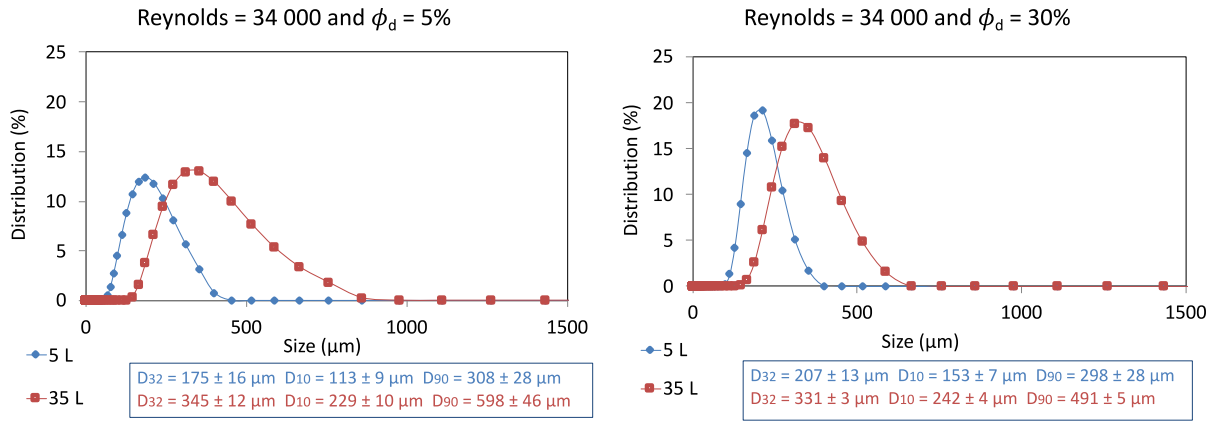


(a) (b)

Figure 5-9 – Droplet size distribution using the Reynolds number for (a) a diluted and (b) a concentrated system with the RT

### 5.3.3 Weber number

Figures 5-10 and 5-11 show a comparison of the droplet size distributions between the scales when using the Weber number as a scale-up criterion with the PBT and the RT for diluted and concentrated systems.

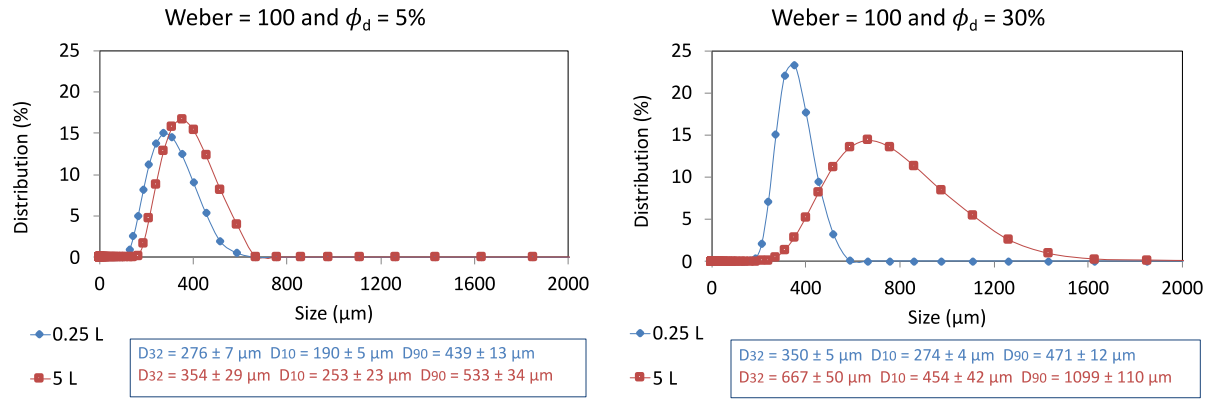


(a) (b)

Figure 5-10 – Droplet size distributions when the same Weber number was used for (a) a diluted system and (b) a concentrated system with the PBT

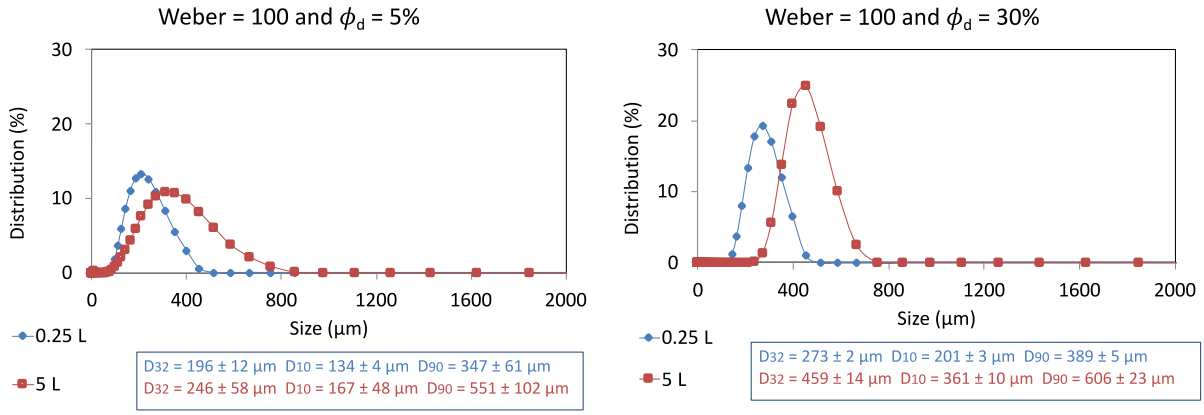


(a) (b)

Figure 5-11 – Droplet size distributions when the same Weber number was used for (a) a diluted system and (b) a concentrated system with the RT

As with the Reynolds number, using the Weber number as a scale criterion resulted in smaller droplets at the smaller scale for the PBT and the RT. This effect was also due to the increase in the energy dissipation rate and the tip speed at the smaller scale (Table 5-3), which generates an

interface, and to the decrease in the circulation time, which reduces coalescence efficiency. However, the Reynolds number decreased at the smaller scale, indicating that this parameter cannot be used to characterize the ability of the system to generate an interface but that it may be related to the coalescence process. It should be noted that achieving a Weber number of 100 at the 35 L scale would not have led to the formation of an emulsion. Indeed, for this condition, the rotational speed would have been too low to enable droplet formation.

### 5.3.4 Power per unit volume

Figures 5-12 and 5-13 present the effect on droplet size distribution of using the energy dissipation rate as a scale-up criterion using the PBT and the RT for diluted and concentrated systems. The experiments were not carried out at the 0.25 L scale due to the high speed required.

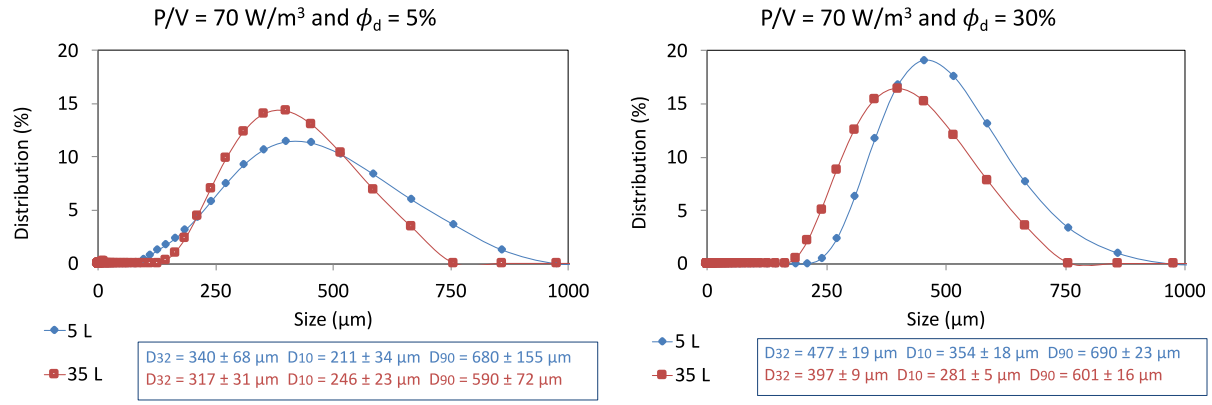


(a) (b)

Figure 5-12 – Droplet size distribution when the same P/V was used for (a) a diluted and (b) a concentrated system with the PBT

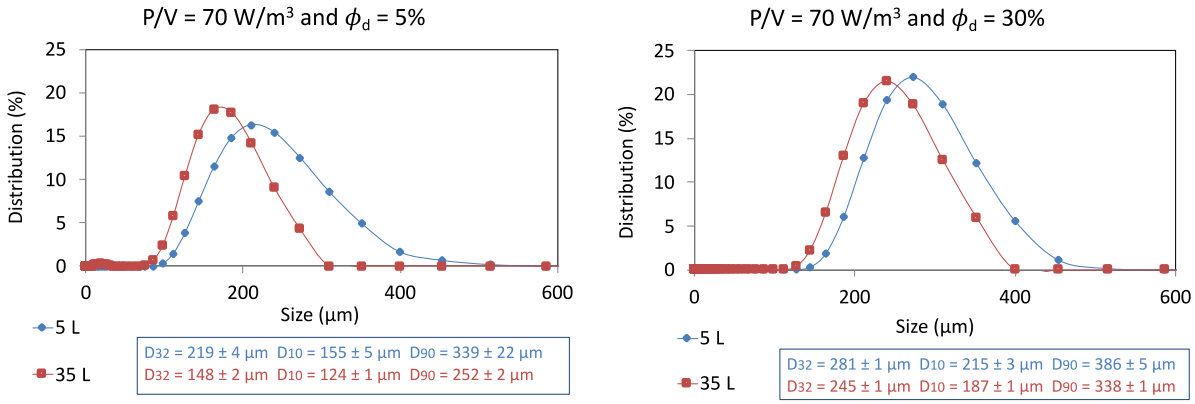


(a) (b)

Figure 5-13 – Droplet size distribution when the same P/V was used for (a) a diluted and (b) a concentrated system with the RT

Increasing the scale resulted in a slightly smaller droplet size for both impellers. This was due to the increase in the capacity of the system to generate an interface following the increase in the ratios of the Weber number, the impeller tip speed, and the Reynolds number, as shown in Figure 5-14 for different $N^3D^2$ representing the variation in the energy dissipation rate. Indeed, Figure 5-14 shows that keeping a constant P/V increased the Weber number, the Reynolds number, and the tip speed at the bigger scale. All these increases improved the emulsification process by producing smaller droplets, which are more stable than bigger droplets. However, the size distributions presented in Figures 5-12 and 5-13 were very close to those obtained when a constant Reynolds number and a constant circulation time were used. These findings suggest that keeping the energy dissipation rate constant can produce a better scale-up. This scale-up criterion is notably used for

slowly coalescing liquid-liquid systems that can be equivalent to solid-stabilized emulsions if the stabilization rate is much higher than the coalescence rate.

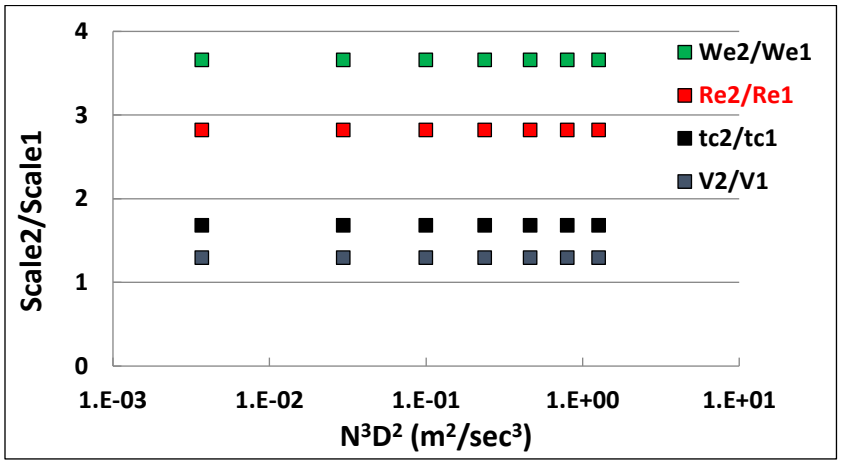


Figure 5-14 – Effect of $N^3D^2$ on the parameters used to characterize the scale-up operation

## 5.3.5 Tip speed

Figures 5-15 and 5-16 present comparisons of droplet size distributions at different scales when using tip speed as a scale-up criterion with the PBT and the RT for diluted and concentrated systems.

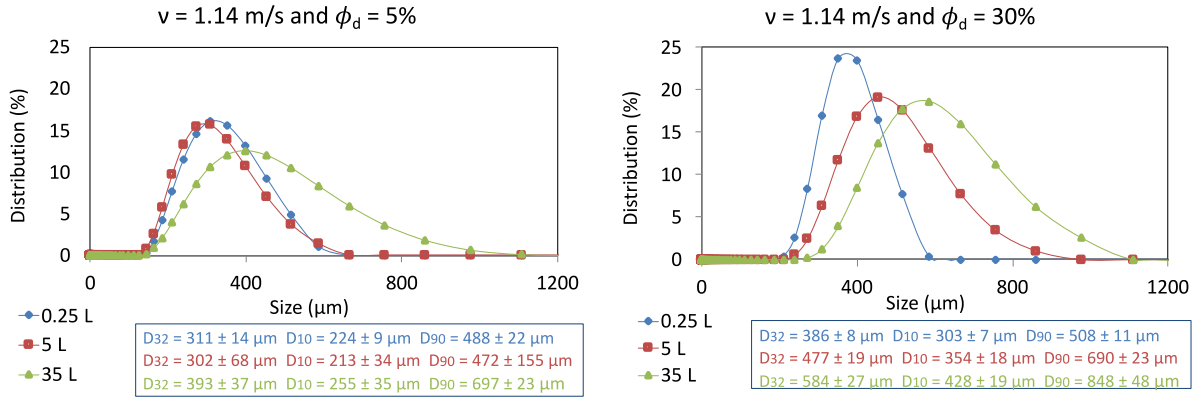


(a) (b)

Figure 5-15 – Droplet size distributions when the same tip speeds were for (a) a diluted and (b) a concentrated system with the PBT

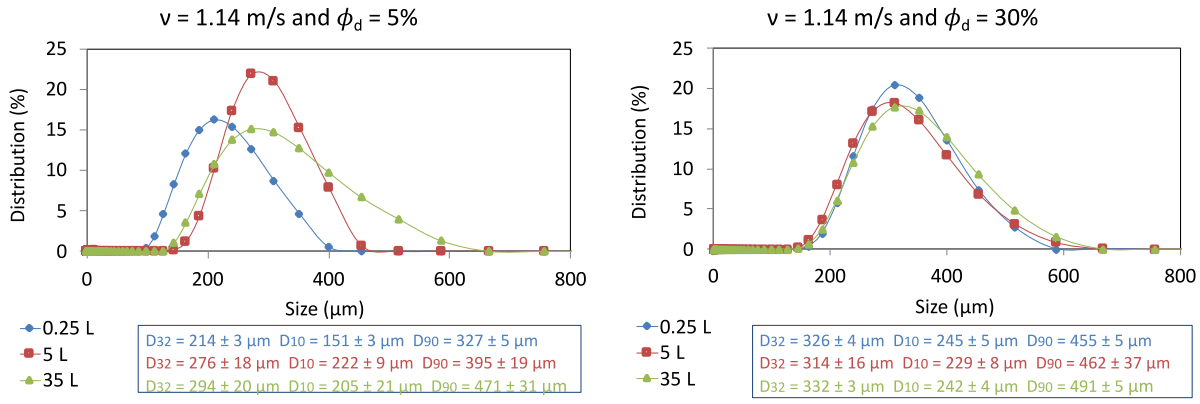


(a) (b)

Figure 5-16 – Droplet size distributions when the same tip speed was used for (a) a diluted and (b) a concentrated system with the RT

Figures 5-15 and 5-16 show that increasing the emulsification scale caused an increase in droplet size. This effect can be attributed to the decrease in the energy dissipation rate since it is the only parameter that decreased when the Weber number was increased (Table 5-3). On the other hand, the results were very close to those of the cases when the Reynolds number or the Weber number were used as a scale-up criterion, which suggests that using tip speed as a scale-up criterion is very close to the conditions required for achieving a consistent scale-up.

### 5.3.6 Summary

Keeping the energy dissipation rate or the impeller tip speed constant provided a more accurate scale-up than keeping the Reynolds number or the Weber number constant. However, an analysis of $d_{32}$ obtained showed that the change in droplet diameter depended on the value of the power-law scale-up exponent (α), as shown in Table 5-8.

Table 5-8 – Difference between $D_{32}$ values

| *Criterion* | *Power law exponent (α)* | *$D_{32}$ (5 L) – $D_{32}$ (35 L)* | *$D_{32}$ (0.25 L) – $D_{32}$ (5 L)* |
|---|---|---|---|
| *Circulation time* | 0 | - | 209 |
| *P/V* | 2/3 | 80 µm | - |
| *Tip speed* | 1 | -91 µm | - |
| *Weber number* | 1.5 | - | -317 |
| *Reynolds number* | 2 | -311 µm | - |

Table 8 shows that when the power per unit volume was used as the scale-up criterion, the droplets were 80 microns larger at the smaller scale (5 L). When the tip speed or the Reynolds number was used as the scale-up criterion, the droplets grew smaller as the scale grew larger. There was thus an inversion of the sign of the size prediction between the case of a constant tip speed and the case of a constant energy dissipation rate (–91 vs 80 µm). The same inversion was observed between the Weber number and the circulation time (–317 and 209 µm) for the two largest scales (5 and 35 L). The inversion of the resulting size at the larger scale suggests that the best-suited scale-up exponent value is between 2/3 and 1. This remains to be proven experimentally, but all the indications presented above point in this direction. The work presented here can be considered as a first step in determining the most appropriate value for a scale-up exponent that is applicable to solid-stabilized emulsions.

## 5.4 Conclusions

The recent interest in the use of solid particles to stabilize emulsions has generated valuable information on the phenomenon at a laboratory scale. This information is helpful for developing formulations and for understanding the basic principles driving emulsification. However, a better understanding of the methods used to scale-up these emulsions is required. Many design rules for conventional liquid-liquid mixtures and for mixing in general are available in the literature. The present work reviewed widely used scale-up criteria and investigated their utility for scaling-up

Pickering emulsions. The Reynolds number, Weber number, impeller tip speed, circulation time, and specific power were used as scale-up parameters using three scales (0.25, 5, and 35 L) and off-centered PBT and RT with geometrically similar unbaffled tanks. None of the scale-up parameters investigated generated equivalent physical properties at different scales suitable for scale-up. However, a further analysis showed that the best-suited power-law exponent would most probably be between 2/3 and 1.

## 5.5 Acknowledgments

The authors gratefully acknowledge the financial support from the Natural Sciences and Engineering Research Council of Canada and from TOTAL.

# CHAPTER 6 ARTICLE 3: SCALING THE PRODUCTION OF SOLID-STABILIZED EMULSIONS. PART II – METHODOLOGY FOR A SCALING FACTOR OF 1000 AND ITS LIMITATIONS

**Alexandre Al-Haiek, Èmir Tsabet, and Louis Fradette**

**Chemical Engineering Department**

**Polytechnique Montréal, 2900 Édouard-Montpetit, Montréal, Canada, H3C 3A7**

**Submitted in *Industrial & Engineering Chemistry Research***

## Abstract

We previously showed (Al-haiek et al. (*submitted*)) that solid-stabilized emulsions (SSEs) cannot be scaled using conventional emulsion scaling rules. We thus performed new experiments to determine the appropriate scaling exponent (α):

$$N_2 = N_1 \left(\frac{D_1}{D_2}\right)^{\alpha} \quad (6.1)$$

The present study was based on results indicating that a suitable power law exponent should be between 0.67 and 1. Identical configurations (off-centered pitched blade and Rushton turbines) were used to produce diluted and concentrated oil-in-water emulsions in unbaffled tanks with four geometrically similar scales (0.25, 5, and 35 L, and a 250 L pilot scale). Silicone oils were used as the dispersed phase, glass beads ($d_{32}$ ≈ 3, 35, and 65 µm) were used as stabilizers, and deionized water was used as the continuous phase.

The emulsions were characterized by droplet size distribution measurements at equilibrium with the laser diffraction method using a Mastersizer 3000 (Malvern). The scaling effect was evaluated by comparing the Sauter mean diameters ($d_{32}$) and two other characteristic diameters ($d_{v10}$ and $d_{v90}$).

A 0.8 scaling exponent was suitable for scaling SSE processes, indicating that a combination of criteria is more appropriate for scaling SSEs than a single criterion as with a standard emulsification. This finding was validated using diluted and concentrated emulsions and a wide range of oil viscosities (10 to 200 cSt), particle sizes, and coverage potentials. The scaling exponent

was then challenged using a 250 L pilot tank and proved to be a suitable scaling criterion for Pickering emulsions in that it can correctly predict the required rotational speed over three size decades.

To better understand the significance of this new scaling exponent, free particle systems were also investigated. The presence of particles reduced coalescence efficiency by reducing the collision frequency between droplets.

**Keywords:** Pickering emulsions, scaling, power-law, emulsification, and stirred tanks.

## 6.1 Introduction

Emulsions are used in many applications in the cosmetics, pharmaceutical, chemical, and other industries (Chappat, 1994). Emulsifying agents are used to stabilize dispersed phase droplets in the continuous phase. Surfactants are commonly used to reduce the interfacial tension of emulsions. However, surfactants are, in many cases, expensive and hazardous and can be solubilized by micelle formation. (Leal-Calderon et al., 2008) The beginning of the 20th century saw increasing interest in solid particles as a new type of stabilizing agent. The ability of solid particles to act as stabilizers was first reported by W. Ramsden (1903) and S.U. Pickering (1907), but it took almost a century for the scientific community to show interest in this kind of application, mainly because of advances in materials science. Many studies have been devoted to the qualitative understanding of SSEs at the laboratory scale since the end of the 20th century. A number of articles on the differences and similarities between solid particles and surfactants have also been published (B.P. Binks, 2002) (R. Aveyard et al., 2003).

The properties of Pickering emulsions have been a major research focus. These properties can be divided into three main categories: emulsion type, emulsion size, and emulsion stability. Particle wettability has been shown to influence emulsion type and stability. Particles of intermediate hydrophobicity produce the most stable emulsions while hydrophilic particles produce oil-in-water (o/w) emulsions and hydrophobic particles produce water-in-oil (w/o) emulsions. Multiple emulsions have also been produced using combinations of particles of opposite wettability. Multiple emulsions such as oil-in-water-in-oil (o/w/o) and water-in-oil-in-water (w/o/w) emulsions (B.P. Binks et al., 2000) (N. Yan et al., 2001) (R. Aveyard et al., 2003) (B.P. Binks et al., 2005) have been produced using ranges of conditions and formulations. Emulsion stability can be improved by adding small monodispersed particles (S. Tarimala et al., 2004), increasing the particle concentration (S. Arditty et al., 2003) (B.P. Binks et al., 2003) (B.P. Binks et al., 2004) (B.P. Binks et al., 2005), decreasing oil viscosity (K. Golemanov et al., 2006) (C.-O. Fournier et al., 2009), increasing the salt concentration to promote partial particle flocculation (B.P. Binks et al., 2005) (B.P. Binks et al., 2006) (T.S. Horozov et al., 2007), and increasing the particle aspect ratio (B. Madivala et al., 2009). The size of droplets decreases with increases in particle concentration (S. Arditty et al., 2003) (Tsabet and Fradette, 2015), decreases in particle size (B.P.

Binks et al., 2001 and S. Tarimala et al., 2004) (Tsabet and Fradette, 2015), and decreases in oil viscosity (Tsabet and Fradette, 2015).

The studies mentioned above have generated a considerable amount of information on SSEs. However, there is a gap in the literature with respect to process design and scale-up rules for these systems. Al-Haiek et al. (*submitted*) evaluated the applicability of the scaling rules used for surfactant-stabilized emulsions and liquid-liquid dispersions, i.e., the Reynolds number, the Weber number, the energy dissipation rate, the circulation time, and the speed of the impeller tip. Although none of these criteria alone was suitable for scaling SSEs, a combination of different criteria with a power-law exponent (α) between 0.67 and 1 would provide an appropriate rule for scaling SSEs:

$$N_2 = N_1 \left(\frac{D_1}{D_2}\right)^{\alpha} \quad (6.2)$$

This supports the assumption that SSEs are solid suspension/liquid dispersion hybrids. Indeed, a power-law exponent of 0.67 represents a constant power per unit of volume criterion that is commonly used for scaling liquid dispersions. In addition, a constant impeller tip speed can be used for solids suspension scaling.

The present work was aimed at confirming our previous results (Al-haiek et al., *submitted*) and determining a suitable rule for scaling SSEs. We used two different impellers (PBT and RT) to investigate a wide range of parameters, including oil viscosity, oil volume fraction, particle size, and particle coverage potential.

## 6.2 Materials and methods

### 6.2.1 Materials

Glass beads (Cospheric and Potters Inc.) were used to stabilize oil-in-water (o/w) emulsions. Particle wettability was determined using the capillary rise method developed by Fournier et al. (2009) and detailed by Al-haiek et al. (*submitted*). Table 6-1 shows particle affinity with different media (air, oil, and water). Particle size distributions (Fig. 6-1) were obtained using a Mastersizer 3000 (Malvern).

Table 6-1 – Properties of glass beads used as dispersion stabilizers

| *Particle size (μm)* | *Density (kg/m$^3$)* | $\theta_{aw}(°)$ | $\theta_{ao}(°)$ | $\theta_{ow}(°)$ | *Supplier* |
|---|---|---|---|---|---|
| 3 | 2520 | $90 \pm 4$ | $81 \pm 1$ | $94 \pm 4$ | Cospheric LLC |
| 35 | 2520 | $74 \pm 2$ | $55 \pm 4$ | $78 \pm 6$ | Potters Inc. |
| 65 | 2520 | $72 \pm 2$ | $26 \pm 3$ | $84 \pm 3$ | Potters Inc. |

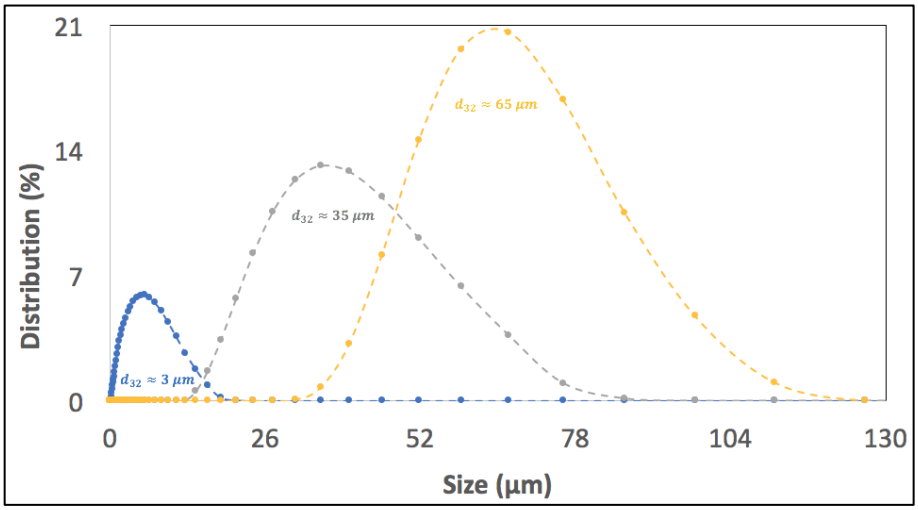


Figure 6-1 – Particle size distribution of each size of glass bead

Pure silicone oils (Clearco Inc., USA) of different viscosities were used as the dispersed phase and deionized water was used as the continuous phase. The physical properties of the oils were confirmed using an MCR502 rotational rheometer (Anton Paar) to measure their dynamic viscosities and an OCA 20 pendant drop instrument (DataPhysics Instruments GmbH) to measure their surface and interfacial tensions (Table 6-2).

Table 6-2 – Properties of the silicone oils

| *Kinematic viscosity (cSt)* | *Density ($kg/m^3$)* | *Dynamic viscosity (mPa.s)* | *Surface tension (N/m)* | *Interfacial tension (N/m)* |
|---|---|---|---|---|
| 10 | 935 | 9.35 | 2.01E-02 | 4.2E-2 |
| 50 | 960 | 48.00 | 2.08E-02 | 4.2E-2 |
| 200 | 968 | 193.60 | 2.10E-02 | 4.2E-2 |

## 6.2.2 Experimental methods

### 6.2.2.1 Emulsification setup

Oil-in-water emulsions were produced in standard unbaffled tanks of different scales (0.25, 5, 35, and 250 L) using a 4-blade PBT or a 6-blade RT (USI-MAX, Canada). The impellers were off-centered (distance from center) to prevent the formation of a vortex (Fig. 6-2). This configuration has the same mixing performance as a baffled tank with a centered impeller (Nishikawa et al., 1979) (Novak et al., 1982) (King et al., 1985) (Karez et al., 2004) (Karez et al., 2005) (Montante et al., 2006).

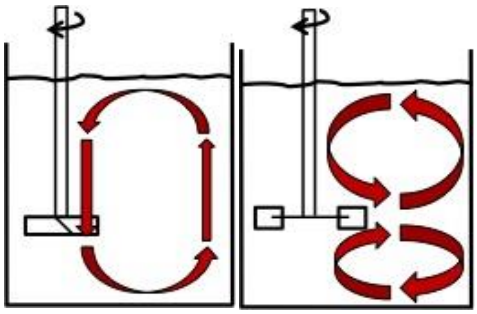

(a) PBT (b) RT

Figure 6-2 – Emulsification systems

Geometrical similarities between the different scales were based on the standard ratios given in Table 6-3, where D is the impeller diameter, T is the tank diameter, $H_{liq}$ is the height of the liquid in the tank, L is the length of the impeller blade, W is the width of the impeller blade, R is the off-

centering distance, and C is the impeller clearance. Table 6-4 gives the geometrical parameters for each scale.

Table 6-3 – Geometrical similarities between the scales

| *T/D* | *$H_{liq}$/T* | *D/L* | *D/W* | *T/R* | *T/C* |
|---|---|---|---|---|---|
| *3* | 1 | 4 | 5 | 6 | 3 |

Table 6-4 – Geometrical parameters for each scale

| *Geometrical parameters* | *Scale 1 - 0.25 L (cm)* | *Scale 2 - 5 L (cm)* | *Scale 3 - 35 L (cm)* | *Scale 4 - 250 L (cm)* |
|---|---|---|---|---|
| Tank diameter (T) | 6.50 | 16.30 | 35.50 | 60.50 |
| Impeller diameter (D) | 2.17 | 5.43 | 11.83 | 20.17 |
| Length of blade (L) | 0.54 | 1.36 | 2.96 | 5.04 |
| Height of blade (W) | 0.43 | 1.09 | 2.37 | 4.03 |
| Baffle thickness (J) | 0.65 | 1.63 | 3.55 | 6.05 |

#### 6.2.2.2 Formulation

Diluted and concentrated oil-in-water (O/W) emulsions ($\phi_d$ = 5% and 30%) were prepared using three silicone oils (10, 50, and 200 cSt).

$$\phi_d = \frac{V_D}{V_D + V_C} \quad (6.3),$$

where $V_D$ is the volume of the dispersed phase and $V_C$ is the volume of the continuous phase, both in $m^3$. Particle concentrations were expressed as their coverage potential. The theoretical coverage potential ($A_{cov}$) was obtained from equations 6.4 to 6.7 (Tsabet and Fradette, 2015 and 2016):

$$V_{1/particle} = \frac{4\,\pi R_p^3}{3} \quad (6.4)$$

$$N_{particles} = \frac{m_p}{\rho * V_{1/particle}} \quad (6.5)$$

$$A_{cov/1p} = \pi\left(R_p \sin\theta_{ow}\right)^2 \quad (6.6)$$

$$A_{cov} = A_{cov/1p} * N_{particles} \quad (6.7),$$

where $R_P$ is the radius of the particle (in m), $V_{1/particle}$ is the volume of the particle (in $m^3$), $m_p$ is the mass of the particles in the system (in kg), $\rho$ is the density of the particles (in $kg/m^3$), $N_{particles}$ is the number of particles in the system, and $\theta_{ow}$ is the oil-water contact angle (in °). Figure 6-3 illustrates the dimensions of a particle.

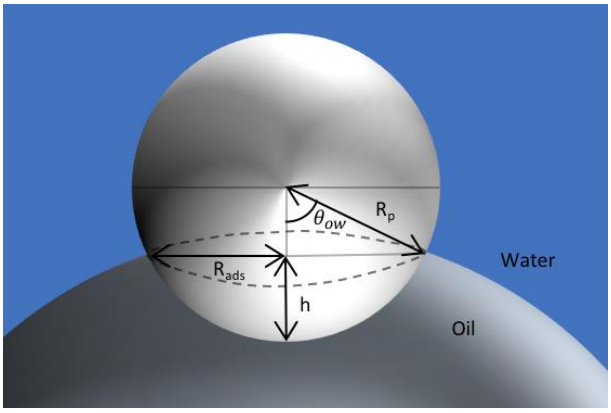


Figure 6-3 – Particle adsorbed to an oil-water interface

The same oil-to-particle volume ratio ($\phi_p = V_D/V_p$) was reproduced at each scale. Table 6-5 gives the equivalence between the theoretical coverage potential and the oil-to-particle volume ratio at each scale for different oil concentrations using 3 µm glass beads (regimes 1 and 2).

Table 6-5 – Equivalence between the oil-to-particle volume ratio ($\phi_p$) and the theoretical coverage potential ($m^2$) at each scale for different oil concentrations ($\phi_d$)

| ***Scales (in L)*** | $\phi_p = 6$ *(Regime 1)* | | $\phi_p = 80$ *(Regime 2)* | |
|---|---|---|---|---|
| | $\phi_d = 5\%$ | $\phi_d = 30\%$ | $\phi_d = 5\%$ | $\phi_d = 30\%$ |
| *0.25* | 53 | 321 | 4 | 25 |
| *5* | 842 | 5 052 | 65 | 387 |
| *35* | 8 700 | 52 199 | 667 | 4 002 |
| *250* | 43 061 | 258 372 | 3 301 | 19 809 |

#### 6.2.2.3 Emulsion preparation

To prepare o/w emulsions, solid particles were gradually added to the desired amount of deionized water under agitation. The particles were dispersed for 10 min at the required rotational speed. The oil was then gently added, and the mixing was continued. Samples were collected after 24 h to characterize the resulting emulsions. Tsabet and Fradette (2016) showed that complete emulsification takes a few hours. Mixing the emulsions for 24 h ensures that the equilibrium droplet size is reached. Figure 6-4 illustrates the emulsification procedure.

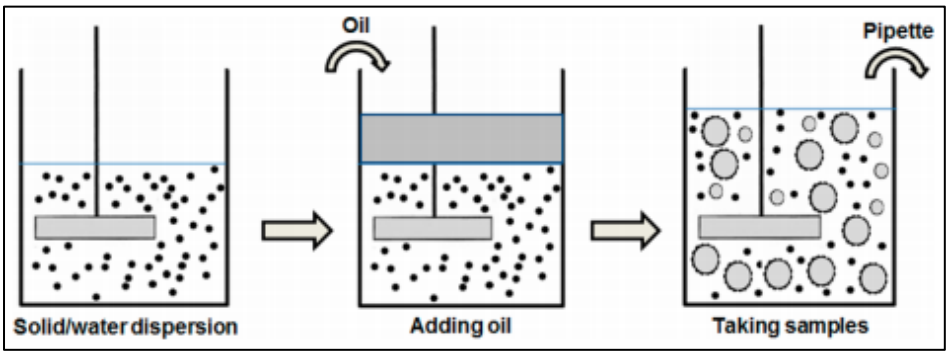


Figure 6-4 – Steps used to prepare a solid-stabilized emulsion [taken from Tsabet and Fradette (2015)]

#### 6.2.2.4 Emulsion characterization

The emulsion type (O/W or W/O) was determined by measuring conductivity using a CON 110 conductivity meter (Oakton). The emulsion size distributions were determined using a Mastersizer 3000 (Malvern). The span was calculated to estimate the distribution widths while the Sauter mean diameter ($d_{32}$) was used as the mean diameter:

$$Span = \frac{d_{90} - d_{10}}{d_{50}} \quad (6.8)$$

$$d_{32} = \frac{6\phi_d}{A_{gen}} \quad (6.9),$$

where $\phi_d$ is the dispersed phase volume fraction (Equation 6-3), $A_{gen}$ is the generated interface (in $m^2$), and $d_{10}$, $d_{50}$, and $d_{90}$ are the diameters (in m) at which 10%, 50%, and 90% of the sample volume is composed of droplets with diameters less than that value.

## 6.3 Results and discussion

According to a previous study (Al-haiek et al., *submitted*), which showed that the suitable power-law exponent ($\alpha$) for SSE scaling should be between 0.67 (constant energy dissipation rate: P/V) and 1 (constant impeller tip speed: $v_{tip}$), exponents located between these two values were tested to find the most suitable one for scaling SSEs. Figure 6-5 gives the Sauter mean diameter at each scale. The only horizontal line that passed through all the average sizes at all the scales and that provided the lowest standard deviation between the scales considered ($\sigma_{d_{32}} = 6\%$) was obtained with a power law exponent of 0.8.

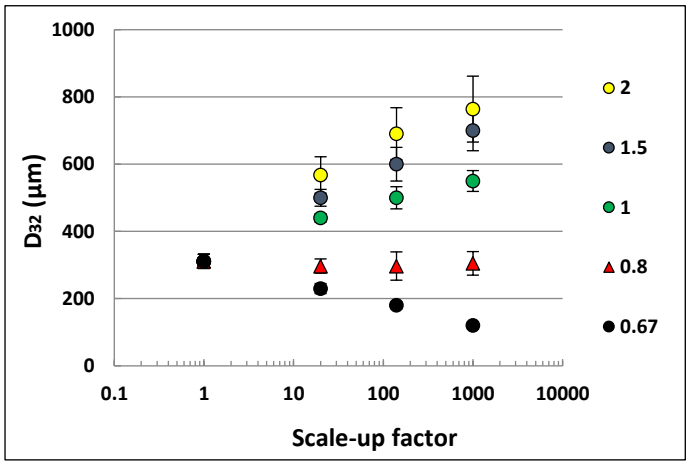


Figure 6-5 – Effect of the power-law exponent on the Sauter mean diameter at different scales using a PBT

The applicability of this exponent was challenged for different formulations using radial and axial impellers (Rushton and pitched blade turbines, respectively) under two different impeller speed regimes (Table 6-6).

Table 6-6 – Impeller speed at each scale based on the 0.8 exponent

| *Scales* | *Impeller speed (rpm)* | |
|---|---|---|
| | Regime 1 | Regime 2 |
| *Scale 1 – 0.25 L* | 1000 | 1200 |
| *Scale 2 – 5 L* | 480 | 576 |
| *Scale 3 – 35 L* | 258 | 309 |
| *Scale 4 – 250 L* | 168 | 202 |

### 6.3.1 Effect of coverage potential

The stabilization of Pickering emulsions is controlled by either the interface generation potential or the coverage potential (Tsabet and Fradette (2016)). Figure 6-6 presents the average drop size as a function of the amount of particles (expressed as $\phi_p$), with oil viscosity as a parameter. A transition occurred in all the curves beyond $\phi_p = 60$, where there are enough particles to cover the generated interface. Based on these results, scaling of the various systems used in our experiments was performed using particle concentrations that allowed both regimes ($\phi_p = 6$ and $\phi_p = 80$) to be tested.

As expected, larger droplets and wider distributions were observed with the 200 cSt silicone oil because the high viscosity lowered the capacity of the system to generate an interface (Fig. 6-6). However, similar results were obtained with both oils, including a plateau zone at a lower $\phi_p$ followed by a diameter increase at a higher $\phi_p$. The zone to the left of $\phi_p$= 60 is the region where emulsification is controlled by the interface generation potential of the system because there are enough particles to cover and stabilize the generated interface (droplets). At higher $\phi_p$values ($\phi_p$ = 60), when the oil/particle mass ratio increased, emulsification was controlled by the coverage potential of the particles, resulting in an increase in droplet size because of a decrease in the amount of particles. Nevertheless, because less interface was generated with the 200 cSt silicone oil, the transition point occurred at an oil-to-particle volume ratio of 60 while the increase in droplet size occurred at a slightly lower value with the 10 cSt silicone oil.

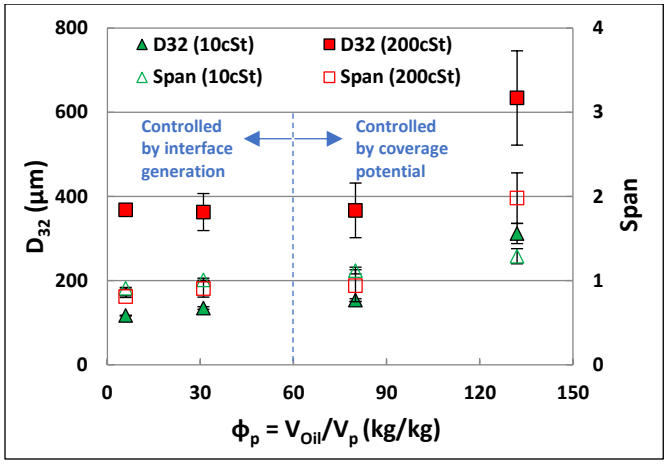


Figure 6-6 – Determination of the emulsification state

Figures 6-7 and 6-8 present the results obtained with the 10 cSt silicone oil and the 200 cSt oil, respectively. The 0.8 exponent was suitable for scaling SSEs at both particle concentrations and for all the conditions considered (oil viscosity and impeller type), with a maximum standard deviation of 1% in the Sauter mean diameter (Table 6-7). This suggested that the 0.8 exponent is not affected by the amount of particles, the droplet size, or the flow pattern. Larger droplets with wider size distributions were obtained with the most viscous oil (200 cSt), and smaller droplets were produced with the RT because it generates higher shear and a lower circulation time than the PBT.

Table 6-7 – Standard deviations for scaling

| | *RT* | | *PBT* | |
|---|---|---|---|---|
| | $\phi_p = 6$ | $\phi_p = 80$ | $\phi_p = 6$ | $\phi_p = 80$ |
| $\sigma_{d_{32}}$ (%) | 0.0 | 1.0 | 1.0 | 0.0 |

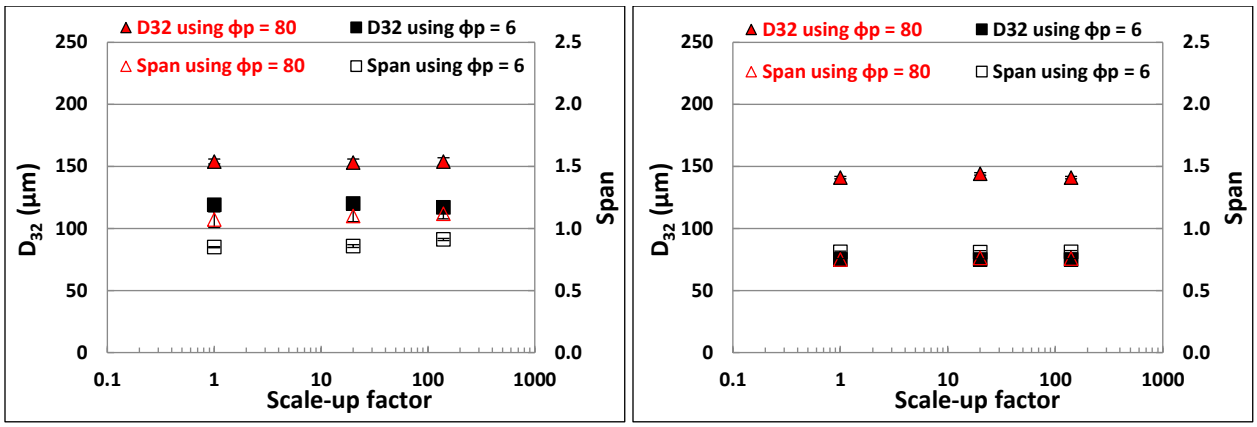


**(a) PBT** **(b) RT**

Figure 6-7 – Effect of particle loading on the scaling of SSEs using 3 $\mu m$ glass beads and 5% (v/v) 10 cSt oil

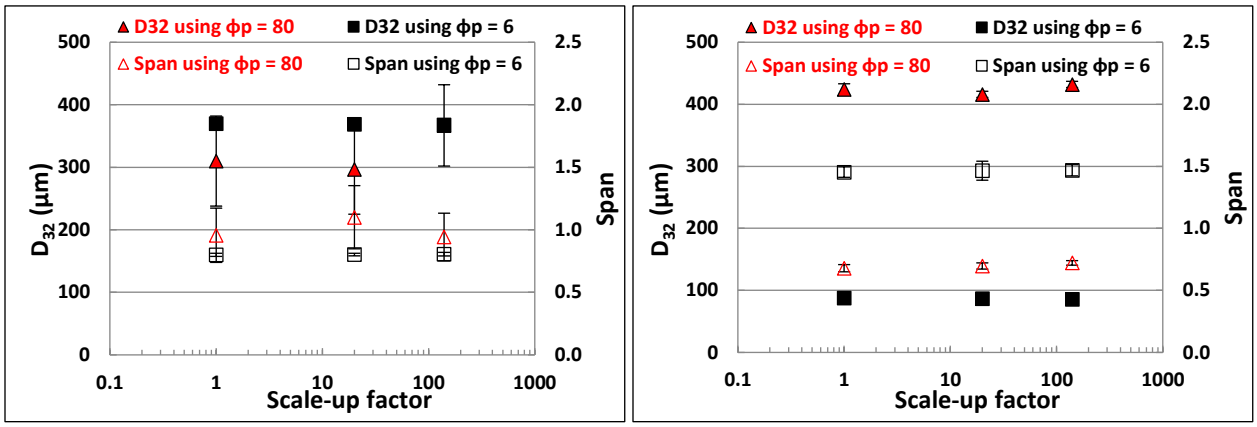


**(a) PBT** **(b) RT**

Figure 6-8 – Effect of particle loading on scaling SSEs using 3 $\mu m$ glass beads and 5% (v/v) 200 cSt oil

## 6.3.2 Effect of particle size

Two different particle sizes (35 and 65 $\mu m$ glass beads) were considered to validate the 0.8 exponent obtained with the 3 $\mu m$ glass beads. The physical properties of the particles are given in Table 6-1. The Sauter mean diameters and spans are shown in Figure 6-9. The associated size distributions were obtained with the PBT and the RT. Slightly larger sizes were obtained with the 65 µm glass beads. Nevertheless, the effectiveness of using an 0.8 exponent for scaling SSEs under

the considered conditions was confirmed. The standard deviations from the predicted sizes were 1% for the 35 µm beads and 3% for the 65 µm beads.

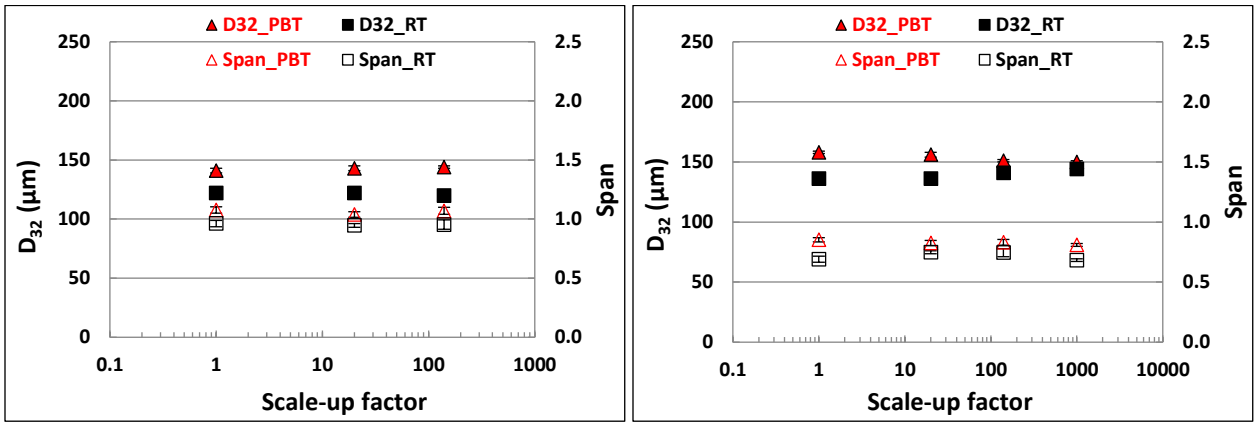


**(a) $d_p$ = 35 µm** **(b) $d_p$ = 65 µm**

Figure 6-9 – Scaling SSEs using (a) 35 µm and (b) 65 µm glass beads

### 6.3.3 Effect of the dispersed phase fraction

Diluted ($\phi_d$ = 5%) and concentrated ($\phi_d$ = 30%) emulsions were prepared using the 50 cSt silicone oil, and the 0.8 exponent was tested with the PBT and RT under both mixing regimes (dominated by coverage potential, with $\phi_p$=6, or dominated by interface generation, with $\phi_p$=80, respectively) (Table 6-5). The Sauter mean diameters and spans obtained at each scale are presented in Figures 6-10 and 6-11.

The effectiveness of using a 0.8 exponent for scaling SSEs with particles was confirmed for both dispersed phase fractions (5% and 30%), with a maximum standard deviation of 6% for the predicted $d_{32}$ and 14% for the span between the different scales (Table 6-8). This again indicated that the scaling exponent is not affected by the flow pattern as the PBT produces one circulation loop while the RT produces two loops pushing sideways (Fig. 6-2).

Increasing the dispersed phase fraction resulted in larger droplets with a wider distribution at each scale. Increasing the coalescence rate and rotational speed resulted in smaller droplets with a narrower distribution, as with conventional emulsions (Arriola-Medellin et al., 2008) and SSEs (Tsabet et al., 2015). The RT generated smaller droplets than the PBT, mainly because the 6-blade RT generates more shear than the 4-blade PBT (Paul et al., 2004). The dispersed phase fraction had less effect on droplet size when the RT was used, indicating that breakage was the dominant

mechanism with the RT while coalescence was the dominant mechanism with the PBT. This behavior can also be explained by the difference in flow patterns because droplets return more rapidly to the high shear zone around the RT impeller.

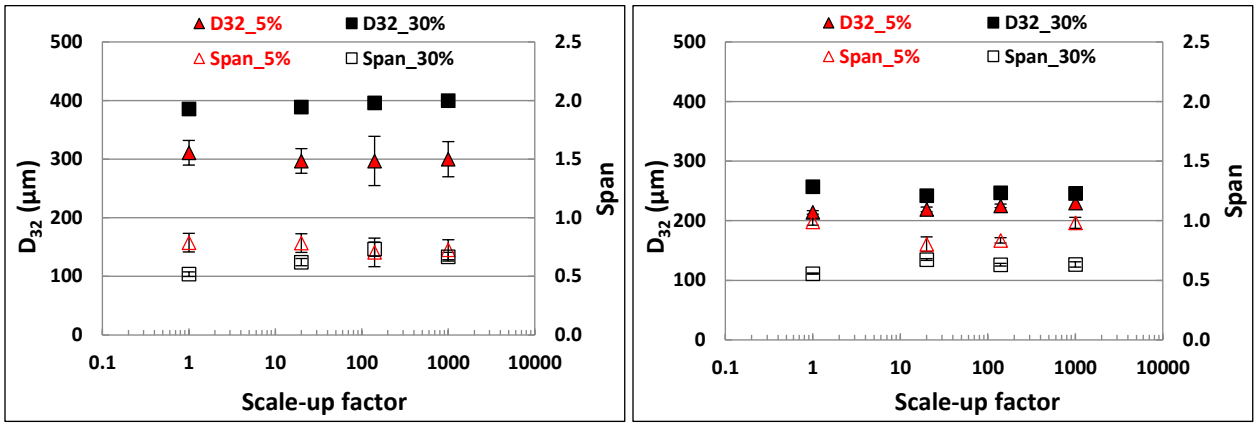


**(a) PBT** **(b) RT**

Figure 6-10 – Effect of the dispersed phase fraction on SSE scaling using 3 $\mu m$ glass beads and 50 cSt oil with Regime 1

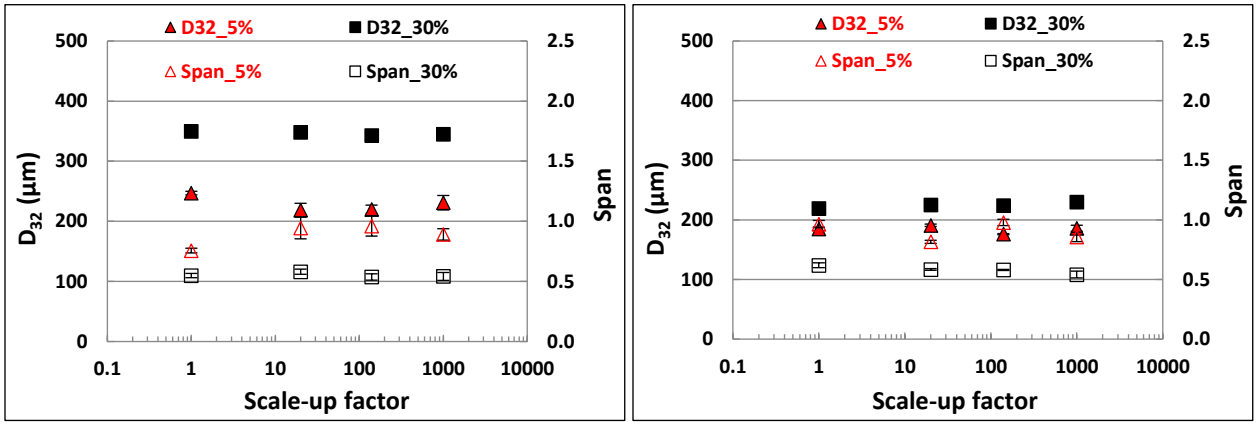


**(a) PBT** **(b) RT**

Figure 6-11 – Effect of the dispersed phase fraction on SSE scaling using 3 $\mu m$ glass beads and 50 cSt oil with Regime 2

Table 6-8 – Standard deviations for the scaling results using the PBT

| | $\phi_d = 5\%$ | | $\phi_d = 30\%$ | |
|---|---|---|---|---|
| | Regime 1 | Regime 2 | Regime 1 | Regime 2 |
| $\sigma_{d_{32}}$ (%) | 2 | 6 | 2 | 1 |
| $\sigma_{Span}$(%) | 6 | 10 | 14 | 4 |

### 6.3.4 Effect of oil viscosity

The 0.8 exponent was also challenged with two other oil viscosities. Figures 6-12(a) and 6-12(b) present the mean diameters and spans obtained with the 10 cSt and 200 cSt silicone oils for a dispersed phase volume fraction of 5% (v/v) using the PBT (Fig. 6-12a) and the RT (Fig. 6-12b). The other parameters were kept constant (coverage potential, $\phi_p$ = 31, and rpms of Regime 1). As expected, increasing the oil viscosity resulted in larger droplets and wider distributions with both impellers. At the highest viscosity, less interface was generated and particle attachment at the droplets surface was hindered. However, comparable sizes were obtained with both impellers, especially with the highest viscosity. This behavior showed that coalescence is less effective in a system equipped with a PBT, suggesting that emulsification is mainly controlled by the breakage process at higher viscosities.

A maximum standard deviation ($\sigma_{d_{32}}$) of 1% was obtained with the 10 cSt silicone oil compared to 13% with the 200 cSt silicone oil at the different scales. The emulsification results again validated the use of the 0.8 value as a suitable exponent for scaling SSEs when the same geometrical parameters are used.

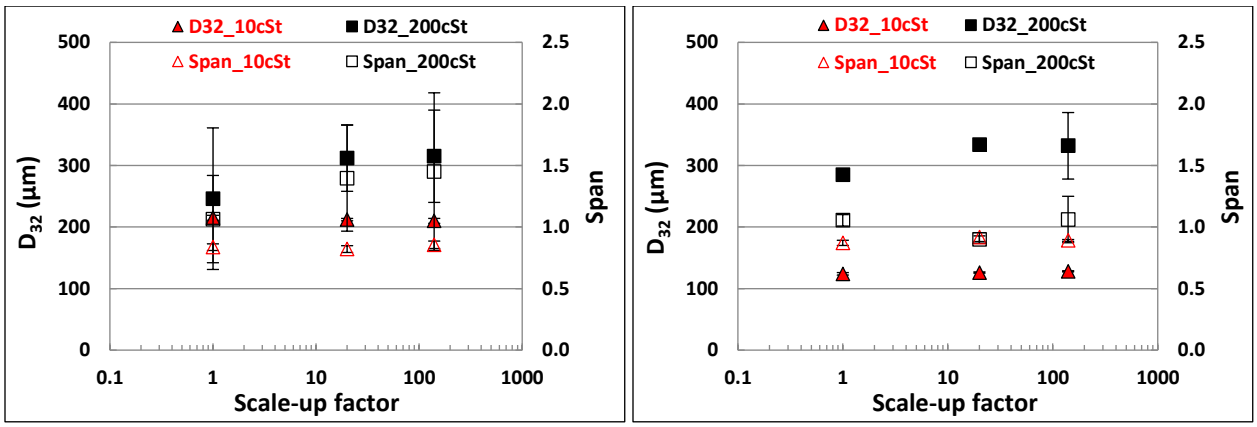


**(a) PBT** **(b) RT**

Figure 6-12 – Effect of dispersed phase viscosity on SSE scaling using 3 $\mu m$ glass beads with $\phi_d$ = 5% (v/v) with Regime 1

### 6.3.5 General discussion: What does the 0.8 value mean?

The applicability of the 0.8 exponent for scaling SSEs was validated with different parameters, including particle fraction and size, oil fraction, oil viscosity, and impeller speed using PBT and RT impellers.

To better understand the origin of this exponent value, the generation of SSEs was divided into the fundamental mechanisms involved, including solids suspension and interface generation, which was sub-divided into breakage, coalescence, and droplet coverage, as described by Tsabet and Fradette (2016). The preliminary analysis presented here might explain why the 0.8 exponent is located between the exponent of a constant energy dissipation rate ($\alpha$ = 0.67) used to scale liquid-liquid dispersions and the exponent of a constant impeller tip speed ($\alpha$ = 1) often used to scale solids suspension systems. Table 6-9 summarizes the effect of using 0.8 as an exponent on the numbers and parameters most widely used to quantify the mechanisms mentioned above.

Is each mechanism reproduced when switching from one scale to another, or is there a complementary effect between the different processes, resulting in the same emulsion properties, or do the mechanisms behave differently from one scale to another.

Table 6-9 – Effect of using a 0.8 exponent on characteristic numbers and parameters

| *Parameter/number* | *Tendency* | *Effect of the 0.8 exponent* | *Effect on scale-up* | *Effect on scale-down* |
|---|---|---|---|---|
| *Reynolds number* | $\sim ND^2$ | $\frac{Re_2}{Re_1} = (scaling\ factor)^{0.40}$ | $\frac{Re_2}{Re_1} > 1$ | $\frac{Re_2}{Re_1} < 1$ |
| *Weber number* | $\sim N^2D^3$ | $\frac{We_2}{We_1} = (scaling\ factor)^{0.47}$ | $\frac{We_2}{We_1} > 1$ | $\frac{We_2}{We_1} < 1$ |
| *Circulation time* | $\sim N^{-1}$ | $\frac{tc_2}{tc_1} = (scaling\ factor)^{0.27}$ | $\frac{tc_2}{tc_1} > 1$ | $\frac{tc_2}{tc_1} < 1$ |
| *Impeller tip speed* | $\sim ND$ | $\frac{V_2}{V_1} = (scaling\ factor)^{0.07}$ | $\frac{V_2}{V_1} > 1$ | $\frac{V_2}{V_1} < 1$ |
| *Specific power* | $\sim N^3D^2$ | $\frac{\varepsilon_2}{\varepsilon_1} = (scaling\ factor)^{-0.13}$ | $\frac{\varepsilon_2}{\varepsilon_1} < 1$ | $\frac{\varepsilon_2}{\varepsilon_1} > 1$ |

To verify this hypothesis, interface generation was separated from the other processes by preparing liquid-liquid dispersions without particles. The 0.8 exponent was applied to scales 2 (5 L) and 3 (35 L) under regimes 1 and 2, which are controlled by interface generation and coverage potential capacity, respectively (Table 6-5), using two different phase fractions (5% (v/v) and 30% (v/v)). Dynamic droplet size distributions were measured with a PVM probe (Mettler Toledo) using the procedure developed by Wan and Fradette (2017).

There was an increase in Sauter mean diameters when moving from scale 2 to scale 3 under both regimes (controlled by interface generation or coverage potential capacity, respectively), suggesting that there was a decrease in the breakage rate or an increase in the coalescence rate, or both (Figures 6-13a and 6-13b).

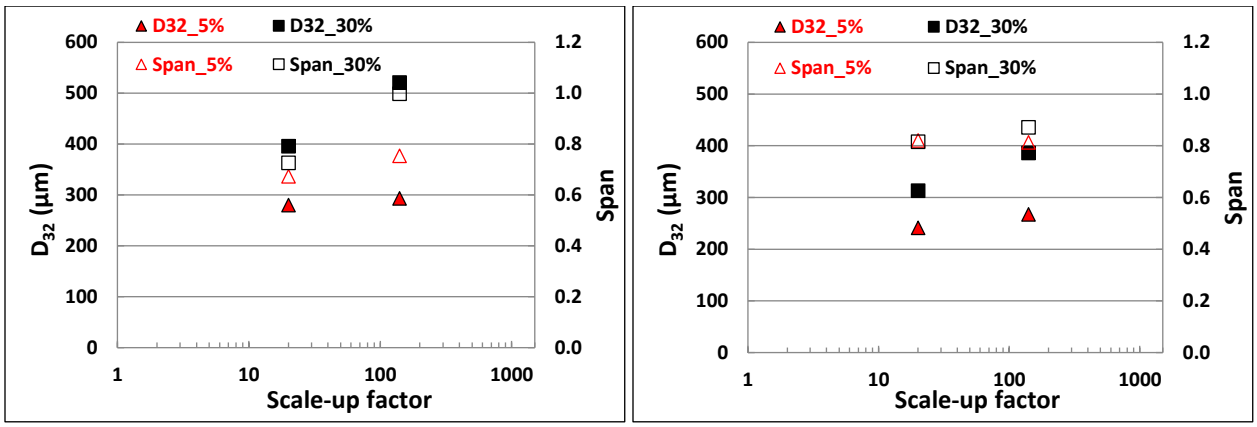


**(a) Regime 1** **(b) Regime 2**

Figure 6-13 – Effect of the dispersed phase fraction on scaling liquid-liquid dispersions without particles using 50 cSt oil

Breakage is generally considered to take place in the impeller zone, and the Sauter mean diameter is usually associated with the Weber number (Equation 6.11) through a balance between the energies or forces favoring droplet generation and those preventing it (Chen et al. (1967), Brown et al. (1970), Van Heuven et al. (1971), Coulaloglou et al. (1976), and Calabrese et al. (1986)):

$$\frac{D_{32}}{D_i} \sim We^{-0.6} \quad (6.10),$$

where

$$We = \frac{\rho_c N_i^2 D_i^3}{\gamma_{ow}} \quad (6.11)$$

The ratio of Sauter mean diameters between the two considered scales is given by:

$$\left(\frac{D_{32}}{D_i}\right)_{Scale\ 3} \Big/ \left(\frac{D_{32}}{D_i}\right)_{Scale\ 2} = (We^{-0.6})_{Scale\ 3} / (We^{-0.6})_{Scale\ 2} \quad (6.12)$$

It can also be given using the energy dissipation rate or the scaling factor X:

$$\frac{(D_{32})_{Scale\ 3}}{(D_{32})_{Scale\ 2}} = \left(\frac{(N_i^3 D_i^2)_{Scale\ 3}}{(N_i^3 D_i^2)_{Scale\ 2}}\right)^{-0.4} = \left(\frac{(\varepsilon)_{Scale\ 3}}{(\varepsilon)_{Scale\ 2}}\right)^{-0.4} = X^{0.052} \quad (6.13)$$

Equation 6.13 gave a ratio of 1.12 for the scales considered in our experiments, which is very close to the experimental results reported in Table 6-10. As the average factor was 1.18, it can be deduced

that the increase in droplet size when scaling up with the 0.8 exponent was due to the decrease in the energy dissipation rate.

Table 6-10 – Ratio of Sauter mean diameters between scale 3 and scale 2

| | *Regime 1* | | *Regime 2* | |
|---|---|---|---|---|
| *Dispersed phase fraction* $\phi_d$ | 5% | 30% | 5% | 30% |
| $\frac{(D_{32})_{Scale\ 3}}{(D_{32})_{Scale\ 2}}$ | 1.05 | 1.32 | 1.11 | 1.23 |

Equation 6.13 can be simplified when a perfect scaling is considered (constant energy dissipation rate), such that:

$$\frac{(N_i)_{Scale\ 3}}{(N_i)_{Scale\ 2}} = \left(\frac{(D_i)_{Scale\ 3}}{(D_i)_{Scale\ 2}}\right)^{-2/3} \quad (6.14)$$

On the other hand, the coalescence rate is generally quantified by the product of droplet collision frequency and coalescence efficiency, as reported by Konno et al. (1988) and Wright et al. (1994):

$$\Gamma(d,d) = \lambda(d,d) \cdot Freq_{Col_{d/d}} \ (6.15),$$

where Γ (d, d′) is the coalescence frequency, λ (d, d′) is the coalescence efficiency, and $Freq_{Col_{d/d}}$ is the collision frequency. Although the collision frequency is also a function of the energy dissipation rate, as noted by Coulaloglou and Tavlarides (1977), Lee et al. (1987), Prince et al. (1990), and Luo (1993), it is also related to the considered scale through the tank volume:

$$Freq_{Col_{d/d}} = C.D_d^{7/3}.\varepsilon_t^{1/3}.V_{tank}.N_d^2/(1+\phi_d) \ (6.16),$$

where C is a constant, $\varepsilon_t$ is the turbulent energy dissipation rate, $D_d$ is the mean diameter of the droplets, $N_d$ is the droplet number density, and $V_{tank}$ is the tank volume.

Coalescence efficiency is based on a film drainage theory such that it is also related to the energy dissipation rate through the collision force, as shown by Chesters (1991).

The ratio of coalescence frequencies at scales 3 and 2 is given by:

$$\frac{\left(Freq_{Col_{d/d}}\right)_{Scale\ 3}}{\left(Freq_{Col_{d/d}}\right)_{Scale\ 2}} = \left(\frac{(\varepsilon)_{Scale\ 3}}{(\varepsilon)_{Scale\ 2}}\right)^{1/3} \cdot \left(\frac{(V_{tank})_{Scale\ 3}}{(V_{tank})_{Scale\ 2}}\right) = X^{0.96} \quad (6.17)$$

Equation 6.17 shows that there is a higher collision frequency at the largest scale because the tank is larger and the circulation time (Equation 6.18) is longer, resulting in higher droplet collision rates and coalescence rates. The breakage rate is simultaneously reduced because the droplets take more time to move back into the impeller zone.

$$t_{circ} = \frac{V_{tank}}{N_q \cdot D_i^3 \cdot N_i} \quad (6.18)$$

Equations 6.17 and 6.18 show that the droplet size increases when scaling up given that coalescence is more significant and breakage is less effective at the larger scale because of the locally lower energy dissipation rate and longer circulation time.

We next investigated the effect of solid particles on scaling. In addition to stabilizing droplets, solid particles also have an effect on the hydrodynamics in the mixing tank. However, particles must first be suspended before they can stabilize droplets. Solids suspension is generally characterized by the just-suspended impeller speed ($N_{js}$), which is the minimum impeller speed required to suspend all the particles in the tank. Numerous correlations have been developed to determine $N_{js}$, but most are based on the empirical correlation developed by Zwietering (1958):

$$N_{js} = A\left(\frac{g(\rho_s - \rho_l)d_p}{\rho_l}\right)^{0.45} \frac{\nu^{0.1}X^{0.13}}{d_p^{0.25}D^{0.85}} \quad (6.19),$$

where g is the acceleration due to gravity (m/s$^2$), $\rho_s$ is the density of the solids (kg/m$^3$), $\rho_l$ is the density of the liquid (kg/m$^3$), $d_p$ is the particle diameter (m), S is Zwietering's constant, ν is the kinematic viscosity (m$^2$/s), D is the impeller diameter (m), T is the tank diameter (m), and X is the particle loading (%).

This correlation was adapted by Ayranci and Kresta (2013) to include the effect of impeller type and geometry under a fully turbulent regime (Re > $10^4$):

$$N_{js} = A\left(\frac{g(\rho_s - \rho_l)}{\rho_l}\right)^{0.5} \frac{d_p^{1/6}X^n}{N_p^{1/3}D^{2/3}}\frac{T}{D} \quad (6.20),$$

where

$$A = S\left(\frac{d_p^{\frac{1}{30}} N_p^{\frac{1}{3}} v^{0.1}}{D^{\frac{11}{60}}}\right)\frac{D}{T}\left(\frac{g\Delta\rho}{\rho_l}\right)^{-0.05} \quad (6.21)$$

The impeller speeds considered in the present work were chosen to exceed the $N_{js}$ calculated using equations 6.20 and 6.21. The fully suspended state was confirmed visually. However, $N_{js}$ is not the only parameter used to design solids suspension procedures, it is also used to stabilize emulsions. Homogeneity, aggregation, and the interaction with turbulence are also very important. These aspects resulted in different scaling rules, depending on the process conditions and objectives ranging from a constant energy dissipation rate (α = 0.67) to a constant impeller tip speed (α = 1). These criteria have been summarized in various publications, notably one by Jafari et al. (2012)

With SSEs, it is important to disperse the particles and avoid the generation of aggregates in order to produce stable droplets with the narrowest size distribution possible. To determine the impact of particles on scaling SSEs, stabilized droplet sizes were compared to the droplet size obtained without particles at different scales using the 0.8 exponent, with different dispersed phase fractions and two different regimes. A decrease in droplet size was observed in many cases when using particles (Table 6-11), indicating that particles affect interface generation through breakage and coalescence.

Table 6-11 – Comparison of droplet size with solids stabilization and without particles under regimes 1 and 2

| | | *Regime 1* | | *Regime 2* | |
|---|---|---|---|---|---|
| *Dispersed phase fraction* $\phi_d$ | | 5% | 30% | 5% | 30% |
| $(D_{32})_{Scale\ 2}$ | Without particles | 280 | 396 | 241 | 313 |
| | With particles | 297 | 389 | 219 | 348 |
| $(D_{32})_{Scale\ 3}$ | Without particles | 293 | 521 | 267 | 386 |
| | With particles | 297 | 396 | 220 | 343 |

The generation of smaller droplets in the presence of particles than in the absence of particles indicated that breakage is promoted when particles are used and that coalescence is prevented. This increase in performance with particles indicated that particles have an impact on the energy dissipation rate since it affected both breakage and coalescence as well as the stabilization process via stabilization efficiencies, as reported by Tsabet and Fradette (2016). It can thus be deduced that the effective energy dissipation rate should be considered when scaling SSEs. The energy dissipation rate is a function of the absolute scale size.

Based on our results, it can also be deduced that the 0.8 exponent is mainly related to the capacity of the system to suspend particles when the properties of the particles allow very fast stabilization given that this exponent is independent of oil viscosity and the oil fraction, the particle size and mass fraction, and the impeller speed and type.

## 6.4 Conclusions

We developed a scaling method for SSEs that can be used with a wide range of oil viscosities (10 to 200 cSt), particle sizes (3 to 65 $\mu m$), dispersed phase volume fractions ($\phi_d$ = 5 to 30%), and coverage potentials ($\phi_p$ = 6 to 80). The method is based on the use of a 0.8 exponent. It was validated with radial- and axial-type impellers at a scaling factor of 1000 (0.25 to 250 L). The value of the exponent remained constant and was independent of the parameters mentioned above. Liquid-liquid dispersion experiments showed that a free particle system cannot be scaled using a 0.8 exponent and that such systems must be scales using a 0.67 exponent, as reported in the literature, since the impeller speed must be increased from one scale to the other to counteract the effect of coalescence. Collision efficiency increased with the scale because of a longer circulation time, which increases the collision frequency and thus the coalescence rate. The presence of particles acted as a barrier, which reduced coalescence. Free particle systems also show that breakage efficiency decreases with scale because droplets take more time to return to the breakage zone. As such, the impeller speed can be lowered in the presence of particles, i.e., the power law exponent can be increased. This behavior is linked to the balance between the two main components of SSEs: particle suspension and liquid-liquid dispersion. The 0.8 exponent lies between the two rules usually used for scale ups.

## 6.5 Acknowledgments

The authors gratefully acknowledge the financial support from the Natural Sciences and Engineering Research Council of Canada and from TOTAL S.A.

# CHAPTER 7 GENERAL DISCUSSSION

As chemical engineers, previous and current students of the *Pickering team* in the URPEI have made it their objective to understand and vulgarize the processing of solid-stabilized emulsions. This is of primary importance in order to properly scale-up end-products that have been subject of numerous researches since the late 1900s. Fournier et al. (2009) described the effect of the dispersed phase viscosity on the generation of solid-stabilized emulsions and, by doing so, developed a method to determine the particle wettability. This method was used in this thesis. Reyjal et al. (2013) explored the thermal transfer within a stabilized emulsion and coupled it with a model. Thermal transfer is of primary importance when it comes to processing. Tsabet and Fradette (2015, 2016) studied the particle adsorption dynamics at a water-oil interface and the effect of numerous processing parameters. It resulted in a semi-empirical correlation that is able to predict droplet size for a wide range of conditions. Recently, Wan and Fradette (2017) described the relation between particle concentration and phase inversion which is crucial regarding the problematic of water emulsified in oil. Bing Wan recently worked on the processing dynamics of particles exchange at the interface.

This thesis has also contributed to the knowledge regarding the processing of solid-stabilized emulsions. As the saying goes: "*Beauty is in simplicity*". Therefore, the processing of these emulsions was approached by decomposing it into simpler, better understood processes. The first step was to assess Pickering emulsions as the combination of a solid suspension and a liquid dispersion process. Doing so, it was noticed that there has been no research on the effect of particle presence on the processing of these emulsions within agitated vessel. However, plenty of papers reported that particles present in a flow will impact the turbulence level. Three particle sizes (3, 35 and 65$\mu m$) and different oil viscosities (10 to 200 cSt) were used in a 5 L unbaffled tank equipped with an off-centred impeller (PBT or RT). A gap between the common literature and collected data was observed. Indeed, when increasing particle concentration for a certain particle size (35 and 65$\mu m$), droplets became larger and not smaller as the literature would have predicted. However, emulsions produced with 3 $\mu m$ particles followed conventional conclusions found in the literature. To show that this behavior is related to particles effect on turbulence and not to the stabilization process, particles wettability was modified making them highly hydrophilic to hinder their

attachment at the interface. Using a particle vision microscope (PVM), it was possible to track droplet size evolution during emulsification.

Results showed that when increasing the concentration of 35 and 65 $\mu m$ particles larger droplets were produced, while 3$\mu m$ particles exhibited the opposite behavior confirming that interface generation is affected through flow conditions. The Stokes number was identified as the dimensionless number describing observed behaviors. It is used to characterize the behavior of solids suspended in a fluid medium. Comparing the particle to the fluid response time, it indicates if particles are following the liquid streamlines (St < 5) or are deviated from them following their own inertia (St > 40). Calculation of Stokes number gives values higher than 10 with 35 and 65 $\mu m$ particles while 3 $\mu m$ particles gives a Stokes number of 1. This conclusion was validated with results obtained using hollow glass beads to investigate the impact of particles density, or by adding glucose to control the continuous phase viscosity.

Based on these findings it was then asked if the scaling of solid-stabilized emulsions is similar to scaling standard emulsification using surfactant or if it is affected by particles suspensions process. Geometrically similar impeller agitated vessels were designed and built with different scaling factor (1, 15, 100, 1000). Both radial- and axial-type impellers were used in order to assess the impact of the flow pattern on the scaling method. Conventional scaling criteria used for either solid suspensions and liquid dispersions were tried over Pickering emulsions. None of them work as to replicate droplet size and size distribution from a 0.25 L beaker to a 250 L tank. Nonetheless, it was observed that there is a sign switch between using a constant power over volume ($\Delta d_i > 0$) and constant impeller tip speed ($\Delta d_i < 0$). This suggested that it might be possible to find a suitable scaling (power-law exponent) criterion between $\alpha = 0.67$ and 1 that would result in $\Delta d_i = 0$. Moreover, results also suggested that the idea of visualising solid-stabilized emulsions as a combination of a solid suspension and liquid dispersion is a valid point of view.

The final objective was to find a suitable scaling criterion and assess if the phenomenon observed with particle sizes (first objective) is scale dependent. The same procedure and apparatuses were used here. It was shown that a power-law exponent equal to 0.8 was able to replicate droplet size and size distribution from a 0.25 L beaker up to a pilot scale of 250 L with both a pitched-blade and Rushton turbine. This exponent was validated for three particle sizes (3, 35 and 65 $\mu m$) both with high and low loadings using dispersed phase viscosities ranging from 10 to 200 cSt. This

exponent ($\alpha$ = 0.8) represents a balance between interface generation and coalescence. Furthermore, it continues to validate the relevance of comparing Pickering emulsions to a mix of two processes: solid suspension and liquid dispersion. Also, the same phenomenon observed in the first objective were larger droplets were obtained with a higher particle loading was seen in larger scales. This concluded that the phenomenon is not scale dependant and that the presence of particles, whatever the vessel size, will impact the energy level.

What where only questions in the beginning where answered and it is without a doubt that knowledge regarding the processing solid-stabilized emulsions has moved forward. This thesis contributed to the understanding of the effect of the presence of particles on the production of emulsions and was able to propose a method for their scaling (x1000) using agitated vessels. This kind of scaling factor is rarely seen in the literature and gives this thesis its originality. Furthermore, the approach used to understand and work with Pickering emulsions, i.e. as a combination of solid suspension and liquid dispersion, is shown to be valid according to results.

# CHAPTER 8 CONCLUSION AND RECOMMENDATIONS

Mixing processes are present in different shapes and forms in numerous industries. It can be found as a standard impeller agitated vessel, a static mixer setup, a rotor-stator configuration or in a more indirect way such as in a fluidized bed or column. However, one thing does not change whatever the mixing configuration or objective is: a science-based approach is still lacking in the industry which has generally relied on trial-and-error. A science-based approach would help reduce the amount of waste generated from bad mixing therefore being also an economical incentive; bad mixing results in millions of dollars in loses every year! Furthermore, a science-based approach would help improve the knowledge in the field of mixing thus opening more *doors*.

As part mixing, emulsification processes are found in many applications such as food (ex. mayonnaise, vinaigrette), pharmaceutical (ex. drug delivery), cosmetic (ex. skin care, sunscreen) and others (ex. paint, bitumen) making them a priority in our lives. Most of nowadays emulsions are produced using surfactants which in some cases, as in pharmaceutical and cosmetics, is not recommended due to their petrochemical origins. Thus, a replacement of surfactants is needed.

In order to replace surfactants and use a science-based approach for problem solving, this thesis considered the use of solid particles, known as solid-stabilized (Pickering) emulsions. If we take a look at the literature, many have studied this type of emulsion from a *chemistry* standpoint. This helped discover the large variety of possible products. What is still missing, however, is the engineering standpoint, i.e. the processing and scaling of these emulsions. Few researchers have considered this standpoint and where presented in Chapters 1 and 2.

The general objective was to *develop a methodology for scaling solid-stabilized emulsions*. In order to achieve this main goal, three specific objectives were completed.

In the first specific objective (Chapter 4), we identified and studied quantitively the impact of the presence of particles on the processing of solid-stabilized emulsions. It was analyzed to identify mechanisms that are relevant for suitable scaling. Two main mechanisms were studied: particle suspension and emulsification. While interface generation and interface stabilization affect the emulsification process, particle suspension has not been studied. We experimentally investigated the effect of particle suspension on SSEs. Oil-in-water emulsions were produced using off-centered pitched blade and Rushton turbines in unbaffled 5-L tanks. Silicone oils were used as the dispersed

phase, glass beads ($d_{32} \approx 3$, 35, and 65 µm) were used as stabilizers, and deionized water was used as the continuous phase. Emulsions were characterized by droplet size distribution measurements using a Malvern Mastersizer 3000. Liquid dispersions were characterized by analyzing images obtained using a particle vision microscope (PVM). The droplet size increased when the particle size or oil viscosity was increased and when the particle concentration was decreased. However, larger droplets could be obtained by increasing the particle concentration under certain conditions. This unexpected behavior was analyzed by examining the interaction between the properties of the solid particles and turbulent energy. An analysis of turbulence length scales showed that this behavior occurs when the particle size is larger than the Kolmogorov scale. We tested different Stokes regimes (flows) and showed that a viscous flow regime (larger fluid response time) exhibits the same behavior as that reported in the literature. On the other hand, high particle concentrations in the inertia flow regime (larger solid response time) stabilized larger droplets.

In the second specific objective (Chapter 5), we verified the applicability of conventional emulsions scaling criteria on Pickering emulsions. Scale-up effects on the production of solid-stabilized emulsions were investigated. Given the geometrical similarities of the three scales used (0.25, 5, and 35 L), emulsions were prepared using off-centered pitched blade and Rushton turbines in unbaffled tanks. Standard criteria for surfactant-stabilized emulsions (constant energy dissipation rate, Weber number, Reynolds number, impeller tip speed, and circulation time) were applied to concentrated and diluted emulsions. Silicone oil (50 cSt) was used as the dispersed phase in water, and glass microspheres ($d_{32} \approx 3$ µm) were used as a stabilizer. A decolorization technique was used to evaluate mixing times. None of the parameters investigated was suitable for use as a scale-up criterion for the production of Pickering emulsions. The use of the Weber number, Reynolds number, and tip speed as scale-up criteria resulted in higher diameters with the largest scale while the opposite tendency was observed with circulation time and energy dissipation. The best scale-up was obtained with the energy dissipation rate and tip speed, suggesting that the suitable scale-up exponent would be between 2/3 (scale-up exponent with the energy dissipation rate) and 1 (scale-up exponent with the tip speed).

In the last and third specific objective (Chapter 6), we identified and quantified parameters regulating the scaling of these emulsions. We thus performed new experiments to determine the appropriate scaling exponent (α). The study was based on results indicating that a suitable power law exponent should be between 0.67 and 1. The scaling effect was evaluated by comparing the

Sauter mean diameters ($d_{32}$) and two other characteristic diameters ($d_{v10}$ and $d_{v90}$). A 0.8 scaling exponent was suitable for scaling SSE processes, indicating that a combination of criteria is more appropriate for scaling SSEs than a single criterion as with a standard emulsification. This finding was validated using diluted and concentrated emulsions and a wide range of oil viscosities (10 to 200 cSt), particle sizes, and coverage potentials. The scaling exponent was then challenged using a 250 L pilot tank and proved to be a suitable scaling criterion for Pickering emulsions. To better understand the significance of this new scaling exponent, free particle systems were also investigated. The presence of particles reduced coalescence efficiency by reducing the collision frequency between droplets.

This thesis contributed to the understanding of processing and scaling of solid-stabilized emulsions. Moreover, it also needs to contribute on what is needed next. Here are some of many more research topics suggested for further investigation:

*Mixing equipment*. We considered, in this thesis, the use of an off-centered impeller within a standard agitated vessel with certain geometrical ratio. However, a large variety of mixing apparatus could also be used such as rotor-stator, static mixer or adding baffles to an agitated vessel can be tested and their impact on the resulting emulsion should be quantified (ex. droplet size and power consumption). This would render data available that would be helpful in choosing the right configuration for large scale design and production as a function of constraint. The scaling method presented in Chapter 6 could be validated on these apparatuses. Moreover, the optimal setup for each application needs to assessed.

*Baffle issues*. In the author's opinion, the use of baffles will encounter numerous issues. First, using baffles in a solid suspension process arise the issue of dead zone. There is a high risk of accumulation zones around the baffles which impacts the homogeneity of the mixing and sends erroneous data. Furthermore, adding a third phase in case of Pickering emulsions will encounter the following problem: one of the two liquid phases will have more affinity to the baffle material…reducing the available interface and increasing the accumulation of particles around the baffles. These are all issues that were observed in the laboratory but were not investigated.

*Emulsions are not only solutions.* Emulsions are also present in the form of a problem rather than a solution (end-use product) if we take the water emulsified in oil as an example. Thus, it is important to dedicate efforts towards the large scale demulsification process using what is now

known. In other words, demulsification is as important as emulsification. Working on how to modify in-situ the particle wettability or aggregate the emulsified water droplet are two distinct possible investigations.

*Transportation of emulsions.* Another major topic is the emulsion transport. To do so, it is important to understand the rheological properties of the product. Thus, it would be interesting to test the emulsion using the double helical ribbon used in Chapter 4 to quantify the viscosity of solid suspensions. The rheology of solid-stabilized emulsions is complex considering that conventional geometries such as bob and cup and cone plate are not useful. Using the same apparatus as in Chapter 4, the emulsion's viscosity can be determined. The author's opinion is that it is plenty feasible with the apparatus found at Polytechnique Montreal.

*Using interface to our advantage.* More phenomena happen at the interface than in the bulk phase. Interface can be used to transport material (ex. minerals) of interest whether by pipeline or by fluidization for example. The use of an emulsification process to render material transportable then to demulsify in-situ is a topic that should be more investigated. Furthermore, the ability of modifying particles properties is a great area of interest when it comes to stimuli responsive materials. It can be used for health benefits such as in drug delivery.

*Scaling emulsions made of a mixture of solid particles and surfactants.* One interesting topic that was not covered in this thesis is the co-stabilization of droplets using a mixture of surfactants and solid particles. Scaling methods should be examined for these kinds of emulsions and the reason is simply: this thesis demonstrated that particle presence reduces the energy left for interface generation. Interface generation capacity, as the Weber number shows, can be increased by reducing the surface tension which can be achieved by using surfactants. Therefore, using a mixture of surfactants and particles can mitigate the reduction of energy left after solid suspension thus generating smaller droplets.

# BIBLIOGRAPHY

Abid, S., & Chesters, A. (1994). The drainage and rupture of partially mobile films between colliding drops at constant approach velocity. *Int. J. Multiphase Flow , 20*, 613-629.

Ait-Kadi, A., P. Marchal, L. Choplin, A.S. Chrissemant, M. Bousmina. (2002) Quantitative analysis of mixer-type rheometers using the Couette analogy, Can. J. Chem. Eng. 80 (6) 1166–1174.

Amani M, Idris M, Abdul Ghani M, Dela Rosa N, Carvero A, et al. (2017) An Experimental Study on the Application of Ultrasonic Technology for Demulsifying Crude Oil and Water Emulsions. J Pet Environ Biotechnol 7:330. doi: 10.4172/2157-7463.1000330

Angst, R., & Kraume, M. (2006). Experimental investigations of stirred solid/liquid systems in three different scales: particle distribution and power consumption. *Chemical Engineering Science , 61* (9), 2864-2870.

Arditty, S., Kahn, J., Schmitt, V., & Leal-Calderon, F. (2004). Materials based on solid-stabilized emulsions. *Journal of Colloid Interface Science , 275* (6), 59-64.

Arditty, S., Whitby, C., Binks, B., Schmitt, V., & Leal-Calderon, F. (2003). Some general features of limited coalescence in solid-stabilized emulsions. *European Physical Journal E, 12*(2), 355-355.

Arriola-Medellin, A.M., Peralta-Martinez, M.V., Palacios-Lozano, E.M. & Sanchez-Sanchez, R. (2008). The Effect of Surfactant Content and Mixing Speed on the Properties of Vacuum Residua in Water Emulsions. *Petroleum Science and Technology, 26*(12), 1449-1458.

Aveyard, R., Binks, B., & Clint, J. (2003). Emulsions stabilised solely by colloidal particles. *Advances in Colloid and Interface Science, 100*, 503-546.

Ayranci, I., Kresta, S. M., & Derksen, J. J. (2013). Experiments and Simulations on Bidisperse Solids Suspension in a Mixing Tank. *Chemical Engineering & Technology*, *36*(11), 1957-1967. DOI: 10.1002/ceat.201300409

Baldyga, J., & Podgorska, W. (2001). Scale-up effects on the drop size distribution of liquid-liquid dispersions in agitated vessels. *Chemical Engineering Science , 56*, 741-746.

Batchelor, G. K. (1977). Effect of Brownian-motion on bulk stress in a suspension of spherical-particles. J. Fluid Mech. 83, 97-117. Journal of Fluid Mechanics. 83. 97 - 117. 10.1017/S0022112077001062.

Berry, J. D., Neeson, M. J., Dagastine, R. R., Chan, D. Y., & Tabor, R. F. (2015). Measurement of surface and interfacial tension using pendant drop tensiometry. *Journal of Colloid and Interface Science , 454*, 226-237.

Bertrand, O., B. Blais, F. Bertrand and L. Fradette. (2018). Complementary methods for the determination of the just-suspended speed and suspension state in a viscous solid-liquid mixing system, Chem. Eng. Res. Des, 136, 32-40.

Bessel, G. German Patent 42 (1877)

Biggs, S., & Proud, A. (1997). Forces between silica surfaces in aqueous solutions of a weak polyelectrolyte. *Langmuir , 13* (26), 7202-7210.

Binks, B., & Lumsdon, S. (2000). Influence of particle wettability on the type and stability of surfactant-free emulsions. *Langmuir, 16*(23), 8622-8631.

Binks, B., & Lumsdon, S. (2001). Pickering emulsions stabilized by monodisperse latex particles: Effects of particle size. *Langmuir, 17*(15), 4540-4547.

Binks, B.P. (2002). Particles as surfactants – similarities and differences. *Current opinion in Colloid & Interface Science, 7*(1-2), 21-41.

Binks, B.P. & Rodrigues, J.A. (2003). Types of Phase Inversion of Silica Particle Stabilized Emulsions Containing Triglyceride Oil. *Langmuir, 19*(12), 4905-4912.

Binks, B.P. & Whitby, C.P. (2004). Silica Particle-Stabilized Emulsions of Silicone Oil and Water: Aspects of Emulsification. *Langmuir, 20*(4), 1130-1137.

Binks, B., & Whitby, C. (2005). Nanoparticle silica-stabilized oil-in-water emulsions: improving emulsion stability. *Colloids and Surfaces A: Physicochemical and Engineering Aspects, 253*(1-3), 105-115.

Binks, B., Murakami, R., Armes, S., & Fujii, S. (2006). Effects of pH and salt concentration on oil-in-water emulsions stabilized solely by nanocomposite microgel particles. *Langmuir, 22*(5), 2050-2057.

Binks, B. (2007). Colloidal particles at liquid interfaces. *Physical Chemistry Chemical Physics, 9*(48), 6298-6299.

Binks, B., & Clint, J. (2002). Solid Wettability from Surface Energy Components: Relevance to Pickering Emulsions. *Langmuir, 18*, 1270-1273

Bird, R., Stewart, W., & Lightfoot, E. (1960). *Transport Phenomena.* New York: Wiley.

Bourne, J., & Hungerbuehler, K. (190). An experimental study of the scale-up of a well-stirred crystallizer. *Transactions of the Institution of Chemical Engineers , 58* (51).

Bragg, J., & Varadaraj, R. (2006). Solids-stabilized oil-in-water emulsion and a method for preparing same. *US Patent No 7.121.339 B2* .

Braisch, B., Kohler, K., Schuchmann, H., & Wolf, B. (2009). Preparation and Flow Behavior of Oil-in-Water Emulsions stabilised by hydrophilic silica particles. *Chemical Engineering & Technology , 32* (7), 1107-1112.

Brito-de la fuente, E., Choplin, L., & Tanguy, P. (1997). MIXING WITH HELICAL RIBBON IMPELLERS: Effect of Highly Shear Thinning Behaviour and Impeller Geometry. *Institution of Chemical Engineers, 75*(1), 45-52.

Brown, D. E. and Pitt, K. (1970). Drop breakup in a stirred liquid–liquid contactor. *Proc. Chemeca* ’70, Melbourne and Sydney, Australia.

Buscall, R., J. I. McGowan, and A. J. Morton-Jones. (1991) *The rheology of concentrated dispersions of weakly attracting colloidal particles with and without wall slip*, J. Rheol. 37, 621–641

Butt, H., Cappella, B., & Kappl, M. (2005). Force measurements with the atomic force microscope: Technique, interpretation and applications. *Surface Science reports , 59* (1-6), 1-152.

Buurman, C., Resoort, G., & Plaschkes, A. (1985). Scaling-up rules for solids suspension in stirred vessels. *Fifth european conference on mixing* .

Cabaret, F., Bonnot, S., Fradette, L., & Tanguy, P. (2007). Mixing time analysis using colorimetric methods and image processing. *Industrial & Engineering Chemistry Research , 46* (14), 5032-5042. Doi: 10.1021/ie0613265.

Calabrese, R.V., Wang, C. Y., & Bryner, N. P. (1986). Drop Breakup in Turbulent Stirred-Tank Contactors Part III: Correlations for Mean Size and Drop Size Distribution. AIChE Journal, 32(4), 677-681.

Capdevila, M., Maestro, A., Porras, M., & Gutiérrez, J. (2010). Preparation of Span 80/oil/water highly concentrated emulsions: Influence of composition and formation variables and scale-up. *Journal of Colloid and Interface Science , 345*, 27-33.

Carrica, P. M., Drew, D., Bonetto, F., & Lahey, R. T. (1999). A polydisperse model for bubbly two-phase flow around surface ship. International Journal of Multiphase Flow, 25(2), 257-305

Chan, D., & Horn, G. (1985). The drainage of thin liquid films between solid surfaces. *Journal of Chemical Physics , 83* (10), 5311-5324.

Chappat, M. (1994). Some applications of emulsions. *Colloids and Surfaces A: Physicochemical and Engineering Aspects, 91*, 57-77. Doi: 10.1016/0927-7757(94)02976-8.

Chelgani, S., Rudolph, M., Kratzsch, R., Sandmann, D., & Gutzmer, J. (2015). A Review of Graphite Beneficiation Techniques. *Mineral Processing and Extractive Metallurgy Review*, 58-68.

Chen, H.T. & Middleman, S. (1967). Drop size distribution in agitated liquid-liquid systems. *AIChE Journal,* 13(5), 989-995.

Chen, S., Gisle Øye & Johan Sjöblom (2005). *Rheological Properties of Aqueous Silica Particle Suspensions*, Journal of Dispersion Science and Technology, 26:4, 495-501, DOI: 10.1081/DIS-200054608

Chesters, A. K. (1991). The Modelling of Coalescence Processes in Fluid Liquid Dispersions: A Review of Current Understanding. *Chem. Eng. Res. & Design, 69(4)*, 259-270.

Chevalier, Y., & Bolzinger, M.-A. (2013). Emulsions stabilized with solid nanoparticles: Pickering emulsions. *Colloids and Surfaces A: Physicochem. Eng. Aspects , 439*, 23-34.

Chong, S. J & B. Christiansen, E & D. Baer, A. (1971). Rheology of Concentrated Suspensions. Journal of Applied Polymer Science. 15. 2007 - 2021. 10.1002/app.1971.070150818.

Colin, C., & Riou, X., (2004), Turbulence and shear-induced coalescence in gas–liquid pipe flows. Fifth International Conference on Multiphase Flow, ICMF'04. Yokohama, Japan.

Coulaloglou, C. A. (1975). Dispersed phase interactions in an agitated flow vessel, PhD Dissertation, Illinois Institute of Technology, Chicago,

Coulaloglou, C. A., & Tavlarides L. L. (1976). Drop size distribution and coalescence frequencies of liquid–liquid dispersions in flow vessels. AIChE Journal, 22(2), 289-297.

Coulaloglou, C. A., & Tavlarides L. L. (1977). Description of interaction processes in agitated liquid–liquid dispersions. Chemical Engineering Science, 32(11), 1289-1297.

Coulson, J., & Richardson, J. (1993). *Chemical Engineering* (Vol. 1). Pergamon Press.
Davis, R., Schonberg, J., & Rallison, J. (1989). The lubrication force between two viscous drops. *Phys. Fluids A , 1*, 77-81.

de Boer, G. B., de Weerd, C., Thoenes, D., & Goossens, H. W. (1987). Laser Diffraction Spectrometry: Fraunhofer Diffraction Versus Mie Scattering. *Part. Charact. , 4*, 14-19.

Dinsmore, A., Hsu, M., Nikolaides, M., Marquez, M., Bausch, A., & Weitz, D. (2002). Colloidosomes: selectively permeable capsules composed of colloidal particles. *Science , 298*.

Dorobantu, L., Yeung, A., Foght, J., & Gray, M. (2004). Stabilization of oil-water emulsions by hydrophobic bacteria. *Appl. Environ. Microbiol. , 70* (633), 3-6.

Drelich, J., Nalaskowski, J., Gosiewska, A., Beach, E., & Miller, J. (2000). Long-range attractive forces and energy barriers in de-inking flotation: AFM studies of interactions between polyethylene and toner. *Journal of Adhesion Science and Technology , 14* (14), 1829-1843.

Drummond, C., Georgaklis, G., & Chan, D. (1996). Fluorocarbons: Surface free energies and van der Waals interaction. *Langmuir , 12* (11), 2617-2621.

Druzhinin, O.A. (2001*) The influence of particle inertia on the two-way coupling and modification of isotropic turbulence by microparticles*, Physics of Fluids 13:12, 3738-3755

Druzhinin, O.A., and Elghobashi, S.E. (1999). *On the decay rate of isotropic turbulence laden with microparticles*, Physics of Fluids, Vol. 11, pp. 602-610

Ebert, F. (1992), Interaction Between the Motion of particles and their turbulent carrier fluid flow. Part. Part. Syst. Charact., 9: 116-124. doi:10.1002/ppsc.19920090116

Einstein, A. (1906). A new determination of molecular dimensions. *Annalen der Physik , 19*, 289-306.

Elghobashi, S.; Truesdell, G. C. (1993) *On the two-way interaction between homogeneous turbulence and dispersed solid particles. I: Turbulence modification*. Physics of Fluids A: Fluid Dynamics, Volume 5, Issue 7, p.1790-1801

Dai, L. L., Tarimala, S. , Wu, C. , Guttula, S. and Wu, J. (2008), The Structure and Dynamics of Microparticles at Pickering Emulsion Interfaces. Scanning, 30: 87-95. doi:10.1002/sca.20087

Fejes, T. (1953). Lagerungen in der Ebene auf der Kugel und im Raum.

Ferrante, A. and Elghobashi, S. E. (2003). *On the physical mechanisms of two-way coupling in particle-laden isotropic turbulence,* Physics of Fluids, Vol. 15, pp. 315-329

Finkle, P., Draper, H. D., & Hildebrand, J. H. (1923). The theory of emulsification. *Journal of the American Chemical Society*, *45*(12), 2780-2788

Fournier, C., Fradette, L., & Tanguy, P. (2009). Effect of dispersed phase viscosity on solid-stabilized emulsions. *Chemical Engineering Research & Design, 87*(4A), 499-506.

Fradette, L. (1999). *Étude de dispersion dans un mélangeur statique Sulzer SMX* (Ph.D. Thesis, École Polytechnique de Montréal).

Frelichowska, J., Bolzinger, M., & Chevalier, Y. (2009). Pickering emulsions with bare silica. *Colloids and Surfaces A: Physicochemical and Engineering Aspects*, *343*(1-3), 70-74.

Fujii, S., Armes, S., Binks, B., & Murakami, R. (2006). Stimulus-responsive particulate emulsifiers based on lightly cross-linked poly(4-vinylpyridine)-silica nanocomposite microgels. *Langmuir , 22* (16), 6818-6825.

Gabriele A, Tsoligkas AN, Kings IN. (2011). Use of PIV to measure turbulence modulation in a high throughput stirred vessel with the addition of high Stokes number particles for both up-and down-pumping configurations. Chem Eng Sci. 66:5862–5874.

Golemanov, K., Tcholakova, S., Kralchevsky, P., Ananthapadmanabhan, K., & Lips, A. (2006). Latex-particle-stabilized emulsions of anti-Bancroft type. *Langmuir, 22*(11), 4968-4977.

Graham, A. L., Steele, R. D., & Bird, R. B. (1984). Particle clusters in concentratedsuspensions. 3. Prediction of suspension viscosity. Industrial & Engineering Chemistry Fundamentals, 23(4), 420–425

Grenville, R., Mak, A., & Brown, D. (2015). Suspension of solid particles in vessels agitated by axial flow impellers. *Chemical engineering research and design , 100*, 282-291.

Griffin, W. C. (1949). Classification of surface-active agents by "HLB". *Journal of Cosmetic Science , 1* (5), 311-326.

Guntzburger, Yoann. (2014). Mixing time measurement using a decolorization method - Images treatment process. URPEI Research Group - Polytechnique Montréal.

Haynes, W., British patent No. 488. Feb. 23: p. 1860.

Herschel, W., & Bulkley, T. (1926). Measurement of consistency as applied to rubber-benzene solutions. *American Society Test Proc. , 26* (2), 621-633.

Hey, M. J., & Kingston, J. G. (2006). Maximum stability of a single spherical particle attached to an emulsion drop. *Journal of Colloid and Interface Science , 298*, 497-499.

Hillier, A., Kim, S., & Bard, A. (1996). Measurement of double-layer forces at the electrode/electrolyte interface using atomic force microscope: potential and anion dependent interactions. *Journal of Physical Chemistry , 100* (48), 18808-18817.

Horozov, T., Aveyard, R., Binks, B., & Clint, J. (2005). Structure and stability of silica particle monolayers at horizontal and vertical octane-water interfaces. *Langmuir , 21* (16), 7405-7412.

Horozov, T., Binks, B.P., & Gottschalk-Gaudig, T. (2007). Effect of electrolyte in silicone oil-in-water emulsions stabilised by fumed silica particles. *Phys Chem Chem Phys*, *9*(48), 6398-6404.

Hsu, M., Nikolaides, M., Dinsmore, A., Bausch, A., Gordon, V., & Chen, X. (2005). Self-assembled shells composed of colloidal particles: fabrication and characterization. *Langmuir , 21* (29), 63-70.

Jafari, R., Tanguy, P. A., & Chaouki, J. (2012). Experimental investigation on solid dispersion, power consumption and scale-up in moderate to dense solid–liquid suspensions . *Chemical Engineering Research and Design , 90*, 201-212.

Jeelani, S., & Hartland, S. (1994). Effect of interfacial mobility on thin film drainage. *Journal of Colloid and Interface Science , 164* (2), 296-308.

Jianren, F., Junmei, S., Youqu, Z. et al. *The effect of particles on fluid turbulence in a turbulent boundary layer over a cylinder.* Acta Mech Sinica (1997) 13: 36. https://doi.org/10.1007/BF02487829

Jones, A., & Wilson, S. (1978). The film drainage problem in droplet coalescence. *Journal of Fluid Mechanics , 87*, 263-288.

Joseph, D., Wang, J., Bai, R., Yang, B., & Hu, H. (2003). Particle motion in a liquid film rimming the inside of a partially filled rotating cylinder. *Journal of Fluid Mechanics , 496*, 139-163.

Karez, J., & Szoplik, J. (2004). An Effect of the Eccentric Position of the Propeller Agitator on the Mixing time. *Chemical Papers, 58*, 9-14.

Karez, J., Cudak, M., & Szoplik, J. (2005). Stirring of a Liquid in a Stirred Tank with an Eccentrically Located Impeller. *Chemical Engineering Science, 60*, 2369-2380.

King, R., & Muskett, M. (1985). Fluid loading and power measurements on an eccentrically mounted pitched blade impeller. *Proceedings of the 5th European Conference on Mixing*, 285-301.

Konno, M., Muto, T., & Saito, S. (1988). Coalescence of dispersed drops in an agitated tank. Journal of Chemical Engineering of Japan, 21(4), 335-338.

Konijn, B.J. & Sanderink, O.B.J. & Kruyt, N.P.. (2014). Experimental study of the viscosity of suspensions: Effect of solid fraction, particle size and suspending liquid. Powder Technology. 266. 61–69. 10.1016/j.powtec.2014.05.044.

Krieger, I., and T. Dougherty. (1959). *A mechanism for non-Newtonian flow in suspension of rigid spheres*, Trans. Soc. Rheol., 3, 137–152

Kruglyakov, P., & Nushtayeva, A. (2004). Phase inversion in emulsions stabilized by solid particles. *Advances in Colloid and Interface Science , 108*, 151-158.

Langevin, D., Poteau, S., Hénaut, I., & Argillier, J. (2004). Crude Oil Emulsion Properties and their Application to Heavy Oil Transportation. *Oil & Gas Science and Technology , 59* (5), 511-521.

Leal-Calderon & Schmitt, V. (2008). Solid-stabilized emulsions. *Current Opinion in Colloid & Interface Science, 13*(4), 217-227.

Lee, C.–H., Erickson, L. E., & Glasgow, L. A. (1987). Bubble breakup and coalescence in turbulent gas–liquid dispersions. Chemical Engineering Communications, 59(1-6), 65-84.

Lee, C.-H. (1987). Bubble breakup and coalescence in turbulent gas-liquid dispersions. *Chem. Eng. Commun , 59* (65).

Lee, Jae-Dong & So, Jae-Hyun & Yang, Seung-Man. (1999). Rheological behavior and stability of concentrated silica suspensions. Journal of Rheology - J RHEOL. 43. 1117-1140. 10.1122/1.551018.

Leikin, S., Parsegian, V., Rau, D., & Rand, R. (1993). Hydration forces. *Annual Review of Physical Chemistry , 44*, 369-395.

Levich, V. (1962). Physicochemical hydrodynamics.

Levine, S., & Bowen, B. (1991). Capillary Interaction of Spherical-Particles Adsorbed on the Surface of an Oil-Water droplet stabilized by the particles I. *Colloids and Surfaces , 59*, 377-386.

Levine, S., Bowen, B., & Partridge, S. (1989). Stabilization of emulsions by fine particles 1. partitioning of particles between continuous phase and oil-water interface. *colloids and surfaces , 38* (4), 325-343.

Levine, S., Bowen, B., & Partridge, S. (1989). Stabilization of emulsions by fine particles 2. Capillary and van der waals forces between particles. *Colloids and surfaces , 38* (4), 345-364.

Li, G. , Gao, Z. , Li, Z. , Wang, J. and Derksen, J. J. (2018), Particle-resolved PIV experiments of solid-liquid mixing in a turbulent stirred tank. AIChE J., 64: 389-402. doi:10.1002/aic.15924

Liang, Y., Hilal, N., Langston, P., & Starov, V. (2007). Interaction forces between colloidal particles in liquid: Theory and experiment. *Advances in Colloid and Interface Science , 134* (35), 151-166.

Lopetinsky, R., Masliyah, J., & Zu, Z. (2006). Solids-stabilized emulsions: A review. *Colloidal Particles at Liquid Interfaces* , 186-224.

Ludovic, D., Allioux, F.-M., Reis, R., & Kong, L. (2014). Qualitative spectroscopic characterization of the matrix–silane coupling agent interface across metal fibre reinforced ion exchange resin composite membranes. *Vibrational spectroscopy , 75*, 203-212.

Luo, H. (1993). Coalescence, breakup and liquid circulation in bubble column reactors. PhD, Dissertation, the Norwegian Institute of Technology, Trondheim.

Madivala, B., Fransaer, J. & Vermant, J. (2009). Self-Assembly and Rheology of Ellipsoidal Particles at Interfaces. *Langmuir, 25*(5), 2718-2728.

Magelli, F., Fajner, D., Nocentini, M., & Pasquali, G. (1990). Solid distribution in vessels stirred with multiple impellers. *Chemical Engineering Science , 45* (3), 615-625.

Magelli, F., Fajner, D., Nocentini, M., Pasquali G, Marisko, V., & Ditl, P. (1991). Solids concentration distribution in slurry reactors stirred with multiple axial impellers. *Chemical Engineering and Processing , 29* (1), 27-32.

Maki, K., & Renardy, Y. (2012). The dynamics of a viscoelastic fluid which displays thixotropic yield stress behavior. *Journal of Non-Newtonian Fluid Mechanics , 181-182*, 30-50

Malvern. (2012, March 28-29). Part I : Rotational Rheometry. *How to measure shear viscosity correctly?*

Mao, Y., Yong, L., Tao, H., Shimin, W., & Yiqian, X. (1998). In-situ measurement of droplet size distribution by light scattering method. *Wuhan University Journal of Natural Sciences , 3* (4), 418-422.

May-Masnou, A., Porras, M., Maestro, A., Gonzalez, C., & Gutiérrez, J. (2013). Scale invariants in the preparation of reverse high internal phase ratio emulsions. *Chemical Engineering Science , 101*, 721-730.

May-Masnou, A., Ribo-Besoli, J., Porras, M., Maestro, A., Gonzalez, C., & Gutiérrez, J. (2014). Scale-up model obtained from the rheological analysis of highly concentrated emulsions prepared at three scales. *Chemical Engineering Science , 111*, 410-420.

McLean, S., Lioe, H., Meagher, L., Craig, V., & Gee, M. (2005). Atomic force microscopy study of the interaction between adsorbed poly(ethylene oxide) layers: Effects of surface modification and approach velocity. *Langmuir , 21* (6), 2199-2208.

Melle, S., Lask, M., & Fuller , G. (2005). Pickering emulsions with controllable stability. *Langmuir , 21* (21), 58-62.

Mewis, J., and N. Wagner. (2012) Colloidal suspension rheology (Cambridge University Press, Cambridge).

Midmore, B. (1998). Preparation of a novel silica-stabilized oil/water emulsion. *Colloids and Surfaces A: Physicochemical and Engineering Aspects , 132* (2-3), 257-265.

Montante, G., Bourne, J., & Magelli, F. (2007). Scale-up of solids distribution in slurry, stirred vessels based on turbulence intermittency. *Industrial and Engineering Chemistry Research , 47* (10), 3438-3443.

Montante, G., Pinelli, D., & Magelli , F. (2003). Scale-up criteria for the solids distribution in a slurry reactors stirred with multiple impellers. *Chemical Engineering Science , 58*, 5363.

Montante, G., Bakker, A., Paglianti, A., & Magelli, F. (2006). Effect of the Shaft Eccentricity on the Hydrodynamics of Unbaffled Stirred tanks. *Chemical Engineering Science, 61*, 2807-2814.

Nai-Ning, W., Hong-Jian, Z., & Xian-Huang, Y. (1992). A versatile Fraunhofer diffraction and Mie scattering based laser particle sizer. *Advanced powder technology , 3* (1), 7-14.

Ngai, T., Auweter, H., & Behrens, S. (2006). Environmental responsiveness of microgel particles and particle-stabilized emulsions. *Macromolecules , 39* (817), 1-7.

Ngai, T., Behrens, S., & Auweter, H. (2005). Novel emulsions stabilized by pH and temperature sensitive microgels. *Chem. Comm. , 33*, 1-3.

Nishikawa, M., Ashiwake, K., Hashimoto, N., & Nagata, S. (1979). Agitation Power and Mixing Time in off-Centering Mxing. *International Journal of Chemical Engineering, 19*, 153-159.

Novak, V., Ditl, P., & Rieger, F. (1982). Mixing in unbaffled vessels the influence of an eccentric impeller position on power consumption and surface aeration. *Proceedings of the 4th European Conference on Mixing*, 57-70.

Ochieng, A., & Lewis, A. (2006). Nickel solids concentration distribution in a stirred tank. *Minerals Engineering , 19* (2), 180-189.

Olhero, Susana & Ferreira, José. (2004). Influence of Particle Size Distribution on Rheology and Particle Packing of Silica-Based Suspensions. Powder Technology. 139. 69–75. 10.1016/j.powtec.2003.10.004.

Ovarlez, G., F. Bertrand, and S. Rodts, (2006). *Local determination of the constitutive law of a dense suspension of noncolloidal particles through magnetic resonance imaging*, J. Rheol. 50, 259-292

Pabst, Willi & Gregorová, Eva & Berthold, Christoph. (2006). Particle Shape and Suspension Rheology of Short-Fiber Systems. Journal of The European Ceramic Society - J EUR CERAM SOC. 26. 149-160. 10.1016/j.jeurceramsoc.2004.10.016.

Patterson, W. I., Carreau, P. J. and Yap, C. Y. (1979), Mixing with helical ribbon agitators: Part II. Newtonian Fluids. AIChE J., 25: 508-516. doi:10.1002/aic.690250317

Paul E.L., Atiemo-Obeng, V.A. & Kresta, S.M. (2004). *Handbook of Industrial Mixing: Science and Practice* (4th edition). New Jersey: John Wiley & Sons, Inc.

Phan, C., Nguyen, A., & Evans, G. (2003). Assessment of hydrodynamic and molecular-kinetic models applied to the motion of the dewetting contact line between a small bubble and a solid surface. *Langmuir , 19* (6796).

PhanThien, N., & Pham, D. (1997). Differential multiphase models for polydispersed suspensions and particulate solids. *Journal of Non-Newtonian Fluid Mechanics , 72* (2-3), 305-318.

Pickering, S. (1907). Emulsions. *J. Chem. Soc., 91*, 2001-2021.

Podgorska, W. (2005). Scale-up effects in coalescing dispersions - comparison of liquid-liquid systems differing in interface mobility. *Chemical Engineering Science , 60*, 2115-2125.

Podgorska, W. (2005). Scale-up effects in coalescing dispersions - comparison of liquid-liquid systems differing in interface mobility. *Chemical Engineering Science , 60*, 2115-2125.

Podgorska, W., & Baldyga, J. (2001). Scale-up effects on the drop size distribution of liquid-liquid dispersions in agitated vessels. *Chemical Engineering Science , 56*, 741-746.

Post Mixing. (2013). *Impellers*. (Post Mixing: Optimization and Solutions, LLC) Retrieved 2016 from Post Mixing: Optimization and Solutions: http://www.postmixing.com/mixing%20forum/impellers/impellers.htm

Prestidge, C., & Simonic, S. (2006). Nanoparticle encapsulation of emulsion droplets. *Int J Pharm, 324*, 92-100.

Princen, H. (1969). Equilibrium shape of interfaces, drops and bubbles, rigid and deformable particles at interfaces. *surface and colloid science , 2*, 1-84.

Prince, M. J., & Blanch, H. W. (1990). Bubble Coalescence and Break-up in Air-Sparged Bubble-Columns. AIChE Journal, 36(10), 1485-1499.

Raji-Asadabadi, M., Abolghasemi, H., Ghannadi Maragheh, M., & Davoodi-Nasab, P. (2013). On the mean drop size of toluene/water dispersion in the presence of silica nanoparticles. *Chemical Engineering Research and Design* , 1739-1747.

Ramsden, W. (1903). Separation of solids in the surface-layers of solutions and suspensions. *Proceedings of the Royal Society of London, 72*, 156-164.

Rapacchietta, A., & Neumann, A. (1977). Force and free energy analyses of small particles at fluid interfaces: II. Spheres. *Journal of Colloid and interface science , 59* (3), 555-567.

Reyjal, Margaux & Tavares, Jason & Virgilio, Nick & Fradette, Louis. (2013). Is the Maxwell-Garnett Continuum Model Valid To Predict the Thermal Conductivity of Particle-Stabilized (Pickering) Emulsions?. Industrial & Engineering Chemistry Research. 52. 10.1021/ie303124p.

Rieger, F., Ditl, P., & Havelkova, O. (1988). Suspension of solids particles, concentration profile and particle layer on the vessel bottom. *Proceedings of the 6th European Conference on Mixing* .

Roscoe, R. (1952). *The viscosity of suspensions of rigid spheres*, Br. J. Appl. Phys., 3, 267–269

Rouzbeh, J., Tanguy, A. P., & Chaouki, J. (2012). Experimental investigation on solid dispersion, power consumption and scale-up in moderate to dense solid–liquid suspensions. *Chemical engineering research and design , 90*, 201-212.

Russell, J., Lin, Y., Boker, A., Su, L., Carl, P., & Zett, J. (2005). Self-assembly and cross-linking of bionanoparticles at liquid-liquid interfaces. *Angew Chem, Int Ed , 44*.

Saboni, A., Gourdon, C., & Chesters, A. (1995). Drainage and Rupture of Partially Mobile films during coalescence in liquid-liquid systems under a constant interaction force. *Journal of Colloid and Interface Science , 175* (1), 27-35.

Scheludko, A., & Nikolov, A. (1975). Measurement of surface tension by pulling a sphere from a liquid. *Colloid and Polymer Science , 253* (5), 396-403.

Schulze, H., & Stockelhuber, W. (1993). Coagulation and flocculation: flotation as a hetero-coagulation process: Possibilities of calculating the propability of flotation. *Edited by Dobias B. and Stechemesser H.* , 455-515.

Shamlou, P. Ayazi. (1993) *Processing of Solid-Liquid Suspensions.* ISBN: 978-0-7506-1134-3, 344 pages. https://doi.org/10.1016/C2013-0-04585-9

Shaw, Duncan J. (1991). *Introduction to colloid & surface chemistry.* 4th edition. ISBN: 0-7506-1182-0, 306 pages

Siebold, A., Walliser, A., Nardin, M., Oppliger, M., & Schultz J. (1997). *Capillary rise for thermodynamic characterization of solid particle surface* (Vol. 186). Journal of Colloid and Interface science.

Simon, S., Theiler, S., Knudsen, A., Oye, G., & Sjoblom, J. (2010). Rheological properties of particle-stabilized emulsions. *Journal of dispersion science and technology , 31* (5), 632-640.

Simonic, S., & Pretidge, C. (2004). Nanoparticles of varying hydrophobicity at the emulsion droplet-water interface: adsorption and coalescence stability. *Langmuir , 20* (83), 57-65.

Singh, P., & Joseph, D. (2005). Fluid dynamics of floating particles. *Journal of Fluid Mechanics , 530*, 31-80.

Stamatoudis, M. and Lawrence L. Tavlarides (1985*). Effect of continuous-phase viscosity on the drop sizes of liquid-liquid dispersions in agitated vessels*, Industrial & Engineering Chemistry Process Design and Development 24 (4), 1175-1181 DOI: 10.1021/i200031a047

Stickel, J., and R. Powell. (2005). *Fluid mechanics and rheology of dense suspension*s, Ann. Rev. Fluid Mech. 37, 129-149

Suarez, M., Gutiérrez, G., Coca, J., & Pazos, C. (2013). Geometric parameters influencing production of O/W emulsions using flat metallic membranes and scale-up. *Journal of Membrane Science , 430*, 140-149.

Sztukowski, D. (2005). *Asphaltene and Solids-Stabilized Water-in-Oil Emulsions.* Thesis, University of Calgary, Department of Chemical and Petroleum Engineering, Calgary.

Tadros, T.F. (2013). *Emulsion Formation and Stability – Chapter 1: Emulsion Formation, Stability, and Rheology*. Pages 1-75, Print ISBN : 9783527319916, Online ISBN : 9783527647941 DOI:10.1002/9783527647941

Tarimala, S., & Dai, L. (2004). Structure of microparticles in solid-stabilized emulsions. *Langmuir, 20*(9), 3492-3494.

Taylor, G. (1932). The viscosity of a fluid containing small drops of another fluid. *Proceeding of the Royal Society of London* , 138-141.

Torres, L., Iturbe, R., Snowden, M., Chowdhry, B., & Leharne, S. (2007). Preparation of o/w emulsions stabilized by solid particles and their characterization by oscillatory rheology. *Colloids and Surfaces A: Physicochemical and Engineering Aspects , 302* (1-3), 439-448.

Tsabet, È. (2014). *De la particule au procédé: modélisation de la production d'émulsions de Pickering.* École Polytechnique de Montréal, Génie chimique. Université de Montréal.

Tsabet, È., & Fradette, L. (2015). Effect of Processing Parameters on the Production of Pickering Emulsions. *Ind. Eng. Chem. Res., 54*(7), 2227-2236.

Tsabet, È., & Fradette, L. (2015). Semiempirical Approach for Predicting the Mean Size of Solid-Stabilized Emulsions. *Industrial & Engineering Chemistry Research, 54*(46), 11661-11677.

Tsabet, È., & Fradette, L. (2016). Study of the properties of oil, particles, and water on particle adsorption dynamics at an oil/water interface using the colloidal probe technique. *Chemical Engineering Research and Design, 109*, 307-316.

Tsouris, C. & Tavlarides, L. L. (1994). Breakage and coalescence models for drops in turbulent dispersions. *AIChE Journal*, 40*(3)*, 395-406.

Tsutsumi, A., Yoshida, K., Yui, M., Kanamori, S., & Shibata, K. (1994). Shear viscosity behavior of 6occulatedsuspensions. Powder Technology, 78(2), 165–172.

Unadkat H, Rielly CD, Hargrave GK. (2009). Application of fluorescent PIV and digital image analysis to measure turbulence properties of solid–liquid stirred suspensions. Chem Eng Res Des. 87:573–586.

Vakarelski, I., Ishimura, K., & Higashitani, K. (2000). Adhesion between silica particle and mica surfaces in water and electrolyte solutions. *J. Colloid Interface Science , 227* (11), 1-8.

van der Werff, J.C., De Kruif, C.G. (Kees. (1989). The shear-thinning behaviour of colloidal dispersions: I. Some theoretical considerations. Physica A: Statistical Mechanics and its Applications. 160. 195-204. 10.1016/0378-4371(89)90416-0.

Van Heuven, J. W., & Beek, W. J. (1971). Power input, drop size and minimum stirrer speed for liquid-liquid dispersions in stirred vessels. Proceeding in International Solvent Extraction Conference, The Hague, the Netherlands, 1, 70-81.

Valentas, K., Bilous, L., & Amundson, A. (1966). Analysis of breakage in dispersed phase systems. *Industrial and engineering chemistry fundamentals , 5* (2), 271-279.

Vargas-Ubera, J., Sanchez-Escobar, J. J., Aguilar, J. F., & Gale, D. M. (2007). Numerical study of particle-size distributions retrieved from angular light-scattering data using an evolution strategy with the Fraunhofer approximation. *Applied Optics , 46* (17), 3602-3610.

Vignati, E., Piazza, R., & Lockhart, T. (2003). Pickering emulsions: Interfacial tension, colloidal layer morphology, and trapped-particle motion. *Langmuir , 19* (17), 6650-6656.

Vrij, A., & Overbeek, J. (1968). Rupture of thin liquid films due to spontaneous fluctuations in thickness. *Journal of American Chemical Society , 90* (12), 3074-3078.

Wan, B. & Fradette, L. (2017). Phase Inversion of a Solid-Stabilized Emulsion: Effect of Particle Concentration. *Canadian Journal of Chemical Engineering*, *95*(10), 1925-1933.

Wang, T. F., Wang, J.F. & Jin, Y. (2005). Theoretical prediction of flow regime transition in bubble columns by the population balance model. *Chem. Eng. Sci., 60(22),* 6199-6209.

Wang, T. F., Wang, J.F. & Jin, Y. (2005). Population balance model for gas–liquid flows: Influence of bubble coalescence and breakup models. *Ind. Eng. Chem. Res., 44(19),* 7540-7549.

Wilkens, R., Henry, C., & Gates, L. (2003). How to scale-up mixing processes in nonnewtonian fluids. *Chem. Eng. Prog. , 99*, 44-52.

Windhab, E., Dressler, M., Feigl, K., Fischer, P., & Megias-Alguacil, D. (2005). Emulsion processing - from single-drop deformation to design of complex processes and products. *Chemical Engineering Science , 60*, 2101-2113.

Wright, H., & Ramkrishna, D. (1994). Factors Affecting Coalescence Frequency of Droplets in a Stirred Liquid-Liquid Dispersion. AIChE Journal, 40(5), 767-776.

Yan, N., Gray, M., & Masliyah, J. (2001). On water-in-oil emulsions stabilized by fine solids. *Colloids and Surfaces A: Physicochemical and Engineering Aspects*, *193*(1-3), 97-107.

Zaman, A. A., Moudgil, B. M., Fricke, A. L., & El-Shall, H. (1996*). Rheological behavior of highly concentratedaqueous silica suspensions in the presence of sodium nitrate and polyethylene oxide*. Journal of Rheology, 40(6), 1191–1210.

Zaman, AA & Moudgil, Brij. (1998). *Rheology of bidisperse aqueous silica suspensions: A new scaling method for the bidisperse viscosity*. Journal of Rheology - J RHEOL. 42. 21-39. 10.1122/1.550935.

Zhou, J., Qiao, X., Binks, B. P., Sun, K., Bai, M., Li, Y., & Liu, Y. (2011). *Magnetic Pickering Emulsions Stabilized by Fe3O4 Nanoparticles* (Vol. 27). Langmuir.

Zhu, W., Aitken, B.G., Sen, S. (2017). *Communication: Non-Newtonian rheology of inorganic glass-forming liquids: Universal patterns and outstanding questions*, J. Chem. Phys. 146, 081103, doi: 10.1063/1.4977085

Zwietering, Th.N. (1958). *Suspending of solid particles in liquid by agitators*. Chemical Engineering Science. 8(3-4), 244-253.

# APPENDICES

## APPENDIX A – NON-DLVO FORCES AND COMPLETE EXPRESSION OF THE STERIC FORCE

Table 8-1 summarizes the non-DLVO forces.

Table 8-1 – Non-DLVO forces during particle/fluid approach [taken from Tsabet (2014)]

| *Forces* | *Type* | *Definition* | *Expression* | *Reference* |
|---|---|---|---|---|
| *Hydration* | Usually repulsive | (1) Attributed to the formation of aqueous molecular layers at interfaces that depend on physico-chemical properties (2) Associated with required energy to remove the water layer adsorbed at the interface | $F(D) = Ke^{-D/D_0}$ | Leikin et al. (1993) |
| *Hydrophobic* | Attractive | Unknown origin but may be associated with the water migration from the gap between two surfaces to the bulk water phase (due to lack of affinity) | $\frac{F}{R} = -C_0 e^{-H/D_0}$ | Drelich et al. (2000) |
| *Hydrodynamic* | Repulsive | Associated with friction induced by the drainage of the thin liquid film between surfaces | $F_{hyd} = 6\pi\eta v \frac{R^2}{D}$ | Chan et al. (1985) |
| *Steric* | Repulsive | Arise when chain molecules attach to surface and form an overlapping structure that prevents approach | $F(D) = 4\pi R P_0(\dots)$ | McLean et al. (2005) |

where $D_0$ is the characteristic decay length, H is the separation distance, $C_0$ is the pre-exponential parameter, D is the separation distance, $\eta$ is the dynamic viscosity of the liquid, $v$ is the approach velocity and R is the sphere radius. McLean et al. (2005) proposed Equation 8.1 for the calculation of the steric force:

$$F(D) = 4\pi R P_0 \left( \frac{2L_0^*}{D} + \left( \frac{D}{2L_0^*} \right)^2 - \left( \frac{D}{2L_0^*} \right)^5 - \frac{9}{5} \right) \quad (8.1)$$

where R is the radius of the particle, $L_0^*$ is the brush thickness at equilibrium, D is the separation distance, $k_B$ is the Boltzmann constant, T is the temperature, N is the sum of all segments in a chain of polymer, $a$ is the length of each segment and $s$ is the average distance between grafting points on the surface. $P_0$ is defined by the following equation:

$$P_0 = \frac{k_B T N}{2} \left( \frac{\pi^2}{12} \right)^{1/3} \frac{a^{4/3}}{s^{10/3}} \quad (8.2)$$

# APPENDIX B – CALCULATIONS OF STABILIZATIONS EFFICIENCIES

## PARTICLE/DROPLET COLLISION EFFICIENCY ($E_{COL}$)

This expression has been presented by Coulaloglou's Ph.D. thesis in 1975,

$$E_{col} \approx \exp\left(-C_1 \frac{t_d}{t_c}\right) \quad (8.3)$$

where $t_d$ is the film drainage time, $t_c$ is the contact time and $C_1$ is a constant. Levich (1962) expressed the contact time using Equation 8.4, which applies in the turbulent regime.

$$t_c \approx C_2 \frac{\left(D_d + D_p\right)^{\frac{2}{3}}}{\varepsilon_t^{\frac{1}{3}}} \quad (8.4)$$

Jeelani and Hartland (1994) defined Equation 8.5 for drainage time calculation.

$$t_d = \frac{3\pi\eta_c R_f^4}{4h_{cr}^2 F_{col}(1 + (3\eta_c l_{circ}/2h_i\eta_d))} \quad (8.5)$$

where $F_{col}$ is the collision force, $R_f$ is the radius of the film, $n_c$ is the continuous phase viscosity, $n_d$ is the dispersed phase viscosity, $h_i$ is the initial film thickness, $h_{cr}$ is the critical film thickness and $l_{circ}$ is the circulation length. Vrij and Overbeek (1968) calculated $h_{rc}$ using Equation 8.6.

$$h_{cr} = 0.267\left(\frac{A_f A_H^2}{6\pi\gamma_{ow}\Delta p}\right)^{\frac{1}{7}} \quad (8.6)$$

where $\gamma_{ow}$ is the interfacial tension between water and oil, $A_f$ is the surface area of the film, $A_H$ is the Hamaker constant and $\Delta p$ is the excess pressure in the film. The surface area of the film can be deduced from the Laplace pressure equation,

$$F_{col} = \Delta p A_f = \frac{2\gamma_{ow}}{R_d} A_f \rightarrow A_f = \frac{F_{col} R_d}{2\gamma_{ow}} \quad (8.7)$$

The radius of the film can be calculated using Equation 8.8. It assumes a spherical deformation and a small film thickness.

$$R_f = R_p \sin\left(cos^{-1}\left(1 - \frac{A_f}{2\pi R_p^2}\right)\right) \quad (8.8)$$

Thus, the collision force can be deduced from these equations proposed by Levich (1962),

$$F_{col} \approx C_3 \frac{\pi}{2} \rho_c \varepsilon_t^{\frac{2}{3}} \left(\frac{D_d D_p}{D_d + D_p}\right)^{\frac{8}{3}} \quad for \quad \left(\frac{D_d D_p}{D_d + D_p}\right) \geq \lambda \quad (8.9)$$

$$F_{col} \approx C_4 \frac{\pi}{4} \rho_c^2 \frac{\varepsilon_t \left(\frac{D_d D_p}{D_d + D_p}\right)^4}{\eta} \quad for \ \left(\frac{D_d D_p}{D_d + D_p}\right) < \lambda \quad (8.10)$$

$$\lambda = (v^3/\varepsilon_t)^{0.25} \quad (8.11)$$

where $F_{col}$ is the collision force, $\varepsilon_t$ is the turbulent energy dissipation rate, $\lambda$ is the Kolmogorov length scale (Equation 8.7), $D_p$ is the particle diameter and $D_d$ is the droplet diameter.

## THREE-PHASE CONTACT LINE EXPANSION EFFICIENCY ($E_{TPCL}$)

This expression was taken from particle/bubble interactions during flotation processes. Schulze et al. proposed it in 1993.

$$E_{TPCL} = 1 - \exp\left(-\frac{t_c}{t_{TPC_{cr}}}\right) \quad (8.12)$$

where $t_c$ can be calculated using Equation 8.4. The time required to reach the critical line radius is calculated using the following equations:

$$t_{i+1} = \frac{R_{TPC}(t_{i+1}) - R_{TPC}(t_i)}{V_{TPC}(t_i)} + t_i \quad (8.13)$$

where $R_{TPC}(t_{i+1})$ is calculated using Equation 8.14,

$$R_{TPC}(t_{i+1}) = R_p \sin\theta_{i+1} \quad (8.14)$$

and $V_{TPC}$ is calculated using Equation 8.15 proposed by Phan et al., (2003),

$$V_{TPC} = \frac{dR_{TPC}}{dt} = \frac{\gamma_{ow}}{9 \ln\left(\frac{R_m}{L_m}\right)\eta}\left(\theta_e^3 - \theta^3(t)\right) \quad (8.15)$$

$$V_{TPC}(t_{i+1} = t_i + \Delta t) = \frac{\gamma_{ow}}{9 \ln\left(\frac{R_m}{L_m}\right)\eta}\left(\theta_e^3 - (\theta_{i+1} = \theta_i + \Delta\theta^3)\right) \quad (8.16)$$

$$\Delta\theta = \frac{\theta_e - \theta_0}{N_\theta} \quad (8.17)$$

where $N_\theta$ is the dynamic contact angle step number and $\theta_0$ is the initial dynamic contact angle (t = 0). Figure 8-1 presents an adsorbed particle at an interface (forming the three-phase contact line).

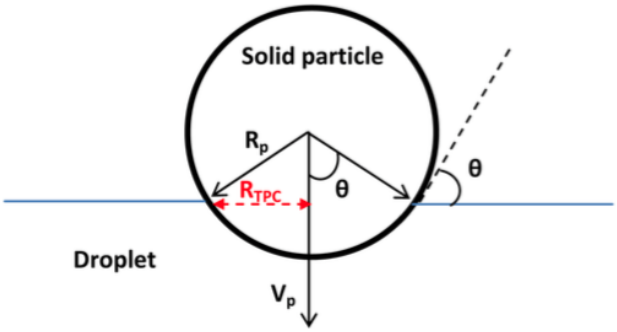


Figure 8-1 – Schematic representation of the three-phase contact line [taken from Tsabet et al. (2015)]

## PARTICLE ATTACHMENT EFFICIENCY ($E_{ATT}$)

Flotation process has also been used to define the particle attachment efficiency. Equation 8.18 presents this efficiency,

$$E_{Att} = 1 - \exp\left(1 - C_{Att}(F_{Att}/F_{Det})\right) \quad (8.18)$$

Scheludko et al. (1975) defined the attachment force ($F_{Att}$) for a sphere particle at a liquid interface,

$$F_{Att} = 2\pi\gamma_{ow}R_p\left(\cos\left(\frac{\theta}{2}\right)\right)^2 \quad (8.19)$$

The detachment force ($F_{Det}$) was considered to be the sum of the hydrodynamic ($F_{Hyd}$), Laplace pressure ($F_{Lap}$) and gravity ($F_g$) forces.

$$F_{Det} = F_{Hyd} + F_{Lap} + F_g \quad (8.20)$$

Jeelani et al. (1994) defined these forces.

$$F_{Hyd} = \frac{4}{3}\pi R_p^3 \rho_p a_t \quad (8.21)$$

where $a_t$ is the acceleration in a turbulent flow field,

$$a_t = \frac{1.9\varepsilon_t^{2/3}}{\left(R_d + R_p\right)^{1/3}} \quad (8.22)$$

$$F_{Lap} = A_p\Delta p = \left(\pi R_p^2 sin^2\theta_{ow}\right)\left(\frac{2\gamma_{ow}}{R_d}\right) \quad (8.23)$$

$$F_g = \frac{4}{3}\pi R_p^3 \rho_p g \quad (8.24)$$

## DROPLET COVERAGE EFFICIENCY ($E_{COV}$)

The droplet coverage efficiency is calculated using Equation 8.25.

$$E_{cov} = \exp\left(-\frac{Freq_{Col_{\frac{d}{d}}} E_{Coalescence}}{Freq_{Col_{\frac{N_p}{d}}}}\right) \quad (8.25)$$

where $Freq_{Col_{d/d}}$ is the droplet/dropet collision frequency, $Freq_{Col_{Np/d}}$ is the particle/droplet collision frequency proposed by Coulaloglou and Tavlarides (1977), Lee et al., (1987), Prince and Blanch (1990) and Luo (1993). $E_{Coalescence}$ is the coalescence efficiency. The first two are calculated using Equations 8.26 and 8.27 respectively. The $E_{Coalescence}$ is calculated using Equation 8.3.

$$Freq_{Col_{Np/d}} = \left(C_5\left(D_p^2 + D_d^2\right)\left(D_p^{\frac{2}{3}} + D_d^{\frac{2}{3}}\right)^{0.5} \varepsilon_t^{\frac{1}{3}} V_{tank} N_d N_{p/Total}\right) \Big/ N_{p/d} \quad (8.26)$$

$$Freq_{Col_{d/d}} = C_6 D_d^{\frac{7}{3}} \varepsilon_t^{\frac{1}{3}} V_{tank} N_d^2 / (1 + \phi_d) \quad (8.27)$$

where C is a constant, $\varepsilon_t$ is the turbulent energy dissipation rate, $D_p$ is average particle diameter, $D_d$ is the average droplet diameter, $N_d$ is the droplet number density, $N_{p/Total}$ is the total particle number density, $N_{p/d}$ is the number of particles required to cover one droplet and $V_{tank}$ is the tank volume.

# APPENDIX C – CALCULATIONS OF DROPLETS DIAMETER BEFORE ($R_{DI}$) AND AFTER PARTICLE ADSORPTION ($R_{DII}$)

The droplet diameter before particle adsorption ($R_{dI}$) has been defined using a Taylor development (Levine et al., 1991):

$$\left(\frac{R_{dII}}{R_{dI}}\right)^3 = 1 + N_{p/d}\left(R_p/4R_{dI}\right)\left(R_p/R_{dI}\right)^2\left[(2+\cos\theta_{ow})(1-\cos\theta_{ow})^2 - \left(9R_p/4R_{dI}\right)sin^2\theta_{ow} + \cdots\right] \quad (8.28)$$

where $R_{dII}$ is defined by Equation 8.29

$$R_{dII} = (D_{mean} - (2R_p - h))/2 \quad (8.29)$$

and $N_{p/d}$ is defined by Equation 8.30

$$N_{p/d} = \frac{A_{cov/1droplet}}{\pi\left(R_p(1-\sin\theta_{ow})\right)^2} \quad (8.30)$$

Figure 8-2 is a schematic representation of the droplet diameter before and after particle adsorption.

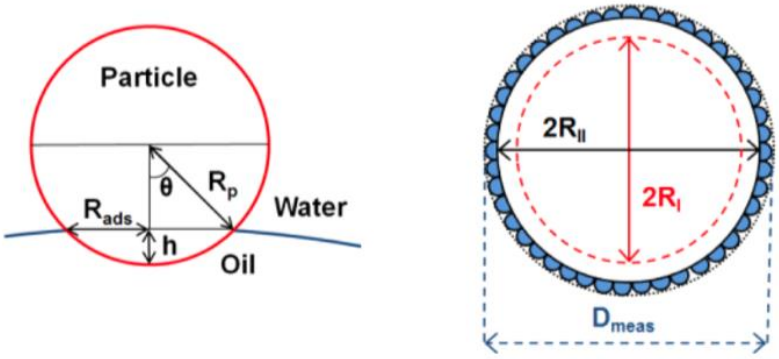


Figure 8-2 – Droplet diameter before and after particle adsorption [taken from Tsabet et al. (2015)]